NEURAL-SPECIFIC ALTERATIONS IN GLYCOSYLATION AND CELL SIGNALING ASSOCIATED WITH TWO NEUROLOGICAL DISEASES.

by

SHANNON WAGNER

(Under the Direction of Michael Tiemeyer)

ABSTRACT

Neurological diseases consist of any disorder that affects the nervous system. Despite being two very different neurological diseases, GM3 Synthase Deficiency (GM3SD) and Alzheimer's Disease (AD) both cause detrimental consequences and symptoms to the body and nervous system. Individuals with GM3SD display seizure activity, hypo- or hyper- pigmented skin as well as cognitive, developmental, psychomotor, speech and hearing impairments. AD is much more common than GM3SD and presents itself in individuals much later in life. These patients experience cognitive impairment and difficulties deciphering spatial relationships. Despite these key differences both diseases share similarities in cellular stress and death. O-linked-β-N-Acetylglucosamine (O-GlcNAc) is a post-translational modification on Ser/Thr residues. It has been shown to act as a signal integrator with the ability to cause or resolve stresses. Using patient-derived induced pluripotent stem cells and derived neural crest cells we observe protein O-GlcNAcylation as a pro-survival mechanism.

INDEX WORDS: Glycosylation, neurological diseases, cell signaling, Alzheimer's Disease, GM3 Synthase Deficiency, peripheral nervous system, human induced pluripotent stem cells, neural crest cells

NEURAL-SPECIFIC ALTERATIONS IN GLYCOSYLATION AND CELL SIGNALING ASSOCIATED WITH TWO NEUROLOGICAL DISEASES.

by

SHANNON WAGNER

B.S., Georgia Southern University, 2019

A Thesis Submitted to the Graduate Faculty of The University of Georgia in Partial Fulfillment of the Requirements for the Degree

MASTER OF SCIENCE

ATHENS, GEORGIA

2022

NEURAL-SPECIFIC ALTERATIONS IN GLYCOSYLATION AND CELL SIGNALING ASSOCIATED WITH TWO NEUROLOGICAL DISEASES.

by

SHANNON WAGNER

Major Professor:	Michael Tiemeyer
Committee:	Lance Wells
	Gerald Hart
	Shelley Hooks

Electronic Version Approved:

Ron Walcott
Vice Provost for Graduate Education and Dean of the Graduate School
The University of Georgia
August 2022

DEDICATION

To my family and friends who have supported me every step of the way.

ACKNOWLEDGEMENTS

I would like to thank my committee Gerald Hart, Shelley Hooks, Lance Wells, and Michael Tiemeyer. A big thank you to Mike for letting me join the lab and guiding me through my project the past three years. An abundance of gratitude to the other individuals that have helped me: Kazuhiro Aoki, Mayumi Ishihara, Katelyn Rosenbalm, and Michelle Dookwah. You all have helped me in so many tremendous ways. I would not be half the scientist I am today without your instruction and friendship.

TABLE OF CONTENTS

Page

LIST OF TABLES

Page

LIST OF FIGURES

Page

CHAPTER 1

INTRODUCTION AND LITERATURE REVIEW

Introduction to Glycosylation

There are a range of post-translational modifications (PTM) that have crucial roles in the cell. Specifically, glycosylation of proteins, lipids and other molecules can modulate and change the fate of transcription, cell signaling, development, differentiation, and migration. This thesis will primarily focus on the consequences of changing a carbohydrate (glycan) modification associated with specific neurological diseases. Lipid glycosylation and O-GlcNAcylation will be discussed in detail in this review and discussed further in diseases associated with the brain and the nervous system.

Glycosphingolipid Biosynthesis

Glycosphingolipids (GSL) are synthesized by combining a glycan to the primary hydroxyl group of a ceramide. Ceramides consist of an amino alcohol that is linked to a fatty acyl chain via an amide linkage (Varki et al., 2015). In mammals the synthesis of ceramide begins at the membrane of the endoplasmic reticulum (ER). Ceramide synthases are found at the cytosolic leaflet of the ER. The acylation of sphingosine forms ceramide (Gault, Obeid, & Hannun, 2010). The pathway illustrated in Fig. 1 begins with the addition of a galactose or glucose residue to ceramide. Glucosylceramide synthase (UGCG) then forms glucosylceramide (GlcCer) by β-glycosidically linking the glucose

residue to the 1-position of the ceramide tail. (Sandhoff & Kolter, 2003). β1,4-galactosyltransferase (LacCer Synthase) encoded by B4GALT6 then produces LacCer by the addition of galactose from UDP-Gal. Glycosyltransferases in the luminal leaflet of the Golgi then catalyzes the addition of additional sugars one by one to form other GSLs and gangliosides. Once extended they can be transported to the plasma membrane by exocytotic membrane flow (Daniotti & Iglesias-Bartolomé, 2011; Lannert, Gorgas, Meißner, Wieland, & Jeckel, 1998). The additional modifications to GSLs can be altered based on changes in substrate or enzyme activity leading to changes in the function of the GSLs (D'Angelo, Capasso, Sticco, & Russo, 2013). It has been shown that the amount of glycosylation varies depending on the glycosyltransferases and donor nucleotide sugars available in the certain tissue or cell type. The donor nucleotide sugars are further regulated by synthetic enzymes in the cytoplasm or nucleus and the nucleotide sugar transporters in the Golgi membrane (Varki et al., 2015). However, with all of this in mind all GSLs will begin with the same starting material lactosylceramide (LacCer). Once a certain pathway of modification has begun, the GSL is committed to that pathway (**Figure 1.1**). One of the most abundant types of GSLs in the brain are gangliosides. Gangliosides contain the ganglio-series backbone and are sialylated. To produce gangliosides, GM3 must be enzymatically produced by GM3 Synthase (ST3Gal5) from the starting material of LacCer. GM3 is the simplest ganglioside that can be further extended to fulfill the remaining possible ganglioside structures in the a-, b-, and c- series (Yu, Tsai, Ariga, & Yanagisawa, 2011). These derived gangliosides contain a ceramide, oligosaccharide, and at least one sialic acid (Palmano, Rowan, Guillermo, Guan, & McJarrow, 2015). Globo and neolacto- series GSLs are two pathways that differ from

gangliosides. They use the same starting material, LacCer, but are neutral or non-sialylated (Varki et al., 2015).

Glycosphingolipids Function

GSLs are the predominate glycosylated lipid in higher organisms compromising over 80% of the glycoconjugates found in the vertebrate brain (Ronald L. Schnaar, 2016; Varki et al., 2015). The increased presence of complex gangliosides such as GM1, GD1a, GD1b, and GT1b are crucial for driving neural differentiation (Russo et al., 2018), neuronal development and brain function (Palmano et al., 2015). They make up 97% of gangliosides in the brain highlighting their overall importance (R. L. Schnaar, Gerardy-Schahn, & Hildebrandt, 2014; Tettamanti, Bonali, Marchesini, & Zambotti, 1973). One reason as to why gangliosides are so crucial for brain function is because they terminate with sialic acid. Gangliosides account for roughly 75% of the sialic acid content in the brain (R. L. Schnaar et al., 2014). Sialic acid is predominately found on the cell surface and acts as receptors for binding proteins. These interactions have been shown to affect inflammatory responses, viral transmission, synaptic plasticity, i.e. (R. L. Schnaar et al., 2014).

GSLs and gangliosides are located primarily on the cell surface where they are found in micro-domains known as lipid rafts (Pike, 2009). Lipid rafts are in the plasma membrane, and laterally partition the membrane through the physiochemical properties of their components (Almeida, 2009). Lipid rafts have been shown to have additional components such as cholesterol, glycosylphosphatidylinositol-anchored proteins (GPI-anchored proteins) and signaling proteins (Brown & Rose, 1992; Schnitzer, McIntosh, Dvorak, Liu, & Oh, 1995; van Meer, Voelker, & Feigenson, 2008). Having these

different domains allows for the domains to indirectly modulate cell signaling by bringing certain molecules in range of each other to interact (Simons & Ikonen, 1997). Gangliosides are also able to modulate cell signaling, specifically neural cell signaling through the carbohydrate- protein or carbohydrate-carbohydrate interactions (Bremer, Hakomori, Bowen-Pope, Raines, & Ross, 1984; Bremer, Schlessinger, & Hakomori, 1986; Kawashima, Yoon, Itoh, & Nakayama, 2009)

O-linked- β- N-Acetylglucosamine (O-GlcNAc) Biosynthesis

O-linked β-N-acetylglucosamine (O-GlcNAc) is a PTM that modifies serine or threonine hydroxyl moieties on nuclear, cytoplasmic, and mitochondrial proteins (Hart, 1997). The addition of O-GlcNAc is very different than other PTMs. Its placement on proteins is solely regulated by two enzymes: O-GlcNAc transferase (OGT) and O-GlcNAcase (OGA) (Hart, 1997). OGT uses uridine diphosphate-N-acetylglucosamine (UDP-GlcNAc) as a donor substrate to modify proteins with the GlcNAc moiety. UDP-GlcNAc is formed through the Hexosamine Biosynthetic Pathway (HBP) (**Figure 1.2**). The HBP begins with the phosphorylation of glucose to produce glucose-6-phoshphate. Glucose-6-phosphate is then converted into fructose-6-phosphate by phosphoglucose isomerase (GPI). Fructose-6-phosphate then goes on to become glucosamine-6-phosphate (GlcN-6P) and glutamate (Glu) by fructose-6-phosphate transaminase (GFAT). GFAT is the first-rate limiting enzyme of HBP (Chiaradonna, Ricciardiello, & Palorini, 2018). GlcN-6P can then be converted into N-acetylglucosamine-6-phosphate (GlcNAc-6P) by glucosamine-phosphate N-acetyltransferase (GNPNAT) using acetyl-Coenzyme A (Ac-CoA) as acetyl group donor. GlcNAc-6P undergoes isomerization to form GlcNAc-1P with the help of GlcNAc phosphomutase (PGM3/AGM1). Then the final UDP-GlcNAc

substrate is produced from UTP and GlcNAc-1P by UDP-N-acetylglucosamine pyrophosphorylase (UAP1) (Hart, 1997). In addition to a different biosynthesis pathway compared to other PTMs, the modification does not get extended and stays as a monosaccharide (Mannino & Hart, 2022).

O-linked- β- N-Acetylglucosamine Function in Cell Signaling

Cell signaling which was once thought to be an "on" and "off" switch is now known to be much more complicated (Comer & Hart, 2000; Mannino & Hart, 2022). It has been shown that the presence of O-GlcNAc and amount of protein O-GlcNAcylation can affect signaling, stress responses, energy metabolism, development, and cell death (Hart & Akimoto, 2009; Mannino & Hart, 2022). To illustrate how necessary O-GlcNAcylation is for proper development and functioning, previous studies completed in OGT and OGA knockout mice were embryonic lethal (Keembiyehetty et al., 2015; Shafi et al., 2000). Many years of research has been carried out to further understand the effect of O-GlcNAcylation on specific proteins. Due to this modification being very transient different amounts of O-GlcNAcylation and O-GlcNAcylation on different sites changes rapidly and these changes can have drastic responses. One of the most notable responses of proteins being modified with O-GlcNAcylation is translocation. Since O-GlcNAcylation occurs mainly on nucleocytoplasmic proteins it often modifies transcription factors. The addition of a O-GlcNAc moiety can cause the transcription factor to translocate to the nucleus. This change in localization allows for increased transcription (Andrali, Qian, & Ozcan, 2007). However, with a protein like β-catenin it can also block gene transcription by changing the localization of it to the plasma membrane (Ha et al., 2014).

As stated previously the production of O-GlcNAc by OGT is based on the availability of UDP-GlcNAc (Kreppel & Hart, 1999; Marshall, Bacote, & Traxinger, 1991; Marshall, Nadeau, & Yamasaki, 2004; Zachara & Hart, 2004). UDP- GlcNAc is produced from the substrate glucose through different enzymatic reactions known as the HBP. The amount of glucose in the blood (hyperglycemia or hypoglycemia conditions) available for the HBP has been linked to different downstream changes in enzyme activity. Specifically changes in O-GlcNAcylation can inhibit or activate enzymes involved in phosphorylation. Under certain circumstances it can initiate pro-survival signaling by aiding in protein folding and cellular homeostasis (Zachara et al., 2004).

Cellular Stress Responses

In addition to changes in nutrient availability there are a variety of different stressors that the cell can experience. Each different stress can elicit different stress responses. A compartment that will be highlighted in this thesis is the endoplasmic reticulum (ER). The ER is the initial compartment in the secretory pathway and is responsible for the production and proper folding of nascent proteins (Almanza et al., 2019; Z. Sun & Brodsky, 2019). Once peptides are synthesized they are co-translationally modified in the ER lumen with the addition of $Glc_3Man_9GlcNAc_2$ (lipid-linked oligosaccharide (LLO) intermediate) to Asn- X- Ser/Thr sequons (Hoseki, Ushioda, & Nagata, 2009). This is completed by oligosaccharyltransferase (OST), an ER membrane protein (Spiro, 2004). Once co-translationally modified, the ER has multiple quality control mechanisms and chaperones to help neutralize protein misfolding and maintain protein homeostasis to avoid cell death (Z. Sun & Brodsky, 2019). Nutrient deprivation, hypoxia, and viruses can all cause ER stress as well an accumulation of misfolded

proteins within the ER lumen (Wodrich, Scott, Shukla, Harris, & Giniger, 2022). Many of these mechanisms have been shown to be regulated by the unfolded protein response (UPR) which is the primary signaling pathway activated by ER stress (Grandjean et al., 2020). The UPR consists of three transmembrane proteins inositol-requiring enzyme (IRE1α), protein kinase RNA-like endoplasmic reticulum kinase (PERK) and activating transcription factor 6 (ATF6) (**Figure 1.3**) (Wodrich et al., 2022). The UPR initially acts with IRE1α and ATF6 which acts as a pro-survival pathway to increase transcription and reduce protein-folding burden on the ER. IRE1α initiates the splicing of X-box binding protein (XBP1) causing its activation (Yoshida, Matsui, Yamamoto, Okada, & Mori, 2001). This activation causes XBP1 to translocate to the nucleus to increase transcription of a wide variety of genes involved in protein trafficking, folding, and degradation (Acosta-Alvear et al., 2007; Lee, Iwakoshi, & Glimcher, 2003). The other branch of the UPR is controlled by PERK, which once activated stops the influx of newly synthesized proteins into the ER by inhibiting translation. PERK does this by phosphorylating eukaryotic initiation factor 2α (eIF2α) (Harding, Zhang, & Ron, 1999). However, a few proteins can still be translated such as activating transcription 4 (ATF4) which will promote cell death when the ER has been stressed for a prolonged amount of time (Lu, Harding, & Ron, 2004).

Recessive GM3 Synthase Deficiency

GM3 Synthase Deficiency (GM3SD) is a rare disorder that is caused by a loss of ST3Gal5 which is one of the initial enzymes in the GSL biosynthesis pathway and is required to make gangliosides (a-, b-, c- series). *ST3GAL5* encodes for the protein GM3 Synthase (ST3 beta- galactoside alpha-2,3-sialyltransferase 5; *ST3GAL5*). Individuals

with this mutation have been identified in three allelic combinations in several different cohorts around the word (Gordon-Lipkin et al., 2018). For the sake of this thesis, we focused our work on two of the initial cohorts found. These two cohorts illustrated seizure activity and skin pigmentation changes giving reason for their names of Amish Infantile Epilepsy Syndrome and Salt and Pepper Syndrome. In addition to the seizure activity and skin pigmentation individuals were also showing cognitive, psychomotor, speech and hearing impairments as well as growth impairments (Gordon-Lipkin et al., 2018).

Amish Infantile Epilepsy Syndrome has become the most predominant form of GM3SD. The variant c.862C > T, is caused by a specific p.Arg288X mutation which lies between the L-sialylmotif and S-sialylmotif found in the luminal catalytic domain of ST3Gal5 (Boccuto et al., 2014). With this mutation, ST3Gal5 is truncated after the L-sialylmotif, or L-motif disrupting proper enzymatic activity. This major consequence is due to the S-motif role in the binding of the donor nucleotide sugar and Lactosylceramide, the acceptor. Whereas the L-motif is necessary for binding of the donor sugar nucleotide, CMP-NeuAc (Audry et al., 2011; A. K. Datta & Paulson, 1995; Arun K. Datta, Sinha, & Paulson, 1998). Individuals diagnosed with the p.Arg288X mutation displayed many of the same symptoms as other variants such as seizures, hyperpigmented skin, developmental delay, lack of proper hearing and sight gastrointestinal issues, and involuntary movements (Bowser et al., 2019; Wang, Bright, Xin, Bockoven, & Paller, 2013). Further research completed by Bowser et al. delved into the mechanistic changes that were occurring. The researchers show that they did not detect GM3, GD3, and any further derived gangliosides by mass spectrometry.

Additionally, they saw an accumulation of LacCer, o-series, and neutral GSLs (Bowser et al., 2019) confirming the disruption of ST3Gal5s' enzymatic activity.

Salt and Pepper Syndrome received its name after the diagnoses of one of the first cases of GM3 Synthase Deficiency. This case contained three siblings all displaying hyper- and hypo- pigmented skin thus giving its name of Salt and Pepper Syndrome. These children also exhibited the classic symptoms of developmental delay, intellectual disability, cranio-facial features, and seizures (Boccuto et al., 2014). Completing whole-exome sequencing a point mutation p.E355K was found in the S-sialyl motif (Boccuto et al., 2014). Once again completing mass spectrometry analysis there was an accumulation of LacCer and other globosides compared to the wildtype (Boccuto et al., 2014). Thus, this point mutation was also shown to inhibit the enzymatic activity of ST3Gal5.

As mentioned previously, gangliosides have been shown to be very crucial in cell signaling and function. Neurons are responsible for relaying the information from the external and internal environment. Myelin helps ensure that nerves can send these signals through the form of action potentials through axons. GD1a and GT1b are derived from LacCer and are the most abundant gangliosides in axonal membranes (Cawley, Jordan, & Wittenberg, 2021; De Vries & Zmachinski, 1980; Russo et al., 2018; Tettamanti et al., 1973). They interact with myelin-associated glycoprotein (MAG), also known as siglec-4. MAG is extremely crucial due to its role in myelination (Cawley et al., 2021). When GM3 Synthase is not present it has been shown in mice that the o-series gangliosides, which are not reliant on ST3Gal5 can bind to MAG with high affinity (Collins et al., 1999). This shows a great compensatory mechanism to maintain proper myelination of axons to ensure proper signaling through action potentials and release of

neurotransmitters. Neurotransmitters are released from synaptic vesicles at the pre-synaptic nerve terminal and transmit across the synaptic cleft to a receptor on the post-synaptic terminal of another nerve (Südhof, 2013). A- and b- series gangliosides which are derived from GM3 have been shown to heavily interact with neurotransmitters and their receptors. AMPA receptors are the main type of excitatory glutamate receptors in the brain. These receptor's efficiency in promoting synaptic transmission is completely dependent on their recruitment and placement at postsynaptic sites (Buonarati, Hammes, Watson, Greger, & Hell, 2019). A previous study analyzing the binding of GSLs, GT1b and GM1, to GluR2 – containing AMPA receptors reported that hippocampal neurons treated with a sialidase treatment, which removes sialic acid, changed the localization of GluR2 – containing AMPA receptors on the cell surface (Prendergast et al., 2014). This change in receptor localization directly affects the activity of neurotransmitters and synaptic plasticity. This study highlights an example of how GTb1 and GM1 which are sialylated gangliosides are needed for proper excitatory signaling. Seeing these crucial roles in cell signaling and proper neuron function indicates the need to further study the lack of ST3Gal5 found with GM3SD variants (Boccuto et al., 2014; Bowser et al., 2019; Gordon-Lipkin et al., 2018).

GM3SD Disease Modeling

Due to the rare and extreme nature of GM3SD it has been previously studied using animal models. However, studies completed on mice did not depict the exact same phenotypical change as seen in humans. Another group completed a study in zebrafish where they compared the changes between wildtype and a knockdown st*3Gal5* model (Boccuto et al., 2014). With only the use of these models previously, it would be ideal to

study GM3SD in human neural tissue specifically tissue from the peripheral nervous system or the brain due to the symptoms associated with this disease. However, obtaining human neural tissue is very difficult in rare diseases such as GM3SD. Thus, using human induced pluripotent stem cells we have the capability to study this rare disease in a neural model to ideally study the phenotypic changes from the loss of ST3Gal5 enzymatic activity.

Alzheimer's Disease

Alzheimer's disease (AD) has become a major interest in research due to the increasingly large population affected and the unknown underlying cellular mechanisms (Chen et al., 2017). AD is the 6th leading cause of death in the US and is associated with neuron loss in multiple regions of the brain (Chi, Chang, & Sang, 2018). It has been specifically shown to cause poor cognitive function, dementia, irritability, and gastrointestinal problems ("2021 Alzheimer's disease facts and figures," 2021). There are two forms of AD: familial and sporadic. Individuals with familial AD inherit the disease in an autosomal dominant manner (Bird, 1993). Familial AD is normally first diagnosed when an individual starts experiencing symptoms prior to the age of 60-65. This earlier diagnosis is referred to as early onset Familial AD and less than 5% of individuals diagnosed with AD have early onset (Brickell et al., 2006). Individuals who start experiencing symptoms later in life are referred to as late onset familial AD. Both forms of familial AD can be screened for and diagnosed in individuals by looking at mutations in the deterministic genes amyloid precursor protein (APP), presenilin 1 (PSEN1), presenilin 2 (PSEN2), and APOE-e4 allele on chromosome 19 (Bird, 1993; Brickell et al., 2006). Sporadic AD received its name due to the fact it is not reliant on being

inherited. However, it has been shown to be influenced by the interactions between risk genes APOE-e4, TREM2 and environmental factors (Guerreiro, Brás, & Hardy, 2013; Sherrington et al., 1995). APOE is a cholesterol carrier important in the transport of lipids and injury repair in the brain. Genetic variation in the e4 allele of APOE has been shown to be strongly correlated with sporadic AD (Chartier-Harlin et al., 1994; C. C. Liu, Liu, Kanekiyo, Xu, & Bu, 2013). The pathophysiological characteristics seen with AD are amyloid-β (Aβ) plaques, neurofibrillary tangles (NFT), synaptic loss, and neural death (Chi et al., 2018).

Aβ plaques have been extensively studied over the years due to their presence around neurons and ability to cause an inflammatory response in individuals diagnosed with AD. One of the first mentions of Aβ plaques was published in Hardy, et al. 1992. They show that the production of Aβ that is seen with AD comes from changes in APP and the gamma-secretase complex. APP is initially cleaved by α- or β- secretase. Cleavage by α-secretase produces smaller monomers to then be further cleaved by gamma-secretase to produce non-amyloidogenic soluble fragments. Gamma-secretase consists of four subunits: nicastrin, PSEN1, PSEN2, and Anterior Pharynx Defective 1. However, if APP possess mutations, it is originally cleaved by β-secretase and then gamma-secretase producing a toxic Aβ peptide (Anderson, Chen, Kim, & Robakis, 1992; Hardy & Higgins, 1992). There are four main sizes that have been shown to be toxic Aβ(1-42), Aβ(1-28), Aβ(25-35), Aβ(17-42) (Peters, Bascuñán, Opazo, & Aguayo, 2016). Despite this wealth of information on Aβ pathogenesis associated with AD, researchers have not been able to define the mechanisms causing AD (X. Sun, Chen, & Wang, 2015). NFTs have also been studied greatly due to their effect on neurons. Tau proteins belong

to a family of microtubule-associated proteins (MAP) that are mainly expressed in neurons. Tau functions in assembly of tubulin monomers into microtubules to constitute the neuronal microtubules network (Evans et al., 2000; Iqbal, Liu, Gong, Alonso Adel, & Grundke-Iqbal, 2009). These microtubules are crucial for maintaining the cell shape and proper function of axons. The longest brain isoform of tau contains 79 Ser or Thr sites (Evans et al., 2000). Thus, in an environment with decreased O-GlcNAc tau can become hyperphosphorylated leading to its aggregation and formation of NFT. In AD it has been shown that it becomes hyperphosphorylated compared to the non-diseased state (F. Liu, Iqbal, Grundke-Iqbal, Hart, & Gong, 2004). This hyperphosphorylation has been shown to cause missorting and aggregation of tau forming NFTs. Similar to Aβ plaques there has been a strong presence of NFTs associated with AD pathogenesis. However, the true mechanistic cause and effect of AD has not been deciphered leading to a need for further studies to be completed.

Due to the lack of a mechanism being discovered for AD other than the correlation with plaque and NFT formation researchers have been interested in identifying other possible mechanisms. Some research has indicated that Aβ monomers and soluble phosphorylated-tau have a large neurotoxic role in the cell prior to plaque and NFT formation (Li & Selkoe, 2020). But in addition to looking at Aβ plaques and NFTs, studies completed using cell culture (J. H. Lin, Li, Zhang, Ron, & Walter, 2009) and post-mortem human brain(Buchanan et al., 2020; Li & Selkoe, 2020) have shown a strong correlation between AD pathogenesis and ER stress markers. Specifically, ER stress markers: PERK and IRE1α have been shown to be highly expressed in AD (Buchanan et al., 2020; Uddin et al., 2020). As stated previously the different ER stress

markers have different roles in UPR (McCarthy et al., 2020). When PERK inhibits protein translation it can possibly lead to declined synaptic plasticity and cognitive functioning having large implications with synapse loss and memory loss in AD (Buchanan et al., 2020). It has been previously shown that phospho-tau is correlated with increased PERK levels in the post-mortem human brain (Buchanan et al., 2020) leading us to question if these two components could be affecting synaptic transmission in AD. IRE1α has been shown to have a large role in the cell by promoting transcription and regulating ERAD. It does this by controlling the expression of the transcription factor XBP1 (Grandjean et al., 2020; Shoulders et al., 2013; Travers et al., 2000). The splicing of XBP1 has been shown to affect the production of UDP-GlcNAc via enzymes in the hexosamine biosynthetic pathway (Buchanan et al., 2020; van der Harg et al., 2017). Thus, it directly affects the amount of UDP-GlcNAc available to be used by OGT. Additionally, IRE1α modulation affects the amount of Aβ oligomers and astrocyte activation (Duran-Aniotz et al., 2017), which are all known components of AD pathogenesis.

Alzheimer's Disease Modeling

Previously a lot of research has been completed trying to further decipher the mechanisms and causes of AD. Once symptoms develop medical professionals can test the cerebral spinal fluid (CSF) for the levels of Aβ and phospho-tau. This procedure is quite intense as it requires a spinal tap in the patient. Gauging biomarkers in patients' blood proves to be a less invasive method, but this method is not always reliable. Other in office methods have also been tested, but no method has shown to have great clinical relevance and reliability. Animal models and post-mortem brain tissue has also been

studied to try to find mechanistic answers, but these results are not always accurate compared to what is occurring in a living human. Thus, there is a great need for better diagnostic criteria and research models to obtain better understanding of the mechanism and biomarkers responsible.

The Peripheral Nervous System

Many neurological diseases focus primarily on the impacts of the disease in the central nervous system (CNS). However, the peripheral nervous system (PNS) is very crucial. It supplies the CNS with information about the external environment and the internal environment of the body. It has two divisions: the somatic and autonomic division. The somatic division includes the sensory neurons that receive information from the skin, muscles, and joints. The autonomic division of the PNS mediates the stomach, intestine, bladder, heart, lungs, and vasculature. It consists of the sympathetic, parasympathetic, and enteric systems. The sympathetic system participates in the body's response to stress and the parasympathetic system acts to conserve body resources and maintain homeostasis. Lastly, the enteric controls the smooth muscle cells of the gut and remaining functions of the PNS (Waxenbaum, Reddy, & Varacallo, 2022). For both chapters of this thesis, we show protein O-GlcNAcylation as a pro-survival mechanism. As stated, protein O-GlcNAcylation is directly reliant on the amount of available glucose to be used by the HBP. The secretory, parasympathetic, and sensory fibers of the PNS regulate the release of glucose from peripheral metabolic tissues and cells (E. E. Lin, Scott-Solomon, & Kuruvilla, 2021). Thus, studying the upstream signal integrators of the PNS in different neurological diseases may prove to be very insightful especially because they have not been studied extensively in the diseases of this thesis.

Human induced Pluripotent Stem Cells and Neural Crest Cells

As stated in the above sections previous research has used animal models or if suitable patient fibroblasts, plasma, or brain tissue to study these different neurological diseases. These models are not always ideal for studying mechanistic changes. For instance, using postmortem human brain tissue which in theory sounds the most reliable can display new challenges such as it is harder to obtain, and it may not be displaying the same characteristics as brain tissue prior to being deceased. Additionally, these models cannot always define cell-type specific mechanistic changes in these diseases that might affect functioning. Many diseases display cell-type specific responses to changes in stress and glycosylation which is crucial to study to try to propose mechanistic interventions. Thus, using human induced pluripotent stem cells (iPSC) we have the capability of differentiating to different neural cell types to study different neurological diseases. iPSC were generated by reprogramming adult somatic cells with four key transcription factors: Oct4, Soc2, Klf4, and c-Myc. These iPSC can then be differentiated to all three germ layers and have the capability to self-renew (Takahashi & Yamanaka, 2006). This allows for studies to be designed ideally looking at the cellular properties of the disease and contexts. We have the capability of perturbing the cells in different ways and testing different treatments to fully discover a mechanism using the patients' cells and specific genetic material.

For these studies highlighted in Chapter 2 and Chapter 3 of this work we will focus on the differentiation to Neural Crest Cells (NCC). NCC are formed at the dorsal most portion of the neural tube during primary neurulation (**Figure 1.4**). These cells then migrate along well-described routes to give rise to the peripheral nervous system such as

peripheral neurons, glia, pigment cells, i.e., (Crane & Trainor, 2006; Gilbert, 2000; Moury & Jacobson, 1990; Rollhäuser-ter Horst, 1977). We decided to differentiate to NCCs due to multiple of our GM3SD patients showing phenotypes consistent with problems in the peripheral nervous system such as cranio-facial defects, skin pigmentation, and enteric innervation defects (Bowser et al., 2019). Contrary to our work on GM3SD variants, AD has not been extensively studied in the PNS. Thus, in the third chapter outlining our studies on AD we wanted to see if there were any molecular changes detected in neural crest cells that are progenitors to the PNS.

Using a protocol adapted from Menendez, et al. NCCs are generated from adding in small molecular inhibitors to iPSC (**Figure 1.4**) (Menendez et al., 2013). It has been shown that during this induction to NCC, BMP and Wnt signaling are crucial to promote an epithelial-to-mesenchymal transition in neuroepithelial cells. This transition consists of a downregulation of E-cadherin adhesion molecules, promotes delamination, and all NCCs to migrate (Ahlstrom & Erickson, 2009). Additionally, during gastrulation, Notch and FGF signaling have also been shown to have an impact on NCC patterning and migration. Many of these initial studies highlighting these molecules were completed in frog, fish, chick, and mouse. Mutating BMP signaling was the only molecule shown to completely inhibit the formation of NCC highlighting the importance of BMP signaling in this transition and process. The cross talk between BMP, Notch, FGF, and Wnt pathways elicits the different migratory pathways of NCCs (Crane & Trainor, 2006; Kulesa & Gammill, 2010). Once completing the epithelial-mesenchymal transition, NCC are divided into different populations along the anterior-posterior axis based on the region: cranial, cardiac, vegal, and trunk. Cranial NCC will differentiate into cartilage

and bone, pigment cells, connective tissue, and sensory/parasympathetic ganglia. Cardiac NCC will terminate as smooth muscle and parasympathetic cardiac ganglia (Kirby, Gale, & Stewart, 1983). Once differentiated vegal Cells become many neuronal cells and glia that make up the enteric nervous system (Yntema & Hammond, 1954). Lastly, the trunk NCC differentiate to neurons of the PNS, sympatho-adrenal cells, and pigment cells in the skin (**Figure 1.4A**) (Burns & Le Douarin, 1998). Following this differentiation process allows for analysis throughout a differentiation as the cells are molecularly changing and developing. This can potentially highlight stress points or key things that are required for differentiating that might not be present in a diseased state. However, there are limitations to completing these experiments using iPSC and the differentiated populations. Specifically, it should be noted that these cells are cultivated in a dish meaning that they may lack environmental exposures and cues. Also, analyzing cell migration and tissue formation are not as always depicted in this model system. With all of this in mind, iPSC and their ability to differentiate into different lineages makes it a very valuable tool for researching human diseases.

Purpose of Study

This dissertation features data on the mechanistic cell signaling changes associated with different neurological diseases using patient-derived induced pluripotent stem cells and derived neural crest cells. Post translational modifications impact different proteins and biological functions (Varki & Kornfeld, 2022). Thus, analyzing these changes in neural cells derived from fibroblasts of these neurological diseases presents new data illustrating cellular changes. Firstly, our previous paper on GM3SD and our current paper in this dissertation is some of the first work defining molecular changes in neural cell types of

GM3SD variants. Using two of the previously defined GM3SD variants we characterized the GSL profile in iPSCs and NCCs. Due to the established role of GSLs in cell signaling, we then looked at cell signaling changes throughout the differentiation to NCCs in our variants to wild type. Chapter two presents a submitted thesis of which I am a co-first author. My experimental contribution to this work was the investigation of O-GlcNAcylation, downstream effects of O-GlcNAcylation, and the impact of modifying O-GlcNAcylation for cell signaling. This work completed shows increased O-GlcNAcylation as a pro-survival mechanism to be further tested for treatments. The remainder of the manuscript presented in chapter two is provided for context and background. Secondly, the third chapter of this dissertation lays the grown work of looking at AD in the neural cell types of the peripheral nervous system which has not been extensively studied at the time of writing this thesis. Using NCC differentiations again we see that after achieving AD NCCs they exhibit significant changes in cellular stress associated with reduced protein O-GlcNAcylation. These results were not accompanied by increased cleaved caspase3 levels indicative of cell death. Thus, we speculate that the PNS in AD may possess compensatory mechanism to alleviate any burden from reduced O-GlcNAcylation.

TABLES AND FIGURES

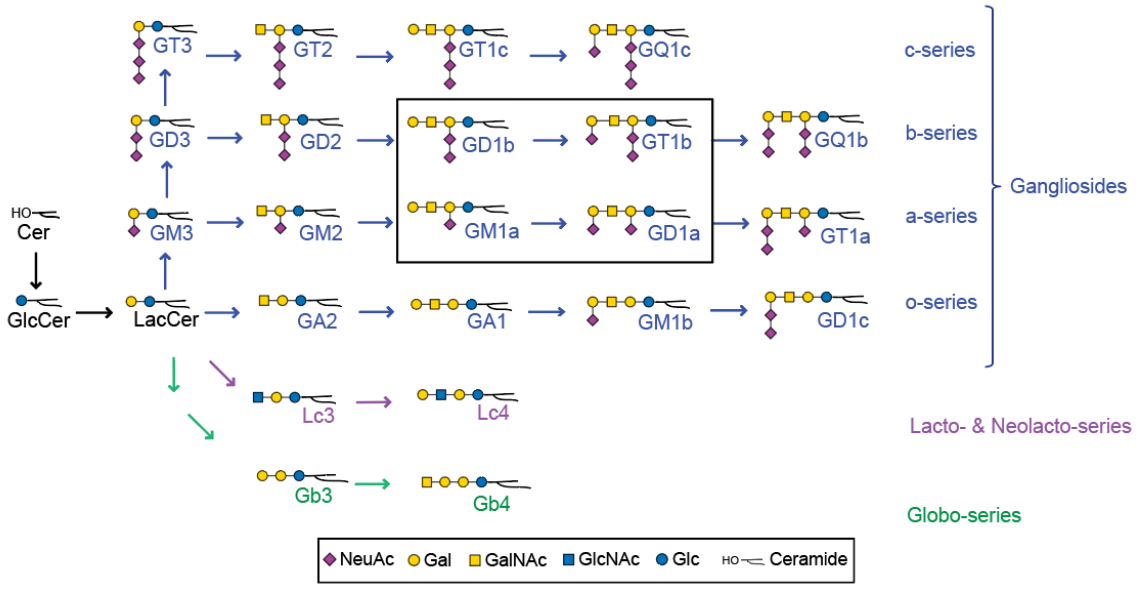

Figure 1.1 Pathways of human glycosphingolipid biosynthesis. Ceramide (Cer) is glucosylated to form glucosylceramide (GlcCer), which is elongated with a galactose to form lactosylceramide (LacCer). LacCer is the precursor for glycosphingolipid (GSL) elongation into multiple biosynthetic pathways, including the globo-, lacto/neolacto-, and ganglio-series. Sialylation of the Gal residue of LacCer by ST3GAL5 (GM3 Synthase) generates the simplest ganglio-series GSL, known as GM3. Graphic representations of GSL monosaccharide residues are consistent with Symbol Nomenclature for Glycans guidelines (SNFG).

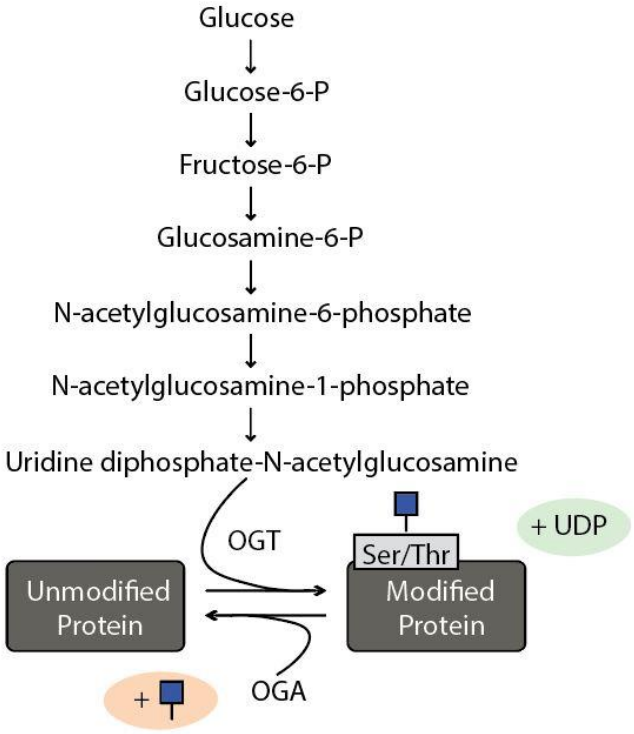

Figure 1.2. Synthesis of UDP-GlcNAc and subsequent donation of GlcNAc to Unmodified Protein. The Hexosamine Biosynthetic Pathway (HBP) generates Uridine diphosphate-N-acetylglucosamine (UDP-GlcNAc) from glucose. UDP-GlcNAc is used by O-GlcNAc Transferase (OGT) as a donor substrate to add GlcNAc to the side chain of Ser/Thr residues on proteins. O-GlcNAcase (OGA) removes the GlcNAc from proteins returning the protein to its unmodified state.

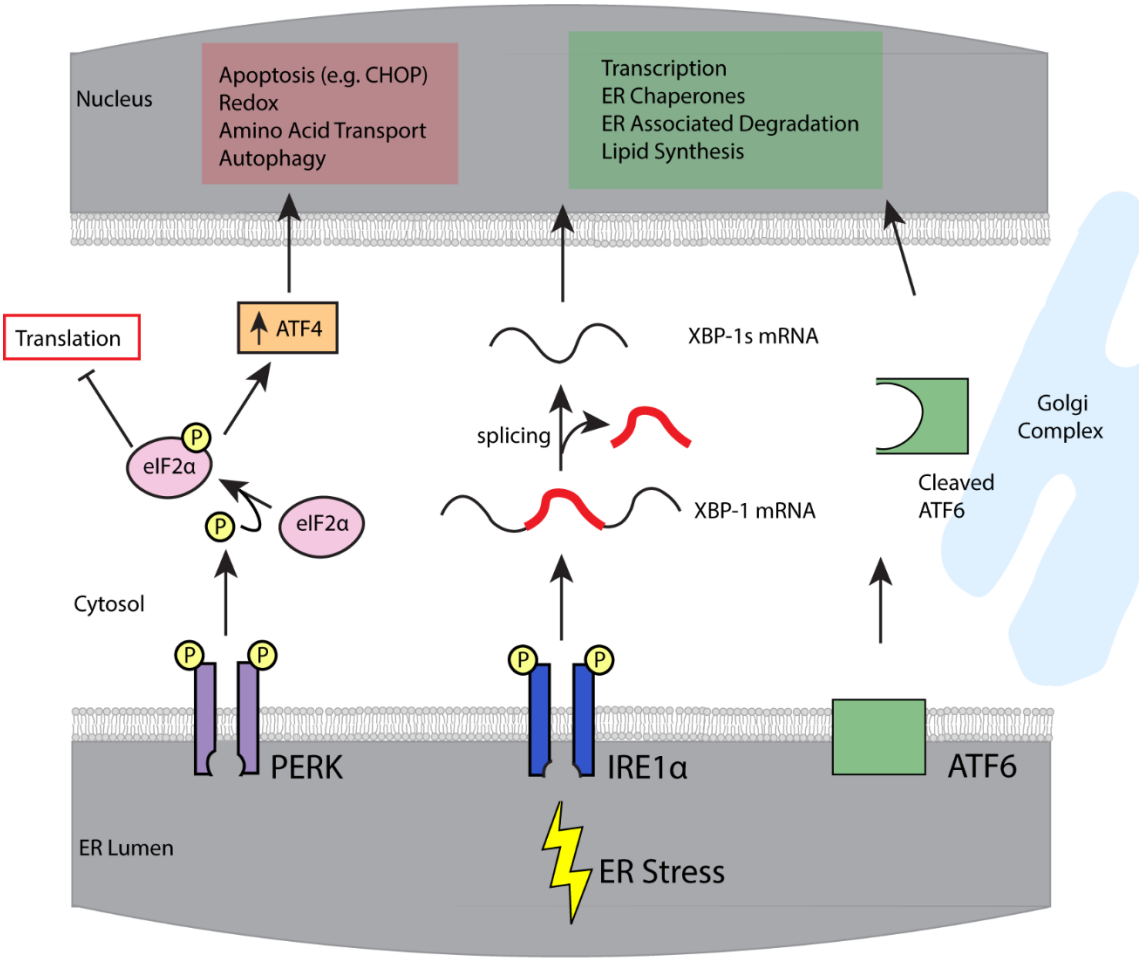

Figure 1.3. Overview of The Unfolded Protein Response in the ER. The unfolded protein response (UPR) acts as a key cell signaling regulator when the endoplasmic reticulum (ER) becomes stressed. The UPR consists of three membrane receptors IRE1α, ATF6, and PERK which all effect the cell in different ways.

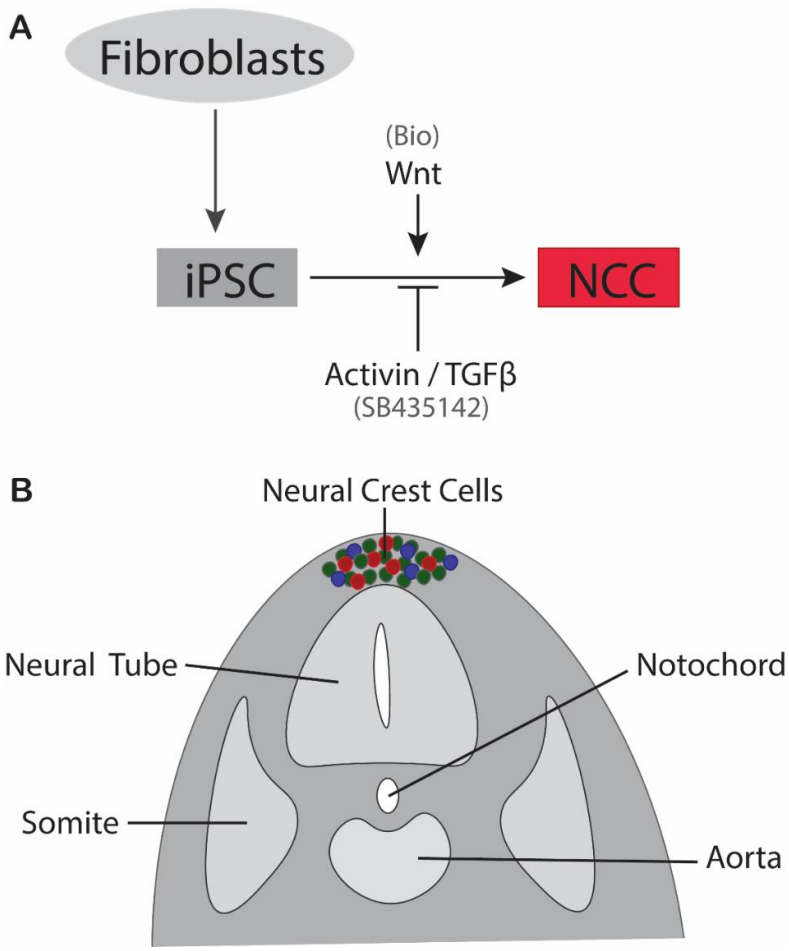

Figure 1.4 Neural Crest Cell Differentiation and Migration. (A) Schematic diagram of induction and differentiation to neural crest cells (NCC). NCC are achieved by dual SMAD inhibition using small molecules SB435142 and Bio. The cells should not express pluripotency markers (SOX2, Oct3/4, SSEA.4) and display NCC markers (AP2, HNK1, and p75) by day 15 of the differentiation. (B) NCC are formed at the dorsal most portion of the neural tube. Where they can then migrate to form neurons of the peripheral nervous system.

REFERENCES

2021 Alzheimer's disease facts and figures. (2021). *Alzheimers Dement, 17*(3), 327-406. doi:10.1002/alz.12328

Acosta-Alvear, D., Zhou, Y., Blais, A., Tsikitis, M., Lents, N. H., Arias, C., . . . Dynlacht, B. D. (2007). XBP1 controls diverse cell type- and condition-specific transcriptional regulatory networks. *Mol Cell, 27*(1), 53-66. doi:10.1016/j.molcel.2007.06.011

Ahlstrom, J. D., & Erickson, C. A. (2009). The neural crest epithelial-mesenchymal transition in 4D: a `tail' of multiple non-obligatory cellular mechanisms. *Development, 136*(11), 1801-1812. doi:10.1242/dev.034785

Almanza, A., Carlesso, A., Chintha, C., Creedican, S., Doultsinos, D., Leuzzi, B., . . . Samali, A. (2019). Endoplasmic reticulum stress signalling - from basic mechanisms to clinical applications. *Febs j, 286*(2), 241-278. doi:10.1111/febs.14608

Almeida, P. F. F. (2009). Thermodynamics of lipid interactions in complex bilayers. *Biochimica et Biophysica Acta (BBA) - Biomembranes, 1788*(1), 72-85. doi:https://doi.org/10.1016/j.bbamem.2008.08.007

Anderson, J. P., Chen, Y., Kim, K. S., & Robakis, N. K. (1992). An alternative secretase cleavage produces soluble Alzheimer amyloid precursor protein containing a potentially amyloidogenic sequence. *J Neurochem, 59*(6), 2328-2331. doi:10.1111/j.1471-4159.1992.tb10128.x

Andrali, S. S., Qian, Q., & Ozcan, S. (2007). Glucose mediates the translocation of NeuroD1 by O-linked glycosylation. *J Biol Chem, 282*(21), 15589-15596. doi:10.1074/jbc.M701762200

Audry, M., Jeanneau, C., Imberty, A., Harduin-Lepers, A., Delannoy, P., & Breton, C. (2011). Current trends in the structure-activity relationships of sialyltransferases. *Glycobiology, 21*(6), 716-726. doi:10.1093/glycob/cwq189

Bird, T. D. (1993). Alzheimer Disease Overview. In M. P. Adam, H. H. Ardinger, R. A. Pagon, S. E. Wallace, L. J. H. Bean, K. W. Gripp, G. M. Mirzaa, & A. Amemiya (Eds.), *GeneReviews((R))*. Seattle (WA).

Boccuto, L., Aoki, K., Flanagan-Steet, H., Chen, C. F., Fan, X., Bartel, F., . . . Schwartz, C. E. (2014). A mutation in a ganglioside biosynthetic enzyme, ST3GAL5, results in salt & pepper syndrome, a neurocutaneous disorder with altered glycolipid and glycoprotein glycosylation. *Hum Mol Genet, 23*(2), 418-433. doi:10.1093/hmg/ddt434

Bowser, L. E., Young, M., Wenger, O. K., Ammous, Z., Brigatti, K. W., Carson, V. J., . . . Strauss, K. A. (2019). Recessive GM3 synthase deficiency: Natural history, biochemistry, and therapeutic frontier. *Mol Genet Metab, 126*(4), 475-488. doi:10.1016/j.ymgme.2019.01.013

Bremer, E. G., Hakomori, S., Bowen-Pope, D. F., Raines, E., & Ross, R. (1984). Ganglioside-mediated modulation of cell growth, growth factor binding, and receptor phosphorylation. *J Biol Chem, 259*(11), 6818-6825.

Bremer, E. G., Schlessinger, J., & Hakomori, S. (1986). Ganglioside-mediated modulation of cell growth. Specific effects of GM3 on tyrosine phosphorylation of the epidermal growth factor receptor. *J Biol Chem, 261*(5), 2434-2440.

Brickell, K. L., Steinbart, E. J., Rumbaugh, M., Payami, H., Schellenberg, G. D., Van Deerlin, V., . . . Bird, T. D. (2006). Early-onset Alzheimer disease in families with late-onset Alzheimer disease: a potential important subtype of familial Alzheimer disease. *Arch Neurol, 63*(9), 1307-1311. doi:10.1001/archneur.63.9.1307

Brown, D. A., & Rose, J. K. (1992). Sorting of GPI-anchored proteins to glycolipid-enriched membrane subdomains during transport to the apical cell surface. *Cell, 68*(3), 533-544. doi:10.1016/0092-8674(92)90189-j

Buchanan, H., Mackay, M., Palmer, K., Tothová, K., Katsur, M., Platt, B., & Koss, D. J. (2020). Synaptic Loss, ER Stress and Neuro-Inflammation Emerge Late in the Lateral Temporal Cortex and Associate with Progressive Tau Pathology in Alzheimer's Disease. *Mol Neurobiol, 57*(8), 3258-3272. doi:10.1007/s12035-020-01950-1

Buonarati, O. R., Hammes, E. A., Watson, J. F., Greger, I. H., & Hell, J. W. (2019). Mechanisms of postsynaptic localization of AMPA-type glutamate receptors and their regulation during long-term potentiation. *Sci Signal, 12*(562). doi:10.1126/scisignal.aar6889

Burns, A. J., & Le Douarin, N. M. (1998). The sacral neural crest contributes neurons and glia to the post-umbilical gut: spatiotemporal analysis of the development of the enteric nervous system. *Development, 125*(21), 4335-4347. doi:10.1242/dev.125.21.4335

Cawley, J. L., Jordan, L. R., & Wittenberg, N. J. (2021). Detection and Characterization of Vesicular Gangliosides Binding to Myelin-Associated Glycoprotein on Supported Lipid Bilayers. *Anal Chem, 93*(2), 1185-1192. doi:10.1021/acs.analchem.0c04412

Chartier-Harlin, M. C., Parfitt, M., Legrain, S., Pérez-Tur, J., Brousseau, T., Evans, A., . . . et al. (1994). Apolipoprotein E, epsilon 4 allele as a major risk factor for sporadic early and late-onset forms of Alzheimer's disease: analysis of the 19q13.2 chromosomal region. *Hum Mol Genet, 3*(4), 569-574. doi:10.1093/hmg/3.4.569

Chen, X., Bisschops, M. M. M., Agarwal, N. R., Ji, B., Shanmugavel, K. P., & Petranovic, D. (2017). Interplay of Energetics and ER Stress Exacerbates Alzheimer's Amyloid-β (Aβ) Toxicity in Yeast. *Front Mol Neurosci, 10*, 232. doi:10.3389/fnmol.2017.00232

Chi, H., Chang, H. Y., & Sang, T. K. (2018). Neuronal Cell Death Mechanisms in Major Neurodegenerative Diseases. *Int J Mol Sci, 19*(10). doi:10.3390/ijms19103082

Chiaradonna, F., Ricciardiello, F., & Palorini, R. (2018). The Nutrient-Sensing Hexosamine Biosynthetic Pathway as the Hub of Cancer Metabolic Rewiring. *Cells, 7*(6). doi:10.3390/cells7060053

Collins, B. E., Ito, H., Sawada, N., Ishida, H., Kiso, M., & Schnaar, R. L. (1999). Enhanced Binding of the Neural Siglecs, Myelin-associated Glycoprotein and Schwann Cell Myelin Protein, to Chol-1 (α-Series) Gangliosides and Novel Sulfated Chol-1 Analogs*. *Journal of Biological Chemistry, 274*(53), 37637-37643. doi:https://doi.org/10.1074/jbc.274.53.37637

Comer, F. I., & Hart, G. W. (2000). O-Glycosylation of nuclear and cytosolic proteins. Dynamic interplay between O-GlcNAc and O-phosphate. *J Biol Chem, 275*(38), 29179-29182. doi:10.1074/jbc.R000010200

Crane, J. F., & Trainor, P. A. (2006). Neural crest stem and progenitor cells. *Annu Rev Cell Dev Biol, 22*, 267-286. doi:10.1146/annurev.cellbio.22.010305.103814

D'Angelo, G., Capasso, S., Sticco, L., & Russo, D. (2013). Glycosphingolipids: synthesis and functions. *Febs j, 280*(24), 6338-6353. doi:10.1111/febs.12559

Daniotti, J. L., & Iglesias-Bartolomé, R. (2011). Metabolic pathways and intracellular trafficking of gangliosides. *IUBMB Life, 63*(7), 513-520. doi:10.1002/iub.477

Datta, A. K., & Paulson, J. C. (1995). The sialyltransferase "sialylmotif" participates in binding the donor substrate CMP-NeuAc. *J Biol Chem, 270*(4), 1497-1500. doi:10.1074/jbc.270.4.1497

Datta, A. K., Sinha, A., & Paulson, J. C. (1998). Mutation of the Sialyltransferase S-sialylmotif Alters the Kinetics of the Donor and Acceptor Substrates *. *Journal of Biological Chemistry, 273*(16), 9608-9614. doi:10.1074/jbc.273.16.9608

De Vries, G. H., & Zmachinski, C. J. (1980). The lipid composition of rat CNS axolemma-enriched fractions. *J Neurochem, 34*(2), 424-430. doi:10.1111/j.1471-4159.1980.tb06613.x

Duran-Aniotz, C., Cornejo, V. H., Espinoza, S., Ardiles Á, O., Medinas, D. B., Salazar, C., . . . Hetz, C. (2017). IRE1 signaling exacerbates Alzheimer's disease pathogenesis. *Acta Neuropathol, 134*(3), 489-506. doi:10.1007/s00401-017-1694-x

Evans, D. B., Rank, K. B., Bhattacharya, K., Thomsen, D. R., Gurney, M. E., & Sharma, S. K. (2000). Tau phosphorylation at serine 396 and serine 404 by human recombinant tau protein kinase II inhibits tau's ability to promote microtubule assembly. *J Biol Chem, 275*(32), 24977-24983. doi:10.1074/jbc.M000808200

Gault, C. R., Obeid, L. M., & Hannun, Y. A. (2010). An overview of sphingolipid metabolism: from synthesis to breakdown. *Adv Exp Med Biol, 688*, 1-23. doi:10.1007/978-1-4419-6741-1_1

Gilbert, S. (2000). *The Neural Crest* [6th edition]*Developmental Biology*.

Gordon-Lipkin, E., Cohen, J. S., Srivastava, S., Soares, B. P., Levey, E., & Fatemi, A. (2018). ST3GAL5-Related Disorders: A Deficiency in Ganglioside Metabolism and a Genetic Cause of Intellectual Disability and Choreoathetosis. *J Child Neurol, 33*(13), 825-831. doi:10.1177/0883073818791099

Grandjean, J. M. D., Madhavan, A., Cech, L., Seguinot, B. O., Paxman, R. J., Smith, E., . . . Wiseman, R. L. (2020). Pharmacologic IRE1/XBP1s activation confers targeted ER proteostasis reprogramming. *Nat Chem Biol, 16*(10), 1052-1061. doi:10.1038/s41589-020-0584-z

Guerreiro, R., Brás, J., & Hardy, J. (2013). SnapShot: genetics of Alzheimer's disease. *Cell, 155*(4), 968-968.e961. doi:10.1016/j.cell.2013.10.037

Ha, J. R., Hao, L., Venkateswaran, G., Huang, Y. H., Garcia, E., & Persad, S. (2014). β-catenin is O-GlcNAc glycosylated at Serine 23: implications for β-catenin's subcellular localization and transactivator function. *Exp Cell Res, 321*(2), 153-166. doi:10.1016/j.yexcr.2013.11.021

Harding, H. P., Zhang, Y., & Ron, D. (1999). Protein translation and folding are coupled by an endoplasmic-reticulum-resident kinase. *Nature, 397*(6716), 271-274. doi:10.1038/16729

Hardy, J. A., & Higgins, G. A. (1992). Alzheimer's disease: the amyloid cascade hypothesis. *Science, 256*(5054), 184-185. doi:10.1126/science.1566067

Hart, G. W. (1997). Dynamic O-linked glycosylation of nuclear and cytoskeletal proteins. *Annu Rev Biochem, 66*, 315-335. doi:10.1146/annurev.biochem.66.1.315

Hart, G. W., & Akimoto, Y. (2009). The O-GlcNAc Modification. In nd, A. Varki, R. D. Cummings, J. D. Esko, H. H. Freeze, P. Stanley, C. R. Bertozzi, G. W. Hart, & M. E. Etzler (Eds.), *Essentials of Glycobiology*. Cold Spring Harbor (NY).

Hoseki, J., Ushioda, R., & Nagata, K. (2009). Mechanism and components of endoplasmic reticulum-associated degradation. *The Journal of Biochemistry, 147*(1), 19-25. doi:10.1093/jb/mvp194

Iqbal, K., Liu, F., Gong, C. X., Alonso Adel, C., & Grundke-Iqbal, I. (2009). Mechanisms of tau-induced neurodegeneration. *Acta Neuropathol, 118*(1), 53-69. doi:10.1007/s00401-009-0486-3

Kawashima, N., Yoon, S. J., Itoh, K., & Nakayama, K. (2009). Tyrosine kinase activity of epidermal growth factor receptor is regulated by GM3 binding through carbohydrate to carbohydrate interactions. *J Biol Chem, 284*(10), 6147-6155. doi:10.1074/jbc.M808171200

Keembiyehetty, C., Love, D. C., Harwood, K. R., Gavrilova, O., Comly, M. E., & Hanover, J. A. (2015). Conditional knock-out reveals a requirement for O-linked N-Acetylglucosaminase (O-GlcNAcase) in metabolic homeostasis. *J Biol Chem, 290*(11), 7097-7113. doi:10.1074/jbc.M114.617779

Kirby, M. L., Gale, T. F., & Stewart, D. E. (1983). Neural crest cells contribute to normal aorticopulmonary septation. *Science, 220*(4601), 1059-1061. doi:10.1126/science.6844926

Kreppel, L. K., & Hart, G. W. (1999). Regulation of a cytosolic and nuclear O-GlcNAc transferase. Role of the tetratricopeptide repeats. *J Biol Chem, 274*(45), 32015-32022. doi:10.1074/jbc.274.45.32015

Kulesa, P. M., & Gammill, L. S. (2010). Neural crest migration: Patterns, phases and signals. *Developmental Biology, 344*(2), 566-568. doi:https://doi.org/10.1016/j.ydbio.2010.05.005

Lannert, H., Gorgas, K., Meißner, I., Wieland, F. T., & Jeckel, D. (1998). Functional Organization of the Golgi Apparatus in Glycosphingolipid Biosynthesis: LACTOSYLCERAMIDE AND SUBSEQUENT GLYCOSPHINGOLIPIDS ARE FORMED IN THE LUMEN OF THE LATE GOLGI*. *Journal of Biological Chemistry, 273*(5), 2939-2946. doi:https://doi.org/10.1074/jbc.273.5.2939

Lee, A. H., Iwakoshi, N. N., & Glimcher, L. H. (2003). XBP-1 regulates a subset of endoplasmic reticulum resident chaperone genes in the unfolded protein response. *Mol Cell Biol, 23*(21), 7448-7459. doi:10.1128/mcb.23.21.7448-7459.2003

Li, S., & Selkoe, D. J. (2020). A mechanistic hypothesis for the impairment of synaptic plasticity by soluble Aβ oligomers from Alzheimer's brain. *J Neurochem, 154*(6), 583-597. doi:10.1111/jnc.15007

Lin, E. E., Scott-Solomon, E., & Kuruvilla, R. (2021). Peripheral Innervation in the Regulation of Glucose Homeostasis. *Trends in Neurosciences, 44*(3), 189-202. doi:https://doi.org/10.1016/j.tins.2020.10.015

Lin, J. H., Li, H., Zhang, Y., Ron, D., & Walter, P. (2009). Divergent effects of PERK and IRE1 signaling on cell viability. *PLoS One, 4*(1), e4170. doi:10.1371/journal.pone.0004170

Liu, C. C., Liu, C. C., Kanekiyo, T., Xu, H., & Bu, G. (2013). Apolipoprotein E and Alzheimer disease: risk, mechanisms and therapy. *Nat Rev Neurol, 9*(2), 106-118. doi:10.1038/nrneurol.2012.263

Liu, F., Iqbal, K., Grundke-Iqbal, I., Hart, G. W., & Gong, C. X. (2004). O-GlcNAcylation regulates phosphorylation of tau: a mechanism involved in Alzheimer's disease. *Proc Natl Acad Sci U S A, 101*(29), 10804-10809. doi:10.1073/pnas.0400348101

Lu, P. D., Harding, H. P., & Ron, D. (2004). Translation reinitiation at alternative open reading frames regulates gene expression in an integrated stress response. *J Cell Biol, 167*(1), 27-33. doi:10.1083/jcb.200408003

Mannino, M. P., & Hart, G. W. (2022). The Beginner's Guide to O-GlcNAc: From Nutrient Sensitive Pathway Regulation to Its Impact on the Immune System. *Front Immunol, 13*, 828648. doi:10.3389/fimmu.2022.828648

Marshall, S., Bacote, V., & Traxinger, R. R. (1991). Discovery of a metabolic pathway mediating glucose-induced desensitization of the glucose transport system. Role of hexosamine biosynthesis in the induction of insulin resistance. *J Biol Chem, 266*(8), 4706-4712.

Marshall, S., Nadeau, O., & Yamasaki, K. (2004). Dynamic actions of glucose and glucosamine on hexosamine biosynthesis in isolated adipocytes: differential effects on glucosamine 6-phosphate, UDP-N-acetylglucosamine, and ATP levels. *J Biol Chem, 279*(34), 35313-35319. doi:10.1074/jbc.M404133200

McCarthy, N., Dolgikh, N., Logue, S., Patterson, J. B., Zeng, Q., Gorman, A. M., . . . Fulda, S. (2020). The IRE1 and PERK arms of the unfolded protein response promote survival of rhabdomyosarcoma cells. *Cancer Letters, 490*, 76-88. doi:https://doi.org/10.1016/j.canlet.2020.07.009

Menendez, L., Kulik, M. J., Page, A. T., Park, S. S., Lauderdale, J. D., Cunningham, M. L., & Dalton, S. (2013). Directed differentiation of human pluripotent cells to neural crest stem cells. *Nat Protoc, 8*(1), 203-212. doi:10.1038/nprot.2012.156

Moury, J. D., & Jacobson, A. G. (1990). The origins of neural crest cells in the axolotl. *Dev Biol, 141*(2), 243-253. doi:10.1016/0012-1606(90)90380-2

Palmano, K., Rowan, A., Guillermo, R., Guan, J., & McJarrow, P. (2015). The role of gangliosides in neurodevelopment. *Nutrients, 7*(5), 3891-3913. doi:10.3390/nu7053891

Peters, C., Bascuñán, D., Opazo, C., & Aguayo, L. G. (2016). Differential Membrane Toxicity of Amyloid-β Fragments by Pore Forming Mechanisms. *J Alzheimers Dis, 51*(3), 689-699. doi:10.3233/jad-150896

Pike, L. J. (2009). The challenge of lipid rafts. *J Lipid Res, 50 Suppl*(Suppl), S323-328. doi:10.1194/jlr.R800040-JLR200

Prendergast, J., Umanah, G. K., Yoo, S. W., Lagerlöf, O., Motari, M. G., Cole, R. N., . . . Schnaar, R. L. (2014). Ganglioside regulation of AMPA receptor trafficking. *J Neurosci, 34*(39), 13246-13258. doi:10.1523/jneurosci.1149-14.2014

Rollhäuser-ter Horst, J. (1977). Artificial neural induction in amphibia. I. Sandwich explants. *Anat Embryol (Berl), 151*(3), 309-316. doi:10.1007/bf00318932

Russo, D., Della Ragione, F., Rizzo, R., Sugiyama, E., Scalabrì, F., Hori, K., . . . D'Angelo, G. (2018). Glycosphingolipid metabolic reprogramming drives neural differentiation. *Embo j, 37*(7). doi:10.15252/embj.201797674

Sandhoff, K., & Kolter, T. (2003). Biosynthesis and degradation of mammalian glycosphingolipids. *Philosophical transactions of the Royal Society of London. Series B, Biological sciences, 358*(1433), 847-861. doi:10.1098/rstb.2003.1265

Schnaar, R. L. (2016). Gangliosides of the Vertebrate Nervous System. *Journal of Molecular Biology, 428*(16), 3325-3336. doi:https://doi.org/10.1016/j.jmb.2016.05.020

Schnaar, R. L., Gerardy-Schahn, R., & Hildebrandt, H. (2014). Sialic acids in the brain: gangliosides and polysialic acid in nervous system development, stability, disease, and regeneration. *Physiol Rev, 94*(2), 461-518. doi:10.1152/physrev.00033.2013

Schnitzer, J. E., McIntosh, D. P., Dvorak, A. M., Liu, J., & Oh, P. (1995). Separation of caveolae from associated microdomains of GPI-anchored proteins. *Science, 269*(5229), 1435-1439. doi:10.1126/science.7660128

Shafi, R., Iyer, S. P., Ellies, L. G., O'Donnell, N., Marek, K. W., Chui, D., . . . Marth, J. D. (2000). The O-GlcNAc transferase gene resides on the X chromosome and is essential for embryonic stem cell viability and mouse ontogeny. *Proc Natl Acad Sci U S A, 97*(11), 5735-5739. doi:10.1073/pnas.100471497

Sherrington, R., Rogaev, E. I., Liang, Y., Rogaeva, E. A., Levesque, G., Ikeda, M., . . . St George-Hyslop, P. H. (1995). Cloning of a gene bearing missense mutations in early-onset familial Alzheimer's disease. *Nature, 375*(6534), 754-760. doi:10.1038/375754a0

Shoulders, M. D., Ryno, L. M., Genereux, J. C., Moresco, J. J., Tu, P. G., Wu, C., . . . Wiseman, R. L. (2013). Stress-independent activation of XBP1s and/or ATF6 reveals three functionally diverse ER proteostasis environments. *Cell Rep, 3*(4), 1279-1292. doi:10.1016/j.celrep.2013.03.024

Simons, K., & Ikonen, E. (1997). Functional rafts in cell membranes. *Nature, 387*(6633), 569-572. doi:10.1038/42408

Spiro, R. G. (2004). Role of N-linked polymannose oligosaccharides in targeting glycoproteins for endoplasmic reticulum-associated degradation. *Cell Mol Life Sci, 61*(9), 1025-1041. doi:10.1007/s00018-004-4037-8

Südhof, T. C. (2013). Neurotransmitter release: the last millisecond in the life of a synaptic vesicle. *Neuron, 80*(3), 675-690. doi:10.1016/j.neuron.2013.10.022

Sun, X., Chen, W.-D., & Wang, Y.-D. (2015). β-Amyloid: The Key Peptide in the Pathogenesis of Alzheimer's Disease. *Frontiers in Pharmacology, 6*. doi:10.3389/fphar.2015.00221

Sun, Z., & Brodsky, J. L. (2019). Protein quality control in the secretory pathway. *J Cell Biol, 218*(10), 3171-3187. doi:10.1083/jcb.201906047

Takahashi, K., & Yamanaka, S. (2006). Induction of pluripotent stem cells from mouse embryonic and adult fibroblast cultures by defined factors. *Cell, 126*(4), 663-676. doi:10.1016/j.cell.2006.07.024

Tettamanti, G., Bonali, F., Marchesini, S., & Zambotti, V. (1973). A new procedure for the extraction, purification and fractionation of brain gangliosides. *Biochim Biophys Acta, 296*(1), 160-170. doi:10.1016/0005-2760(73)90055-6

Travers, K. J., Patil, C. K., Wodicka, L., Lockhart, D. J., Weissman, J. S., & Walter, P. (2000). Functional and genomic analyses reveal an essential coordination between the unfolded protein response and ER-associated degradation. *Cell, 101*(3), 249-258. doi:10.1016/s0092-8674(00)80835-1

Uddin, M. S., Tewari, D., Sharma, G., Kabir, M. T., Barreto, G. E., Bin-Jumah, M. N., . . . Ashraf, G. M. (2020). Molecular Mechanisms of ER Stress and UPR in the Pathogenesis of Alzheimer's Disease. *Molecular Neurobiology, 57*(7), 2902-2919. doi:10.1007/s12035-020-01929-y

van der Harg, J. M., van Heest, J. C., Bangel, F. N., Patiwael, S., van Weering, J. R., & Scheper, W. (2017). The UPR reduces glucose metabolism via IRE1 signaling. *Biochim Biophys Acta Mol Cell Res, 1864*(4), 655-665. doi:10.1016/j.bbamcr.2017.01.009

van Meer, G., Voelker, D. R., & Feigenson, G. W. (2008). Membrane lipids: where they are and how they behave. *Nat Rev Mol Cell Biol, 9*(2), 112-124. doi:10.1038/nrm2330

Varki, A., Cummings, R. D., Esko, J. D., Stanley, P., Hart, G. W., Aebi, M., . . . Seeberger, P. H. (2015). Essentials of Glycobiology. In A. Varki, R. D. Cummings, J. D. Esko, P. Stanley, G. W. Hart, M. Aebi, A. G. Darvill, T. Kinoshita, N. H. Packer, J. H. Prestegard, R. L. Schnaar, & P. H. Seeberger (Eds.), *Essentials of Glycobiology*. Cold Spring Harbor (NY): Cold Spring Harbor Laboratory Press

Varki, A., & Kornfeld, S. (2022). Historical Background and Overview. In th, A. Varki, R. D. Cummings, J. D. Esko, P. Stanley, G. W. Hart, M. Aebi, D. Mohnen, T. Kinoshita, N. H. Packer, J. H. Prestegard, R. L. Schnaar, & P. H. Seeberger (Eds.), *Essentials of Glycobiology* (pp. 1-20). Cold Spring Harbor (NY).

Wang, H., Bright, A., Xin, B., Bockoven, J. R., & Paller, A. S. (2013). Cutaneous dyspigmentation in patients with ganglioside GM3 synthase deficiency. *American journal of medical genetics. Part A, 161A*(4), 875-879. doi:10.1002/ajmg.a.35826

Waxenbaum, J. A., Reddy, V., & Varacallo, M. (2022). Anatomy, Autonomic Nervous System. In *StatPearls*. Treasure Island (FL).

Wodrich, A. P. K., Scott, A. W., Shukla, A. K., Harris, B. T., & Giniger, E. (2022). The Unfolded Protein Responses in Health, Aging, and Neurodegeneration: Recent Advances and Future Considerations. *Frontiers in Molecular Neuroscience, 15*. doi:10.3389/fnmol.2022.831116

Yntema, C. L., & Hammond, W. S. (1954). The origin of intrinsic ganglia of trunk viscera from vagal neural crest in the chick embryo. *J Comp Neurol, 101*(2), 515-541. doi:10.1002/cne.901010212

Yoshida, H., Matsui, T., Yamamoto, A., Okada, T., & Mori, K. (2001). XBP1 mRNA is induced by ATF6 and spliced by IRE1 in response to ER stress to produce a highly active transcription factor. *Cell, 107*(7), 881-891. doi:10.1016/s0092-8674(01)00611-0

Yu, R. K., Tsai, Y.-T., Ariga, T., & Yanagisawa, M. (2011). Structures, biosynthesis, and functions of gangliosides--an overview. *Journal of oleo science, 60*(10), 537-544. doi:10.5650/jos.60.537

Zachara, N. E., & Hart, G. W. (2004). O-GlcNAc a sensor of cellular state: the role of nucleocytoplasmic glycosylation in modulating cellular function in response to nutrition and stress. *Biochim Biophys Acta, 1673*(1-2), 13-28. doi:10.1016/j.bbagen.2004.03.016

Zachara, N. E., O'Donnell, N., Cheung, W. D., Mercer, J. J., Marth, J. D., & Hart, G. W. (2004). Dynamic O-GlcNAc modification of nucleocytoplasmic proteins in response to stress. A survival response of mammalian cells. *J Biol Chem, 279*(29), 30133-30142. doi:10.1074/jbc.M403773200

CHAPTER 2

NEURAL-SPECIFIC ALTERATIONS IN GLYCOSPHINGOLIPID BIOSYNTHESIS AND CELL SIGNALING ASSOCIATED WITH TWO HUMAN GANGLIOSIDE GM3 SYNTHASE DEFICIENCY VARIANTS.

Shannon K. Wagner[*], Michelle Dookwah[*], Mayumi Ishihara, Seok-Ho Yu, Heidi Urichs, Michael J. Kulik, Nadja Zeltner, Kevin A. Strauss, Kazuhiro Aoki, Richard Steet, Michael Tiemeyer

* Denotes co-equal first authors

Submitted to Human Molecular Genetics

ABSTRACT

GM3 Synthase Deficiency (GM3SD) is a neurodevelopmental disorder resulting from pathogenic variants in the *ST3GAL5* gene, which encodes GM3 synthase, a glycosphingolipid (GSL)-specific sialyltransferase. This enzyme adds a sialic acid to the terminal galactose of lactosylceramide (LacCer) to produce the monosialylated ganglioside GM3. In turn, GM3 is extended by other glycosyltransferases to generate nearly all the complex gangliosides enriched in neural tissue. Pathogenic mechanisms underlying the neural phenotypes associated with GM3SD are unknown. To explore how loss of GM3 impacts neural-specific glycolipid glycosylation and cell signaling, GM3SD patient fibroblasts bearing one of two different *ST3GAL5* variants were reprogrammed to induced pluripotent stem cells (iPSCs) and then differentiated to neural crest cells (NCCs). GM3 and GM3-derived gangliosides were undetectable in cells carrying either variant, while LacCer precursor levels were elevated compared to wildtype (WT). NCCs of both variants synthesized elevated levels of neutral lacto- and globo-series, as well as minor alternatively sialylated GSLs compared to WT. Ceramide profiles were also shifted in GM3SD variant cells. Altered GSL profiles in GM3SD cells were accompanied by dynamic changes in the cell surface proteome, protein O-GlcNAcylation, and receptor tyrosine kinase abundance. GM3SD cells also exhibited increased apoptosis and sensitivity to erlotnib-induced inhibition of epidermal growth factor receptor signaling. Pharmacologic inhibition of O-GlcNAcase rescued baseline and erlotnib-induced apoptosis. Collectively, these findings indicate aberrant cell signaling during differentiation of GM3SD iPSCs. Thus, human GM3SD cells provide a novel platform to investigate structure/function relationships connecting GSL diversity to cell signaling, cell survival, and neural differentiation.

INTRODUCTION

GM3 Synthase Deficiency (GM3SD) is an autosomal recessive disorder characterized by infantile-onset epileptic encephalopathy, global developmental delay, postnatal microcephaly, congenital hearing loss, cortical visual impairment, and hyper- and hypo-pigmented epidermis (Saul, Wilkes, & Stevenson, 1983). GM3SD is caused by pathogenic variants in the *ST3GAL5* gene that encodes for the sialyltransferase known as GM3 synthase. ST3GAL5 catalyzes the production of the ganglioside GM3, which is the precursor for all complex a- b-, and c-type ganglioside glycosphingolipids (GSLs) in the human brain (**Figure 2.1**). Gangliosides account for >80% of brain glycans and have been implicated in neural-glial cell interactions, neuronal proliferation and survival, membrane microdomain formation, and cell signaling (Schnaar, Gerardy-Schahn, & Hildebrandt, 2014; Sipione, Monyror, Galleguillos, Steinberg, & Kadam, 2020). The significant clinical consequences of GM3SD are not entirely unexpected, in light of the impact of targeted biosynthetic knockouts in mice, and of the accumulated data highlighting in vitro functions of gangliosides (Lloyd & Furukawa, 1998; Schnaar, 2016; Yamashita et al., 2003). Nonetheless, the functional impact of altered ganglioside biosynthesis on neural cell differentiation, signaling, and survival in the context of neural cells in culture has not been studied, leaving gaps in our understanding of the neuronal pathogenesis associated with GM3SD.

GM3SD has been associated with several cohorts worldwide, exhibiting allelic diversity based in part on genetic ancestry. Salt & Pepper Syndrome was described as one of the first cohorts of GM3SD, affecting a single family in South Carolina, USA(Boccuto et al., 2014; Saul et al., 1983). The variant associated with Salt & Pepper Syndrome, *ST3GAL5* c.1063G>A (p.Glu355Lys), encodes for a mutant form of the enzyme lacking

any enzymatic activity (Indellicato et al., 2019). A more prevalent variant identified in the Amish population, c.862C>T (p.Arg288Ter), encodes for a truncated and inactive enzyme (Indellicato et al., 2019; Simpson et al., 2004). The Amish variant is estimated to have a carrier frequency of 5-6% within this population, which translates to approximately 1 in 1200 births (Bowser et al., 2019). The p.Arg288Ter variant has also been reported in French and Pakistani cohorts (Fragaki et al., 2013; Gordon-Lipkin et al., 2018). Additional variants, compound heterozygous ST3GAL5 mutations (p.Gly201Arg and p.Cys195Ser), were identified in two Korean siblings (Lee et al., 2016). All of the currently identified and characterized pathogenic ST3GAL5 variants are null for enzymatic activity and share significant overlap in their clinical presentations (Li & Schnaar, 2018).

To investigate the molecular and neural-specific changes resulting from loss of GM3, we generated induced pluripotent stem cells (iPSCs) from Salt & Pepper (p.Glu355Lys) and Amish cohort (p.Arg288Ter) fibroblasts. These cells were subsequently differentiated towards the neural crest cell (NCC) lineage, and the impact of GM3 synthase deficiency on neural-specific glycosphingolipid biosynthesis and cellular signaling responses was monitored across the differentiation time course. Neural crest was chosen as an initial lineage of study based on skin pigmentation phenotypes described in patients, high homogeneity of the NCC population derived from iPSCs, and the broad impact of neural crest derivatives on somatic function. This investigation identified several common GSL profile alterations in the two variants, including changes in ceramide structures and loss of complex gangliosides. These GSL changes were accompanied by broad fluctuations in multiple cell signaling pathways and an abnormal abundance of several lipid raft-associated cell surface proteins in the two patient lines. The implications of these findings

for the neuronal pathogenesis of GM3SD and molecular phenotypes that distinguish the two patient lines are discussed. These results establish a baseline for the use of patient-derived cells for further investigating the impact of GSL diversity on cell signaling and differentiation in multiple tissue and cell-specific lineages.

MATERIALS AND METHODS

Generation of induced pluripotent stem cells

Wild-type iPSC lines hiPSK3 and hiC3 were, respectively, acquired from Steve Duncan, University of Wisconsin, or generated from ATCC CRL-1509 human fibroblasts (Si-Tayeb et al., 2010). Generation of p.Glu355Lys iPSCs (from *ST3GAL5* c.1063G>A (p.Glu355Lys) patient fibroblasts) and p.Arg288Ter iPSCs (from *ST3GAL5* c.862C>T (p.Arg288Ter) patient fibroblasts) was performed using the CytoTune-iPS Sendai Reprogramming Kit (Invitrogen, # A13780) and the CytoTune-iPS 2.0 Sendai Reprogramming Kit (ThermoFisher, # A16517), respectively, using the manufacturer's conditions and as described previously (Menendez et al., 2013). The p.Glu355Lys donor was a 13 year old male of African-American descent and the p.Arg288Ter donor was a 12 year old male and a member of the Amish community. A single iPSC clone was generated for the p.Glu355Lys variant and 3 independent clones were generated for the p.Arg288Ter variant. Each subclone was passaged at least 10 times to ensure removal of residual reprogramming virus before further characterization. Loss of virus was monitored by staining with anti-Sendai virus antibody (Invitrogen, cat #14649482).

iPSC clones were initially tested for pluripotency by assessing expression of pluripotency markers Oct4 (Cell Signaling, # C30A3), SSEA3/4 (Santa Cruz, # sc-21704), and Sox2 (R&D, # MAB2018), and by inducing differentiation into neuroectodermal

cells(Cederquist et al., 2020). For neuroectoderm differentiation, iPSCs were seeded at 260,000 cells/cm^2 in 6 wells in Essential 8 media on matrigel. The next day, the media was changed to Essential 6 containing 100 nM LDN, 10 µM SB and 2 µM XAV until day 2 when the media was changed to Essential 6 containing 100 nM LDN, 10 µM SB. Cells were fixed and stained for PAX6 (Biolegend, # 901301/B201255) and DAPI at day 4 and exhibited efficient differentiation into the neuroectodermal lineage (**Supplement Figure 2.7**). All iPSCs were tested for mycoplasma every 2 weeks. The three independent iPSC clones derived from p.Arg288Ter donor fibroblasts and the single clone derived from p,Glu355Lys donor fibroblasts exhibited equivalent differentiation potential and growth characteristics (**Supplement Figure 2.7 – 2.9**). In the absence of any observable differences in the growth and differentiation characteristics of the three p.Arg288Ter clones, the p.Arg288Ter.2.1a was selected for the glycolipidomic and biochemical analyses described here (**Supplement Figure 2.7**).

Neural Crest differentiation of iPSCs

Patient and WT iPSCs were differentiated to neural crest cells (NCCs) according to (Menendez et al., 2013). Briefly, a 60 mm dish of ~90% confluent iPSCs was dissociated with Accutase (Innovative Cell Technologies, # AT104) and resuspended to a density of ~$9.2x10^4$ cells per cm^2 on Geltrex-coated plates in neural crest media composed of DMEM/F12 without glutamine (Cellgro), 2% Probumin, Life Science Grade (Millipore), 1x Non-essential amino acids (Cellgro), 2 mM GlutaGro (Cellgro), 1x Antibiotic/Antimycotic (Cellgro), 10 µg/ml Human Transferrin, (Athens Research & Tech),1x Trace elements A, B, & C (Cellgro), 50 µg/ml L-Ascorbic acid 2-phosphate sesqimagnesium salt hydrate (Sigma), 10 ng/ml Heregulin β (Peprotech), 200 ng/ml Long

R3-IGF1 (SAFC/Sigma), 8 ng/ml bFGF (RnD Systems), 2 µM GSK3 inhibitor IX (BIO) (Tocris), and 20 µM SB431542 (Tocris). Media was changed daily, and at confluence, cells were split 1:4-1:6 (vol/vol) onto Geltrex-coated plates. Cells exhibited NCC morphology between day 7-10 of differentiation. By Day 15, cells tested positive by immunohistochemistry for NC markers HNK1 (Sigma Aldrich, # C6680) and p75 (Advanced Targeting Systems, # AB-N07), and negative for iPSC markers Oct4, SSEA3/4, and Sox2 (**Supplement Figure 2.7-9**). When assessing cell characteristics at specific time points of differentiation, cells were collected on specified days by scraping, spun down at 200 x g for 5 minutes, and frozen after aspiration of the supernatant. Successful differentiation of WT and GM3SD variant iPSCs to NCCs was monitored by endpoint analysis for the acquisition of NCC markers and loss of pluripotency markers by immunofluorescence as described below. Marker assessment was performed over multiple independent differentiations and repeated upon thaw of each new aliquot of an iPSC line. In all cases, the iPSCs acquired NCC and lost pluripotency markers as expected based on previous publications (Menendez et al., 2013).

Immunofluorescence staining

Antibodies and dilutions were as follows: Anti-HNK-1 antibody (Sigma Aldrich, Monoclonal Anti-HNK-1/N-CAM (CD57), # C6680), 1:200 dilution in 5% donkey serum prepared in 0.2% Triton X-100 in PBS (PBS-T); Anti-Sox2 antibody (R&D, # MAB2018), 1:200 dilution in 5% donkey serum in PBS-T; Anti-Oct4 antibody (Santa Cruz, # sc-8628), 1:200 dilution in 5% donkey serum in PBS-T; Anti-Pax6 antibody (Santa Cruz, # sc-81649), 1:200 dilution in 5% donkey serum prepared in 0.05% Tween-20 in PBS (PBS-T); Anti-SSEA3/4 antibody (Santa Cruz, # sc-21704), 1:200 dilution in 5% donkey serum in

PBS-T; Anti-p75 antibody (Advanced Targeting Systems, # AB-N07), 1:100 dilution in PBS-T. All antibodies were incubated overnight at 4ºC. Immunofluorescent images were captured using an Olympus Fluoview FV1000 laser confocal microscope or a LionheartFX (BioTek) fluorescence microscope.

Extraction and preparation of GSLs

iPSCs or iPSC-derived NCCs were homogenized and extracted with organic solvents to precipitate proteins and recover GSLs as described previously (K. Aoki et al., 2007). Briefly, cell pellets were Dounce homogenized in 50% methanol on ice. Ice-cold water (W), methanol (M) and chloroform (C) were added to give final ratio of C:M:W::4:8:3. The suspension was then transferred into a Teflon-lined screw cap glass tube, agitated for 2 hours at room temperature, and clarified by centrifugation. The supernatant was saved and the resulting pellet was re-extracted three times with fresh 4:8:3 solvent. All supernatants were combined as the lipid extract. Lipid extracts were dried under a nitrogen stream and subjected to saponification to remove glycerophospholipids (Silva, Videira, & Sackstein, 2017). Saponification was completed using 0.5M KOH in methanol-water (95:5, M/W, v/v) at 37 ºC for 6 hours. Following neutralization with 10% acetic acid on ice, the solution was adjusted to 50% M/W, and then directly loaded onto a Sep-Pak tC18 cartridge column (Waters, Sep-Pak Vac 1cc, 100 mg resin) equipped with a glass syringe (10 ml) that was previously washed with methanol and pre-equilibrated with distilled water. The initial flow-through from the loading was collected and re-applied to the column to enhance recovery. The loaded column was washed with a total of 30 ml of water. GSLs were then eluted with 3 ml of methanol and dried under a nitrogen stream. Free fatty acids resulting from saponification of glycerophospholipids were removed from

the dried GSLs by wash with hexane and redrying under nitrogen. Initial analyses of WT and GM3SD GSLs were performed by TLC using the following solvent systems: C/M/W (60:35:8) for neutral GSLs; C/M/0.2% $CaCl_2$ (55:45:10) for gangliosides; C/M/W (60:40:10) for GSL mixtures. Orcinol–H_2SO_4, resorcinol, Dittmer-Lester, and Ninhydrin reagents were used for the detection of sugar, sialic acid, phosphate, and primary amine groups, respectively.

Analysis of GSLs by mass spectrometry

Nanospray ionization mass spectrometry (NSI-MS) was performed on permethylated glycolipids. For MS of permethylated glycolipids in positive ion mode,~0.4 nmol of permethylated total glycolipids were dissolved in 50 µl of 1 mM sodium acetate in methanol/water (1:1) for infusion into a linear ion trap mass spectrometer (Orbi-LTQ; ThermoFisher Scientific) using a nanospray source at a syringe flow rate of 0.40 µl/min and capillary temperature set to 210 ^{o}C (Anumula & Taylor, 1992; K. Aoki et al., 2007; Silva et al., 2017; Vukelić et al., 2005). The instrument was tuned with a mixture of permethylated standard neutral or ganglioside GSLs. For fragmentation by collision-induced dissociation (CID) in MS/MS and MS^n, a normalized collision energy of 30 – 35% was used.

Detection, structural identification, and quantification of individual glycolipids were accomplished using full MS, total ion mapping (TIM), and neutral loss scan (NL scan) functionalities of the Xcalibur software package version 2.0 (ThermoFisher Scientific) as previously described (Kazuhiro Aoki, Heaps, Strauss, & Tiemeyer, 2019; K. Aoki et al., 2007). Quantification of the amount of each permethylated GSL (as pmol/1x10^6 cells) was achieved by referencing GSL peak heights in full MS spectra to the peak height of a known

quantity of a permethylated glycan standard, maltotetraose (Dp4), which was spiked into the sample prior to MS, as previously described (Kazuhiro Aoki et al., 2019; Mehta et al., 2016). For TIM, the m/z range from 600 to 2000 was automatically scanned in successive 2.8 mass unit windows with a window-to-window overlap of 0.8 mass units, which allowed the naturally occurring isotopes of each glycolipid species to be summed into a single response, thereby increasing detection sensitivity. Most glycolipid components were identified as singly, doubly, and triply charged, sodiated species (M + Na) in positive mode. Peaks for all charge states were summed for quantification. Preliminary analysis demonstrated that the major fragment ions in CID MS/MS scans of glycolipid preparations correspond to the neutral loss of the ceramide moiety, leaving intact glycolipid oligosaccharide ions. Therefore, an MS workflow was defined for NL scans in which the highest intensity peak detected by full MS was subjected to CID fragmentation. If an MS/MS profile contained an ion with m/z equivalent to loss of the most prevalent ceramide moiety, MS^n fragmentation was initiated. Following this data-dependent acquisition, the workflow returned to full MS, excluded the parent ion just fragmented, and chose the peak of next highest intensity for the same MS/MS and MS^n analysis. Graphic representations of GSL monosaccharide residues are consistent with the Symbol Nomenclature For Glycans (SNFG) as adopted by the glycomics and glycobiology communities (Varki et al., 2015). Glycomics data and metadata were obtained and are presented in accordance with MIRAGE standards and the Athens Guidelines (Wells, Hart, & Athens Guidelines for the Publication of Glycomics, 2013; York et al., 2014). All raw mass spectrometric data, both glycomic and proteomic, were deposited at GlycoPost, Accession #XXXX (Rojas-Macias et al., 2019).

Selective Exo-Enzymatic labeling of cell surface glycoproteins

Selective Exo-Enzymatic Labeling (SEEL) installs a biotin moiety onto the N-linked glycans of cell-surface glycoproteins, allowing their subsequent high-affinity capture and enrichment for proteomic analysis (Mbua et al., 2013). SEEL and subsequent proteomic analysis of tagged proteins were conducted on WT and p.Glu355Lys iPSCs and NCCs according to previously described methods(Mbua et al., 2013). Recombinant rat α-(2,6)-sialyltransferase (ST6GAL1) was prepared as previously described (Meng et al., 2013). Biotinylated CMP-sialic acid was synthesized as described previously according to (Mbua et al., 2013). For labeling of cell-surface glycoproteins, approximately $9x10^7$ NCCs from WT and p.Glu355Lys lines were dissociated from the cell culture dish by manual trituration in Dulbecco's phosphate-buffered saline (DPBS) and the cells were transferred to Eppendorf tubes. The cells were pelleted and resuspended in serum-free DMEM with 42 µg/ml ST6Gal1, 34 µM CMP-Sia-C5-biotin, 13.3 µg/ml BSA, 13.3 µg/ml alkaline phosphatase and 2 µl (in 50% glycerol) *Arthrobacter ureafaciens* (AU) neuraminidase. Each reaction was in a final volume of 350 µl per tube and was incubated for 2 hours at 37 °C. After the SEEL labeling incubation, labeled cells were lysed in RIPA buffer and biotinylated proteins were captured by immunoprecipitation (IP) from 1 mg total lysate protein using anti-biotin antibody. Precipitated proteins were resolved by SDS-PAGE and visualized by silver stain. The resulting gels were cut into two pieces corresponding to regions of the gel that contained proteins with apparent molecular weight between 75-150 kD or greater than 150 kD. Each gel region was then subjected to in-gel trypsinization as previously described (Mbua et al., 2013). The resulting peptides and glycopeptides from each gel region were separately analyzed by LC-MS/MS using a Lumos Tribrid mass

spectrometer (ThermoFisher). Proteins identified by peptides detected at <10 spectral matches (PSMs) were excluded from analysis, as were peptides identified as nuclear or cytosolic by GO annotation. Spectral counts for cell surface and secreted proteins that met threshold criteria were normalized to the number of spectral counts detected for human transferrin receptor in WT and p.Glu355Lys IPs.

Identification of Receptor Tyrosine Kinases in WT and GM3SD cells

Protein was harvested from WT and p.Glu355Lys iPSC and NCC lysates (d19 of differentiation) using the manufacturer's Receptor Tyrosine Kinase (RTK) array protocol in Lysis buffer 17 (R&D Systems, # ARY001B). RTK arrays were blocked for 1 hour at room temperature in Array Buffer 1 (manufacturer's protocol). An amount of protein (300 µg) from each cell lysate was diluted in Array Buffer 1 to a volume of 1.5ml and added to the blocked RTK arrays. Arrays were then incubated with gentle rocking overnight at 4 ºC. The arrays were then washed 3X with 1X Wash Buffer (manufacturer's protocol) and subsequently probed with HRP-conjugated pan-phosphotyrosine antibody diluted in Array Buffer 2 (manufacturer's protocol). Following incubation with gentle rocking for 2 hours at room temperature, the blots were washed with Wash Buffer and RTK capture/phosphorylation was detected by chemiluminescence.

Western blot analysis

Antibodies for detection of cell surface proteins by western blot of cell lysates were used as provided and were from the following sources: anti-ERBBB3 (Cell Signaling, HER3/ERBB3, D22C5 XP Rabbit mAb, # 12708) at 1:1000 dilution with detection by goat anti-mouse secondary at 1:2500 dilution; anti-EGFR (Santa Cruz, EGFR A-10, # sc-373746) at 1:1000 dilution with detection by goat anti-mouse secondary at 1:2500 dilution;

anti-caspase 3 (Santa Cruz, caspase-3 Antibody 31A1067, # sc-56053) at 1:1000 dilution with detection by goat anti-mouse secondary at 1:2500 dilution; anti-sortilin (BD Biosciences, Neurotensin Receptor 3 antibody, # 612100) at 1:1000 dilution with detection by goat anti-mouse secondary at 1:2500 dilution; anti-NOTCH2 (DSHB, NOTCH2 C651.6DbHN) at 1:500 dilution with detection by goat anti-rat secondary at 1:3000 dilution; anti-β-actin (Santa Cruz, Actin Antibody 2Q1055, # Sc-58673) at 1:5000 dilution with detection by goat anti-mouse secondary at 1:2500 dilution. O-GlcNAcylation of proteins in cell lysates was detected by western blot with anti-O-GlcNAc monoclonal antibody RL-2 (Enzo Life Sciences, ALX-804-11-R100) at 1:1000 dilution with detection by goat anti-mouse secondary at 1:10000. Actin was detected in parallel with O-GlcNAc by incubation with anti-β-actin (Cell Signaling Technology, Actin Antibody 13E5, #4790) at 1:5000 with detection by goat anti-rabbit secondary at 1:10000.

Protein concentrations in lysates were measured by BCA assay and aliquots containing 25 µg were reduced, alkylated, resolved by SDS-PAGE, and transferred to PVDF membranes for probing with primary antibodies. Primary antibody binding was detected by HRP-conjugated secondary antibodies and chemiluminescence. Densitometric quantification was performed with ImageJ Software. For developmental time courses that assessed the change in abundance of receptors across differentiation from iPSC to NCC, signal intensities for receptor proteins were normalized to ß-actin (loading control) and then expressed as $\log_2$-fold changes relative to the normalized signal intensity detected in iPSC (d0 of differentiation).

Pharmacologic inhibition of EGFR signaling by erlotinib and of O-GlcNAcase by thiamet-G

WT and p.Glu355Lys iPSCs were differentiated to NCCs for 10 days. Beginning at d10, vehicle (2% DMSO final) or erlotinib in vehicle (100 μM final concentration in media) or thiamet-G in vehicle with or without erlotnib (10 μM thiamet-G ± 100 μM erlotnib final concentration in media) was added to a media change and the cells were incubated for 24 or 48 additional hours prior to harvest for analysis. At harvest timepoints, the media was removed from the wells and centrifuged to collect floating cells. Adherent cells were also scraped and pelleted for collection. Adherent and floating cells were lysed prior to analysis by BCA assay and analyzed separately by western blot for the relative abundance of cleaved and uncleaved caspase 3.

Statistical analysis

Western blot analyses were performed on cells harvested at indicated time points from between 3-6 independent differentiation courses. Multiple parametric tests were utilized to assess the statistical significance of the resulting data. One-way ANOVA was used to identify significant changes across the three cell populations: WT, p.Glu355Lys, and p.Arg288Ter. Z-scores were calculated and subjected to Z-test to assess the distribution of WT and GM3SD population data for EGFR and ERBB3 expression, where the large number of independent replicates allowed for reasonable estimation of the standard deviation of the entire population. Pairwise T-tests were also used to assess the similarity of one population compared to another for specific features, especially for assessing pharmacologic effects on smaller sample sets. For all three tests, a P-value less than or equal to 0.05 was considered indicative of a significant difference between the tested

populations. The results of pairwise T-tests and Z-tests identified the same population differences as significant; for simplicity of presentation, only the pairwise T-tests are presented for direct comparisons. In tables and graphs, population means are reported ± standard error of the mean. For the analysis of EGFR and ERBB3 expression, immunoblot band intensities for each receptor were normalized to actin intensity in order to control for loading variability and then presented as $\log_2$ of the ratio for each timepoint relative to day 0 of the differentiation course. For the analysis of cleaved Caspase3, the ratio of the immunoblot intensity associated with the cleavage product at 17kD was divided by the ratio of the intensity associated with the intact protein at 34kD detected in the same lane; normalization to actin was not performed since the ratios are independent of sample load.

RESULTS

GM3 synthase deficiency impacts neural-specific GSL biosynthesis

Characterization of the distribution and abundance of GSLs in WT and GM3SD cell populations by thin-layer chromatography (TLC) and mass spectrometry demonstrates broad similarity as iPSCs, but highly divergent profiles in the differentiated NCC populations. The GSL profiles of iPSCs and NCCs are detectably different by TLC, whether the cells are WT or GM3SD (**Figure 2.2**). WT and GM3SD iPSC GSL profiles are dominated by hexosyl-, lactosyl-, globotriaosyl- and globotetraosylceramide (LacCer, Gb3, and Gb4, respectively). While the analysis presented here cannot distinguish between LacCer and a dihexosylceramide of alternative monosaccharide composition, the only other dihexosylceramide previously described in vertebrate cells is Galα4GalCer, a Gala-series GSL whose expression has been described as a minor component of the GSL profile of the thymus, kidney, meconium, and myelocytic cancer cells in humans as well as of the

heart in chickens (Bouchon & Portoukalian, 1985; Bouchon, Portoukalian, & Bornet, 1985; Chatterjee, Khullar, & Shi, 1995; Jennemann, Felding-Habermann, Geyer, Stirm, & Wiegandt, 1987; Karlsson & Larson, 1981; Klock, D'Angona, & Macher, 1981; Macher, Klock, Fukuda, & Fukuda, 1981). Upon differentiation of WT iPSCs to NCCs, LacCer is efficiently shunted toward the production of GM3, along with the more complex gangliosides derived from GM3, such as GD3, GM1, and GD1 (see **Figure 2.1** for nomenclature). However, differentiation of GM3SD iPSCs results in accumulation of LacCer without production of GM3.

Higher resolution analysis of GSL profiles by NSI-MS^n of their permethylated derivatives validated the lack of GM3 in GM3SD iPSCs and NCCs and the resulting lack of a-, b-, or c-series gangliosides **(Figure 2.3, 2.4)**. By this method, the induced pluripotent stem cell marker SSEA-3 (Gal-extended globotetraosylceramide), itself a GSL, was also detected in WT and GM3SD iPSC GSL profiles. The complex sialylated GSLs of GM3SD NCCs were detected only as o-series gangliosides; these alternatively sialylated GSLs are sialylated on their external Gal residue (GM1b, GD1c, see **Figure 2.1**). In the absence of GM3 and GM3-derived GSLs, the GM3SD NCCs retained high levels of LacCer and elevated levels of Gb3 and Gb4 compared to wildtype NCCs.

While the GSL profiles of p.Glu355Lys and p.Arg288Ter iPSCs and NCCs presented similar deficiencies in GM3 and the major GM3-derived GSLs, more subtle differences were detected between the cells derived from the two GM3SD variants. The alternatively sialylated gangliosides GM1b and GD1c were increased in p.Glu355Lys NCCs compared to p.Arg288Ter NCCs (**Table 2.1**). Additionally, GSLs with N-acetyl-lactosamine (LacNAc) repeats uncapped by sialic acid at their non-reducing termini were

more abundant in p.Arg288Ter NCCs, whereas extended LacNAc structures were more likely to be sialylated in p.Glu355Lys NCCs (**Figure 2.5,** see **Supplement Figure 2.1** for validation of the extended LacNAc GSL structures). In general, the major shifts in GSL profiles were conserved across the two GM3SD variants when compared to WT, but p.Glu355Lys NCCs synthesized a higher abundance of alternatively sialylated gangliosides and p.Arg288Ter cells retained greater relative abundance of LacCer and ceramides with higher mass. (**Figure 2.6A**).

GSL ceramide moieties impart physicochemical characteristics that facilitate their incorporation into specialized membrane microdomains referred to as lipid rafts and as detergent resistant membranes(Deborah A. Brown & London, 1997). Heterogeneity in GSL ceramides derives from the chemical nature of the sphingosine base and its amide-linked fatty acid. These components can differ based on degree of saturation, hydrocarbon chain length, and presence or absence of a sphingosine hydroxyl group. The heterogeneity of GSL ceramides is well resolved by NSI-MS^n, in which each GSL glycan head group is detected in association with a family of m/z values that reflect lipid differences (**Figure 2.3, 2.4**). The ratio of longer chain fatty acid-containing ceramides to shorter chain-containing ceramides was higher in the iPSCs of GM3SD patients compared to wild-type; LacCer and globoside Gb4 exhibit this difference particularly well in iPSCs (**Figure 2.3, 2.6A**). The relative abundance of the longest chain (C24:0 and C26:0) and shortest chain (C16:0) fatty acids did not change appreciably as WT iPSCs differentiated to NCCs, although the relative abundance of intermediate chain lengths (C18:0, C20:0, C22:0, C22:1) was redistributed (**Figure 2.6B**). Similarly, the relative abundance of the longest and shortest chain fatty acids did not change significantly as p.Arg288Ter iPSCs

differentiated to NCCs, although the p.Arg288Ter NCCs (similar to their iPSC precursors) maintained a much higher abundance of the longer chain species than WT NCCs (**Figure 2.6B**). In contrast, the pGlu355Lys NCCs exhibited reduced relative abundance of the longest chain fatty acids compared to their iPSC precursors and to WT and p.Arg288Ter NCCs (**Figure 2.6B**).

GM3 synthase deficiency alters the cell surface proteome

GM3 and several of its precursors and products are components of lipid rafts, plasma membrane microdomains enriched in proteins, frequently GPI-anchored, that participate in multiple cellular functions including adhesion and signaling. We employed a robust cell-surface capture technology (Selective Exo-Enzymatic Labeling or SEEL) to assess whether altered GSL profiles in GM3SD cells impacted the abundance of cell surface proteins, in particular those associated with lipid rafts (Deborah A. Brown & London, 1997; D. A. Brown & Rose, 1992; K. Sandhoff & Kolter, 2003; Simons & Ikonen, 1997). SEEL installs a biotin moiety onto desialylated N-linked glycans of cell surface glycoproteins, allowing their subsequent high-affinity capture and enrichment for proteomic analysis (Mbua et al., 2013). We applied SEEL to NCCs derived from WT and p.Glu355Lys iPSCs at day 35 of differentiation, captured the resulting biotinylated proteins by immunoprecipitation with anti-biotin antibody, and resolved the precipitated proteins by SDS-PAGE (**Figure 2.7A**).

Subsequent in-gel tryptic digestion and LC-MS/MS analysis identified 120 proteins in WT and 160 proteins in p.Glu355Lys detected at > 10 spectral counts (range 10-460). Gene Ontology (GO) analysis indicated that 96% of the identified proteins were cell surface or cell-surface associated and 4% were nuclear or cytoplasmic. Thus, our SEEL

method achieved a stringent enrichment of cell-surface glycoproteins and provided a pool of protein identities for further analysis. After filtering the total protein identifications to exclude the low-level of contamination with cytoplasmic and nuclear proteins, quantification by spectral counts demonstrated that 73% of the identified cell surface proteins were increased and 27% were decreased in abundance in p.Glu355Lys NCCs compared to WT NCCs.

To assess the impact of GM3SD on the membrane raft and the endocytic pathway proteome, we filtered the identified membrane proteins for GO assignments to the ontologic terms “membrane raft” (GO:0045121) and “endosome” (GO:0005768). Of the total protein identifications, 28% of WT (33 proteins) and 20% of p.Glu355Lys (32 proteins) were annotated with these GO classifications. Among the membrane raft protein identifications, 11 were increased and 3 were decreased in p.Glu355Lys compared to WT (**Figure 2.7B**). Among the raft-associated proteins, several adhesion receptors (CAD13, CAD15, ICAM1) were detected in WT NCCs that were absent or significantly reduced in p.Glu355Lys NCCs, while other adhesion receptors (DAG1, ITA1, CAD2) were enriched in p.Glu355Lys NCCs compared to WT. Several endocytic receptors, signaling, and adaptor proteins were increased in abundance at the plasma membrane in p.Glu355Lys NCCs in comparison to WT, while a single signaling receptor, a receptor tyrosine kinase (ERBB2) and two peptide hormone processing enzymes (ECE1, LNPEP) were reduced.

A major component of raft/endosomal membrane trafficking, sortilin (SORT1), was not detected on p.Glu355Lys NCCs following SEEL-based enrichment, but was detected at the surface of WT NCCs. However, western blot analysis of whole cell lysates demonstrated that p.Glu355Lys cells express SORT1 at levels similar to WT NCCs

(**Supplement Figure 2.2A**). Likewise, NOTCH2, a cell surface receptor important for NCC differentiation into peripheral neurons and other NC-derived cell types, was also not detected following SEEL in p.Glu355Lys NCC cells, but was detected at the surface of WT NCCs, despite being expressed and detected in whole cell lysates (**Supplement Figure 2.2B**). These results indicate that decreased ability to detect these cell surface receptors in GM3SD cells, compared to WT cells, was not due to lack of expression.

GM3 synthase deficiency disrupts protein O-GlcNAcylation, a downstream effector of multiple cell signaling pathways

Protein O-GlcNAcylation is a dynamic modification found on many nuclear and cytoplasmic proteins and is responsive to a broad range of cellular signaling activities, similar to protein phosphorylation. To assess the fidelity of protein O-GlcNAcylation in the absence of complex gangliosides, we probed whole cell lysates for the presence of O-GlcNAc in iPSCs and NCCs derived from WT and GM3SD cells (**Figure 2.8**). For both WT and GM3SD cells, the abundance of O-GlcNAc modified proteins increased upon differentiation of iPSCs to NCCS (**Figure 2.8** and **Supplement Figure 2.3**). For WT cells, the increase in O-GlcNAcylation in NCCs reached statistical significance ($P<0.02$) compared to iPSCs. For p.Glu355Lys and p.Arg288Ter cells, O-GlcNAcylation levels were also increased in NCCs, but the variance in the detected levels was too great to reach statistical significance. Nonetheless, the fold-increase in O-GlcNAcylation in NCCs relative to iPSCs for each separate differentiation was comparable for WT, p.Glu355Lys, and p.Arg288Ter: 3.4 ± 0.9 in WT, 4.1 ± 1.1 in p.Glu355Lys, and 3.6 ± 0.8 in p.Arg288Ter cells ($p>0.05$ for pairwise comparisons, n=3 independent differentiations for each cell type). The apparent molecular weight profile of proteins detectable by western blot of one-

dimensional SDS-PAGE gels was also different in iPSCs compared to NCCs, but was not qualitatively altered across genotypes (**Supplement Figure 2.3**).

Receptor tyrosine kinases are impacted by GM3 synthase deficiency

To assess whether GM3SD broadly impacts cell surface signaling events that lie upstream of protein O-GlcNAcylation, we used an array-based approach to query receptor tyrosine kinase (RTK) activity in whole-cell lysates prepared from WT and p.Glu355Lys iPSCs and NCCs at day 19 of differentiation. This method takes advantage of immobilized antibodies to capture RTKs from cell lysates for subsequent detection of the phosphorylation status of the captured RTKs following incubation of the blots with a pan-phosphotyrosine antibody. The major RTKs detected in WT and GM3SD iPSC lysates were EGFR, ERBB3, INSR, and IGF2, each of which were detected at approximately equal intensity comparing WT to GM3SD (**Supplement Figure 2.4A**). Upon differentiation to NCCs, ERBB3 intensity was increased, while EGFR, INSR, and IGF1 intensities were not substantially modified (**Supplement Figure 2.4B**). EGFR was similar to WT in GM3SD NCC lysates, while INSR and IGF-1 intensities were slightly decreased. Most striking, however, was the loss of ERBB3 detection in GM3SD NCC lysates. This array-based method reports changes in the overall phosphorylation of the represented RTKs but does not resolve whether the changes relate to altered activity or differences in protein expression. Therefore, we independently assessed the steady-state levels of EGFR and ERBB3 receptors during NCC differentiation.

EGFR (also known as ERBB1) possesses a binding domain in its extracellular region that interacts with gangliosides, in particular GM3 (Miljan et al., 2002). EGFR also forms a heterodimer with ERBB3, thought to be a poor kinase by itself, to facilitate

signaling in response to heregulin/neuregulin binding (Black, Longo, & Carroll, 2019; Shih, Telesco, & Radhakrishnan, 2011; Steinkamp et al., 2014). To understand whether the differences in ERBB3 detected on the array blots resulted from altered phosphorylation or from differential protein expression/stability, we probed cell lysates with phosphorylation-independent antibodies for EGFR and ERBB3 across the time course of differentiation from iPSCs to NCCs (**Supplement Figure 2.4C,D,E**). As WT iPSCs differentiate toward NCCs, they exhibit a reproducible and complementary expression profile in which EGFR increases early in differentiation compared to iPSCs and then decreases upon completion of the differentiation process (**Figure 2.9A**). ERBB3 mirrors the EGFR profile, exhibiting an early decrease in abundance that transforms into increased abundance in NCCs compared to iPSCs. The evolving time course of EGFR and ErbB3 expression during differentiation from iPSCs to NCCs was highly reproducible across biological replicates, with the maximum variability occurring during times of greatest change in receptor expression (d0-d15 of differentiation).

We assessed EGFR and ERBB3 expression in p.Glu355Lys and p.Arg288Ter cells across the same differentiation course from iPSCs to NCCs and compared the GM3SD cells to WT (**Figure 2.9B,C** and **Table 2**). Both the p.Glu355Lys and p.Arg288Ter cell populations exhibit significant variation from WT across all timepoints of differentiation. For EGFR, significant differences across the three cell populations were detected during mid (d11-22) and late (d3-32) stages of differentiation (ANOVA $p<0.01$ and $p<0.001$, respectively). Pairwise comparisons demonstrated that EGFR expression in p.Glu355Lys was significantly decreased compared to WT at late stages ($p<0.05$), while expression in p.Arg288Ter was significantly increased in mid and late stages ($p<0.01$ and $p<0.05$,

respectively). For ERBB3, significant differences were also detected in GM3SD cells compared to WT, especially at mid stages of differentiation (ANOVA $p<0.05$). Pairwise comparisons demonstrated that ERBB3 expression in p.Glu355Lys was significantly reduced at this stage ($p<0.05$) but p.Arg288Ter was not significantly different from WT. Pairwise comparisons of EGFR and ERBB3 expression between p.Glu355Lys and p.Arg288Ter further highlight subtle differences between the two GM3SD cell populations, with EGFR expression more highly impacted in p.Arg288Ter and ERBB3 more impacted in p.Glu355Lys cells. Furthermore, the deviation detected for EGFR and ERBB3 in the p.Glu355Lys cells is consistent with the RTK blot, namely ERBB3 was affected more than EGFR at d19 of differentiation (see **Supplement Figure 2.4**).

EGFR/ERBB3-dependent cell survival is compromised in GM3 synthase deficiency cells

EGFR and ERBB3 signaling support cell survival (Holbro et al., 2003; Wee & Wang, 2017). Fluctuations in these signaling pathways may therefore lead to decreased survival of differentiating cells. We investigated the impact of altered abundance of these essential RTKs on cell survival by assessing the appearance of cleaved caspase3, an apoptotic effector, in differentiating GM3SD cells (**Figure 2.10**). While cleaved caspase3 was detected in WT and both GM3SD iPSCs, it decreased to undetectable levels in WT cells by the mid-point of differentiation to NCCs (**Figure 2.10A**). In contrast, levels of cleaved caspase3 remained detectable through d13 in differentiating p.Glu355Lys cells (**Figure 2.10B**) and through d17 in p.Arg288Ter cells (**Figure 2.10C**). This result suggested that GM3SD cells are more prone to programmed cell death during differentiation to NCCs, a phenotype that may relate to altered EGFR/ERBB3 abundance.

In order to test the hypothesis that altered ganglioside and glycolipid biosynthesis increases the likelihood of cell death, we stressed the EGFR/ERBB3 signaling pathway by exposing cells to erlotinib, a pharmacologic inhibitor of EGFR signaling, at the midpoint (d11 – d13) of iPSC differentiation to NCCs(Rukazenkov et al., 2009). We observed that treatment with erlotnib resulted in significant detachment of presumably apoptotic cells from the surface of the tissue culture well. GM3SD cells dissociated from the surface of the culture well to a much greater extent than WT cells and significant levels of cleaved caspase3 were detected within the floating cell population (**Supplement Figure 2.5A**). Exposure of WT cells to 100 µM erlotinib for 24 - 48 hours resulted in a consistent and time-dependent increase in the ratio of cleaved to full-length caspase3, although the increase did not achieve statistical signifcance (**Table 3** and **Figure 2.10D**). In both populations of GM3SD cells, cleaved caspase3 levels were markedly more variable than in WT with or without erlotnib treatment. Upon erlotnib challenge, p.Glu355Lys and p.Arg288Ter cells exhibited statistically significant increases in cleaved caspase3 at one or more timepoints whether the GM3SD cells were compared to erlotnib-treated or vehicle-treated WT cells (**Table 3** and **Figure 2.10D**). Collectively, these findings demonstrate an increased sensitivity of the GM3SD cells to erlotinib during NCC differentiation, a phenotype that may relate to unregulated expression/abundance of RTKs such as EGFR/ERBB3 during critical stages of differentiation.

Pharmacologic inhibition of O-GlcNAcase rescues viability of GM3 synthase deficiency cells

Protein O-GlcNAcylation is responsive to many cellular response pathways and has been proposed to serve as a signal integrator that regulates downstream effectors(Hart,

2019). The increase in O-GlcNAcylation that we detected in WT NCCs compared to iPSCs and the indication that absolute levels of protein O-GlcNAcylation are more variable in GM3SD cells than in WT (see **Figure 2.8**), suggested that pharmacologic manipulation of O-GlcNAcylation might attenuate the impact of altered EGFR/ERBB3 expression in GM3SD cells. To test this hypothesis, we treated WT and p.Arg288Ter cells with thiamet G, a specific inhibitor of the hexosaminidase (O-GlcNAcase) responsible for removing O-GlcNAc from nuclear and cytoplasmic proteins, with or without co-treatment with erlotnib (**Figure 2.10E** and **Supplement Figure 2.5B**). Since p.Arg288Ter cells exhibited greater cleaved caspase than p.Glu355Lys cells during unperturbed differentiation (compare **Figure 2.10B,C**) and following 48-hour treatment with erlotnib (**Figure 2.10D**), we chose to treat this population of cells as a more stringent test of the hypothesis. While thiamet G treatment tended to decrease cleaved caspase3 in WT cells, the decreases were not significant when comparing thiamet G treatment to vehicle alone, erlotnib alone, or to thiamet G + erlotnib treatment at 24 or 48 hours of exposure (**Table 4**). Dual treatment of p.Arg288Ter cells with erlotnib and thiamet G resulted in cleaved caspase3 levels that were reduced compared to erlotnib alone (compare **Figure 2.10D,E**). Although trending upwards from 24 to 48 hours of dual exposure in p.Arg288Ter cells, the cleaved caspase ratio was statistically indistinguishable from erlotnib treated WT cells at 24 and 48 hours of exposure, indicating that increased O-GlcNAcylation rescued erlotnib-induced apoptosis of GM3SD cells (**Figure 2.10E** and **Table 4**).

DISCUSSION

Complex gangliosides are essential components of the extracellular leaflet of the plasma membrane of neural cells. Subsets of these GSLs, including GM3, preferentially partition into lipid microdomains that are also enriched in cell-signaling receptors and adhesion molecules(D. A. Brown & Rose, 1992; K. Sandhoff & Kolter, 2003). Therefore, mutations in the biosynthetic enzymes responsible for generating GSLs would be expected to impart significant pathology. Surprisingly, however, the first reports of a mouse knockout of *St3gal5* described a relatively normal animal capable of surviving and reproducing(Yamashita et al., 2003). Subsequent analysis demonstrated more subtle defects such as cochlear neuronal cell death, reduced male fertility, altered insulin receptor signaling, and skewed inflammatory responses (R. Sandhoff et al., 2005; Yamashita et al., 2003; Yamashita et al., 2005; Yoshikawa et al., 2015; Yoshikawa et al., 2009). The relatively mild nature of the mouse *St3gal5* knockout phenotype has been proposed to result from the ability of that organism to efficiently sialylate extended GSL cores on external Gal residues to generate o-series GSLs (**Figure 2.1**). These gangliosides, which we refer to here as alternatively sialylated gangliosides, were proposed to be capable of at least partially compensating for loss of the a-, b-, and c-series gangliosides (Collins et al., 1999). Our previously published work on p.Glu355Lys patient fibroblasts demonstrated that human fibroblasts do not possess a robust capacity to produce significant amounts of o-series, alternatively sialylated gangliosides (Boccuto et al., 2014). It was thought that in the absence of this alternative GSL biosynthetic capacity, patients with GM3SD manifest significant neurologic complications that are not currently well modeled in the mouse. Therefore, we took advantage of iPSC technology to investigate the cellular consequences

of altered ganglioside biosynthesis during human neural cell differentiation in two different GM3SD variants.

Consistent with our previous report on p.Glu355Lys fibroblasts, GSL profiles of iPSCs and NCCs from both GM3SD variants were devoid of GM3 and GM3-derived GSLs (Boccuto et al., 2014; Simpson et al., 2004). Other than loss of GM3, the GSL profile of GM3SD iPSCs was strikingly similar to WT, suggesting that GM3SD should be expected to have a minimal impact on the maintenance of pluripotency and, perhaps, of neural stem cell populations in developing or mature brains. However, the value of modeling human disease in iPSC-derived cell populations became apparent upon differentiation of GM3SD cells to NCC, as neural-specific and variant-specific changes in GSL profiles became evident. In GM3SD NCCs, the absence of a-, b-, and c-series gangliosides was associated with large increases in LacCer, the precursor to GM3, and parallel increases in globo- and lacto-series GSLs compared to WT. Other neural-specific changes in GM3SD cells included enhanced production of the alternatively sialylated gangliosides GM1b and GD1c in p.Glu355Lys and greater retention of LacCer in p.Arg288Ter cells compared to each other and to WT. Another more subtle difference between the GSL profiles of GM3SD cells was noted in the detection and characterization of minor GSLs with extended LacNAc structures. Non-sialylated extended LacNAc structures were more abundant in p.Arg288Ter NCCs, whereas extended LacNAc structures were more likely to be sialylated in p.Glu355Lys NCCs. Thus, a hallmark of human GM3SD is the retention and partial rerouting of LacCer into other biosynthetic pathways. The extent to which the clinical phenotypes of GM3SD arise from elevated LacCer, reduced complex ganglioside biosynthesis, or a combination of both remains unknown, but the iPSCs and NCCs we

describe here provide a useful platform to investigate the impact of GSL imbalance at the cellular level.

It is important to note that neither the p.Glu355Lys or p.Arg288Ter variant polypeptides have yet been detected as endogenously expressed proteins in human tissues or derived cells. However, both proteins are produced when expressed as epitope-tagged forms in HEK cells but lack measurable transferase activity (Indellicato et al., 2019). Thus, while both variants are functionally null, it remains to be determined whether mRNA produced from an endogenous variant *ST3GAL5* gene locus can lead to the translation of a stable enzyme variant. The molecular nature of the two ST3GAL5 protein variants fails to suggest an obvious mechanism by which either might differentially impact alternative sialylation. Thus, the mechanism for the retention of LacCer precursor or for the production of alternatively sialylated GSLs most likely entails a nuanced, but yet-to-be characterized, shift in the functional organization of GSL processing in the secretory pathway. Such a reorganization might arise from altered cell-surface signaling or from the association of non-functional ST3GAL5 protein with other glycosyltransferases. The latter of these non-exclusive possibilities has been proposed as a general feature of enzymes involved in GSL biosynthesis (H. J. Maccioni, Quiroga, & Ferrari, 2011; H. J. F. Maccioni, Quiroga, & Spessott, 2011).

SEEL-based capture of cell surface glycoproteins in WT and p.Glu355Lys NCCs identified both enrichment and loss of membrane raft associated proteins whose GO functions indicate roles in cell adhesion, cell signaling, axon pathfinding, neurogenesis, nervous system development, and cell migration. Neuropathological data at cellular resolution is not yet available for GM3SD brain tissue, making it difficult to associate

specific cellular and developmental processes (neuroblast/neural stem cell proliferation and migration, axonal/dendritic outgrowth, neuropil expansion, myelination, etc.) with altered ganglioside biosynthesis. However, delayed neurologic development and reduced cranial growth are characteristic of GM3SD and point to likely impairments in the types of functions associated with the proteins whose presence we detected as altered at the cell surface of GM3SD cells (Bowser et al., 2019). Minimally, these changes are consistent with material changes in the physicochemical nature of the plasma membrane and in membrane subdomains relevant for signaling and adhesion.

Although the molecular mechanisms by which specific GSLs contribute to the self-associative generation or stabilization of signaling microdomains remain elusive, direct interactions between GM3 and RTKs such as EGFR have been functionally and structurally demonstrated (Bremer, Hakomori, Bowen-Pope, Raines, & Ross, 1984; Bremer, Schlessinger, & Hakomori, 1986; Laine & Hakomori, 1973; Miljan et al., 2002; Wang, Sun, & Paller, 2003). Weak, potentially disruptive binding between EGFR or other RTKs and the alternatively sialylated GSLs produced by GM3SD cells may significantly impact the efficiency of receptor partition into signaling domains, the efficacy of their signaling activity, or the extent of their residence time at the cell surface (**Figure 2.11**). As pluripotent WT cells proceed down any particular differentiation pathway (e.g. to NCCs), receptor signaling activates and inhibits various cellular effector functions to appropriately tune or balance responses toward achieving a particular endpoint. Phosphorylation and O-GlcNAcylation of effector proteins are frequently responsible for driving these responses (**Figure 2.11A**).

We propose that GM3SD generates aberrant populations of signaling domains that may be more heterogeneous in their size and/or functionality compared to WT (**Figure 2.11B**). Some domains may be too small or unstable to accommodate the signaling machinery of specific receptors while others may be larger than in WT, resulting in suppressed or enhanced signaling, respectively, and/or altered residence time for receptors at the surface. We propose that the confluence of multiple effects associated with altered glycosphingolipid biosynthesis generates unstable and highly variable signaling responses, such as shown here for EGFR and ERBB3. The origin of the variability of these responses in GM3SD cells is biological and not technical in nature since WT cells that are grown, differentiated, and assayed at the same time as GM3SD cells exhibit reproducible trends with minimal variability across the course of independent differentiations from iPSC to NCC (**Figure 2.9A**). Together, the impact of the modified membrane domains may result in altered effector responses that impact survivability and other yet-to-be identified characteristics of GM3SD cells. Although beyond the scope of our current characterization, the GM3SD cells we describe here provide novel opportunities to assess the impact of altered GSL biosynthesis on the biophysical characteristics and GSL-dependent enrichment of proteins and lipid types associated with lipid microdomains in any cell type that can be derived from iPSCs.

While protein phosphorylation is well recognized as a regulatory post-translational modification, many nuclear and cytoplasmic proteins are also modified by the addition of O-linked GlcNAc at Ser/Thr residues in response to a broad range of cellular signaling activities. O-GlcNAcylation is dynamically driven by the cellular micro-environment, nutrient availability, cell stress, cell cycle, growth factors and associated developmental

events, as well as other signals (Hart, 2019). Thus, like phosphorylation, the profile of O-GlcNAcylated proteins reflects the integration of signals through multiple pathways. We demonstrated that protein O-GlcNAcylation increased as WT and GM3SD iPSCs differentiated to NCCs but the amount of O-GlcNAc modification was much more broadly distributed in GM3SD cells. By pharmacologically enhancing O-GlcNAcylation with thiamet G, cleaved caspase3 levels were significantly reduced in WT and GM3SD cells in the presence or absence of erlotnib (Jiang et al., 2017; Yuzwa et al., 2008). This intervention suggests that, despite broad variation in the expression of primary signaling receptors like EGFR and ERBB3, modulation of downstream effectors can rescue the impact of altered GSL biosynthesis on basic cellular processes in neural lineages (**Figure 2.11B**).

An important caveat for the studies reported here is that our observations are based on iPSCs derived from a single representative of each of the p.Glu355Lys and p.Arg288Ter variants. It will be essential to continuously evaluate individual-to-individual variation in patient-derived cell types as more patient samples become available. Nonetheless, significant individual-to-individual variation in plasma GSL abundance and ceramide diversity was not previously detected in the p.Arg288Ter GM3SD patient population (Kazuhiro Aoki et al., 2019). Comparing 8 unrelated p.Arg288Ter individuals to the mean value for 19 non-affected individuals in this prior study, the fold-increase in LacCer abundance was 1.9 ± 0.1 (CV%=5.2%) and the fold-increase in the higher mass ceramides of LacCer was 1.6 ± 0.2 (CV%=12.5%). Thus, at least within the p.Arg288Ter patient population, the major changes in GSL diversity and abundance are well conserved across unrelated individuals. While additional p.Glu355Lys patients are unlikely to become

available for future study, expanded efforts to acquire a broader range of p.Arg288Ter and other variant cell types will greatly enhance our understanding of the biochemical corelates of clinical presentation.

The relevance of iPSC-derived cell types for understanding biochemical and physiologic responses to disease-causing gene variants in patient tissues should be evaluated on a disease-by-disease basis. Previously published results characterized the fatty acid distribution of the ceramides associated with LacCer in wildtype (non-affected human subjects) and GM3SD (p.Arg288Ter homozygous subjects) patient populations (Kazuhiro Aoki et al., 2019). Analysis of the fatty acid distributions of the LacCer ceramide moieties detected in iPSCs and NCCs of WT and p.Arg288Ter revealed striking similarities between patient plasma, patient-derived iPSCs, and differentiated NCCs (**Supplement Figure 2.6**). While WT and GM3SD cells exhibited distinct fatty acid profiles, both were consistent with the plasma profiles of wildtype and p.Arg288Ter patients, respectively. Thus, despite cellular reprogramming and subsequent differentiation to NCCs, derived cells grown in tissue culture media exhibited ceramide fatty acid profiles consistent with the plasma profiles of a population of patients with the same *ST3GAL5* genotype. While the implications of such seemingly nutrient-independent fatty acid utilization remain to be determined, the conservation of ceramide heterogeneity in iPSCs and derived cell types adds support for the validity of modeling GSL-mediated cellular responses in the patient-derived cells we report here.

Our results demonstrate the importance of investigating glycosylation changes associated with mutations in glycan biosynthetic enzymes in appropriate cell types. We previously described collateral changes in N-linked and O-linked glycosylation of

glycoproteins expressed by p.Glu355Lys fibroblasts (Boccuto et al., 2014). Such collateral changes are of interest because ST3GAL5 does not act on glycans linked to proteins; it is absolutely GSL-specific. Thus, the matrix of regulatory processes that control cellular glycosylation are responsive to changes that span glycan classes. This phenomenon has also recently been demonstrated in glyco-engineered human cell lines (Huang et al., 2021). The results presented here provide the first characterization of GSL biosynthetic, cell signaling, and cellular survival changes associated with human-derived neural cells in GM3SD. We have identified global changes in GSL biosynthesis that correspond to substantial alterations in cell signaling and residence of glycoproteins at the plasma membrane. We have also identified more subtle changes that may provide differential characteristics capable of distinguishing GM3SD variants. As additional cohorts of GM3SD patients are identified and become available for analysis at the cellular level, the results reported here will provide a framework for assessing functional differences that may provide insight into clinical phenotypes. The iPSC platform we have characterized also presents opportunities to assess the potency of molecular and small-molecule therapeutic interventions that might resolve these cellular phenotypes and impact broader glycomic and pathophysiologic consequences associated with GM3SD.

TABLES and FIGURES

Table 1. GSL abundance in iPSC and NCC of WT and GM3SD variant cells quantified by mass spectrometry.

GSL[a]	Cell type and Genotype											
	iPSC						NCC					
	Wildtype		p.Glu355Lys		p.Arg288Ter		Wildtype		p.Glu355Lys		p.Arg288Ter	
	%[b]	pmol[c]	%	pmol	%	pmol	%	pmol	%	pmol	%	pmol
LacCer	33.3	277.8	38.5	230.4	29.0	90.1	11.1	35.1	42.4	138.4	75.7	390.4
Gb3	39.1	326.1	26.6	158.9	34.8	108.1	1.0	3.1	2.4	7.9	3.2	16.5
Lc3	--[d]	--	--	--	0.2	0.4	0.4	1.2	2.8	9.0	2.1	10.6
Gb4, Lc4	20.8	173.8	31.5	188.4	21.2	66.0	3.7	11.8	7.8	25.6	16.0	82.3
Fuc-Lc4	1.7	14.1	--	--	14.7	45.8	--	--	2.6	8.5	1.4	7.2
GM3	4.0	33.6	--	--	--	--	46.1	145.6	--	--	--	--
GM2	--	--	--	--	--	--	0.3	1.0	--	--	--	--
GM1a	0.3	2.6	--	--	--	--	1.5	4.6	--	--	--	--
GM1b	0.7	6.0	3.4	20.6	0.1	0.2	13.2	41.8	28.2	92.1	1.6	8.1
GD3	--	--	--	--	--	--	20.2	63.7	--	--	--	--
GD1a	--	--	--	--	--	--	0.5	1.6	--	--	--	--
GD1b	--	--	--	--	--	--	0.3	0.8	--	--	--	--
GD1c	--	--	--	--	--	--	1.8	5.5	13.6	44.5	0.1	0.7

[a]Graphical representations of quantified glycosphingolipids are shown in Figure 1 along with their abbreviations, except Fuc-Lc4, a terminally fucosylated lactotetraosylceramide (see Figures 3, 4).

[b]GSL relative abundance, denoted "%," is given as the percent that each individual GSL contributes to the total lipid profile for each cell type/genotype.

[c]GSL amount, denoted "pmol," is given as pmol/1x10^6 cells.

[d]Double dash denotes GSL not detected.

Table 2. EGFR and ERBB3 expression in iPSC and NCC of WT and GM3SD variant cells.

Differentiation Time (Days)	Receptor Expression (log2 normalized to actin)			ANOVA P-value	Pairwise T-Test P-Value		
	Wildtype Mean ± SEM (n)	**p.Glu355Lys** Mean ± SEM (n)	**p.Arg288Ter** Mean ± SEM (n)		**p.Glu355Lys *vs.* Wildtype**	**p.Arg288Ter *vs.* Wildtype**	**p.Glu355Lys *vs.* p.Arg288Ter**
EGFR							
Early (3-10)	0.61 ± 0.36 (6)	-0.10 ± 0.20 (6)	0.49 ± 0.58 (9)	0.5806	0.0572	0.8778	0.2170
Mid (11-22)	0.18 ± 0.18 (12)	0.63 ± 0.31 (12)	1.73 ± 0.38 (18)	0.0046	0.1112	0.0018	0.0235
Late (23-32)	-0.37 ± 0.18 (9)	-1.06 ± 0.20 (9)	1.44 ± 0.79 (5)	0.0005	0.0101	0.0130	0.0009
ERBB3							
Early (3-10)	-0.77 ± 0.62 (7)	-1.78 ± 0.75 (11)	-0.69 ± 0.87 (9)	0.5269	0.3586	0.9489	0.3543
Mid (11-22)	1.39 ± 0.28 (12)	-0.60 ± 0.90 (16)	1.47 ± 0.46 (16)	0.0429	0.0370	0.4473	0.0245
Late (23-32)	1.24 ± 0.48 (7)	2.68 ± 0.79 (10)	1.51 ± 0.46 (7)	0.2691	0.0945	0.7029	0.1378

P>0.05	P<0.05	P<0.01	P<0.001

Table 3. Cleaved Caspase3 in WT and GM3SD variant cells at mid-differentiation with and without EGFR inhibition by erlotnib.

Treat-ment	Cleaved Caspase3 Ratio (cleaved/uncleaved)[a]			ANOVA P-value	Pairwise T-test P-value					
	WT[b]	p.E355K	p.R288*		p.E355K *vs.* WT	p.R288* *vs.* WT	p.E355 *vs.* p.R288*	WT Erlotnib *vs.* WT Vehicle	p.E355K Erlotnib *vs.* WT Vehicle	p.R288* Erlotnib *vs.* WT Vehicle
Vehicle	0.026 ± 0.013	0.151 ± 0.076	0.368 ± 0.261	0.1506	0.0251	0.0868	0.4701	--	--	--
24 hr Erlotnib	0.115 ± 0.053	0.498 ± 0.143	0.040 ± 0.027	0.0093	0.0080	0.3826	0.0344	0.1343	0.0008	0.5805
48 hr Erlotnib	0.158 ± 0.070	0.291 ± 0.095	0.593 ± 0.202	0.0637	0.3054	0.0179	0.2484	0.0958	0.0047	0.0019

P>0.05	P<0.05	P<0.01	P<0.001

[a]Cleaved Caspase3 Ratios are given as the mean ± SEM of 3-6 independent differentiations.

[b]Cell types are abbreviated as WT (wildtype), p.E355K (p.Glu355Lys), and p.R288* (p.Arg288Ter)

Table 4. Cleaved Caspase3 in WT and GM3SD variant cells at mid-differentiation in presence of EGFR (erlotnib) and O-GlcNAcase (thiamet G) inhibition.

Treatment	Cleaved Caspase3 Ratio (cleaved/uncleaved)[a]		Pairwise T-test P-value			
	Wildtype	p.Arg288Ter	Wildtype Thiamet G *vs.* Wildtype Vehicle[b]	Wildtype Erlotnib + Thiamet G *vs.* Wildtype Thiamet G	Wildtype Erlotnib[b] *vs.* Wildtype Erlotnib + Thiamet G	p.Arg288Ter Erlotnib + Thiamet G *vs.* Wildtype Erlotnib[b]
Vehicle[b]	0.026 ± 0.013	0.368 ± 0.261	0.2455	--	--	--
Thiamet G alone	0.002 ± 0.001	0.012 ± 0.005	--	--	--	--
24 hr Erlotnib + Thiamet G	0.016 ± 0.007	0.048 ± 0.031	--	0.1101	0.2462	0.4326
48 hr Erlotnib + Thiamet G	0.028 ± 0.016	0.245 ± 0.064	--	0.1911	0.2531	0.4569

P>0.05

[a]Cleaved Caspase3 Ratios are given as the mean ± SEM of 3-6 independent differentiations.

[b]Values for these Cleaved Caspase3 Ratios taken from Table 3.

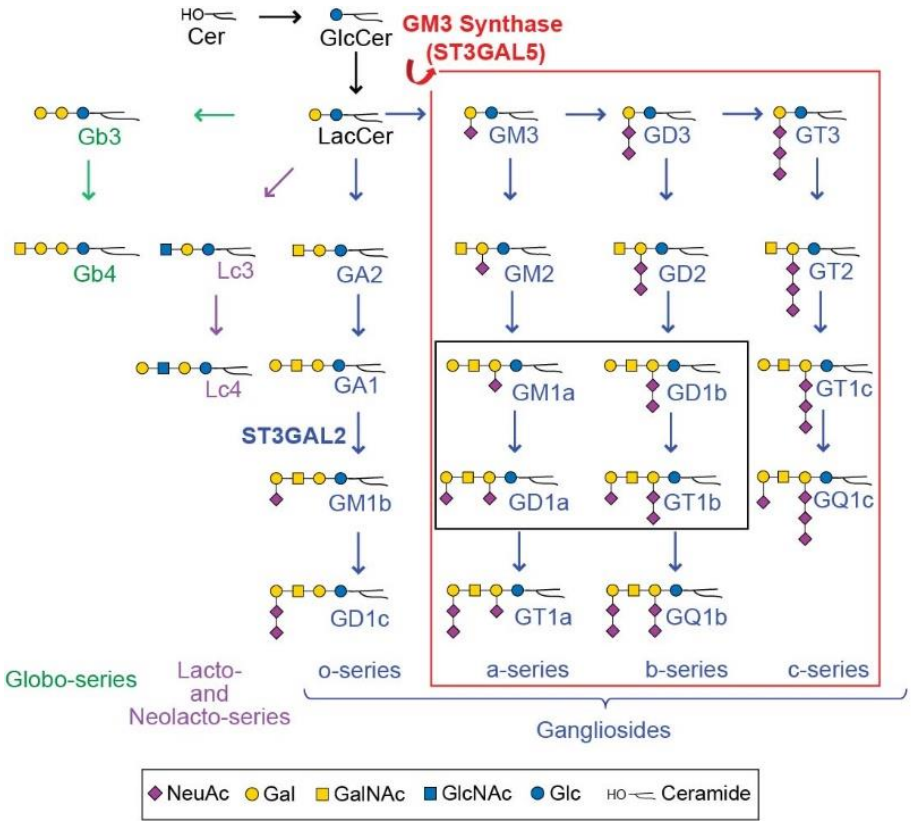

Figure 2.1. Pathways of human glycosphingolipid biosynthesis. Ceramide (Cer) is glucosylated to form glucosylceramide (GlcCer), which is elongated with a galactose to form lactosylceramide (LacCer). LacCer is the precursor for glycosphingolipid (GSL) elongation into multiple biosynthetic pathways, including the globo-, lacto/neolacto-, and ganglio-series. Sialylation of the Gal residue of LacCer by ST3GAL5 (GM3 Synthase) generates the simplest ganglio-series GSL, known as GM3. GM3 is the essential precursor for the production of all a-, b-, and c- series gangliosides (***red box***). Of these gangliosides, four are the most abundant GSLs found in neural tissue, GM1a, GD1a, GD1b and GT1b (***black box***). Graphic representations of GSL monosaccharide residues are consistent with Symbol Nomenclature for Glycans guidelines (SNFG).

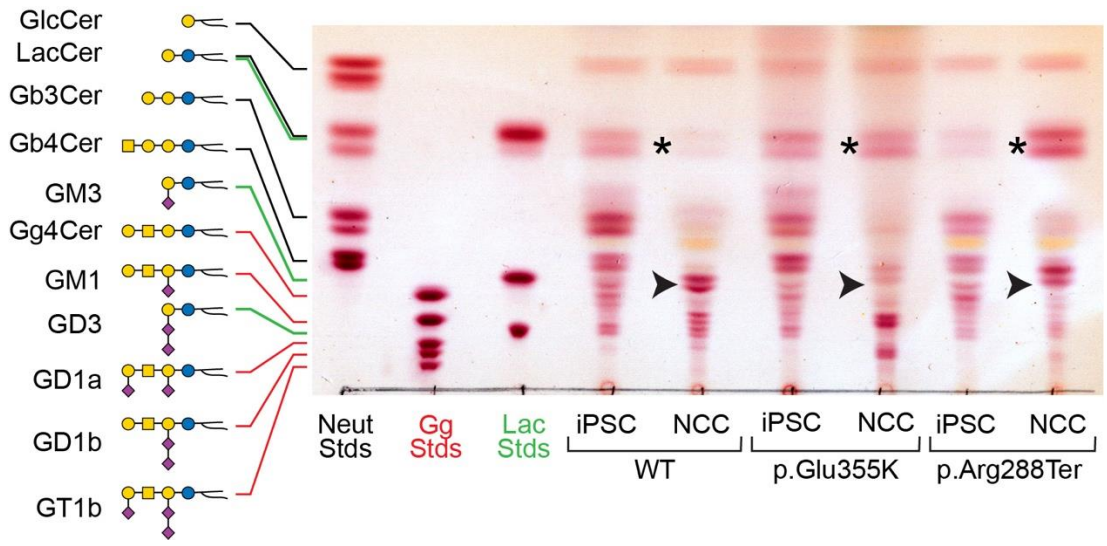

Figure 2.2. iPSCs and NCCs derived from GM3SD variants fail to produce GM3 and accumulate LacCer. GSLs extracted from WT and GM3SD patient cell types were resolved by thin-layer chromatography and visualized by staining with orcinol reagent. The mobility of three sets of GSL standards are shown for reference (***Neut***, GSLs with neutral cores of increasing length up to globotetraosylceramide, indicated by black lines; ***Gg***, GSLs with gangliotetraose cores carrying 0, 1, 2, or 3 sialic acids, indicated by red lines; ***Lac***, GSLs with a LacCer core carrying 0, 1, or 2 sialic acids, indicated by green lines). In iPSCs of all three genotypes, the GSL profile is dominated by LacCer and globo-series GSLs. Upon differentiation of WT iPSCs to NCCs, LacCer abundance decreases (***asterisk***) and the appearance of gangliosides is evident, among which GM3 is the most abundant (***arrowhead***). NCCs derived from both GM3SD genotypes retain high levels of LacCer and do not generate GM3.

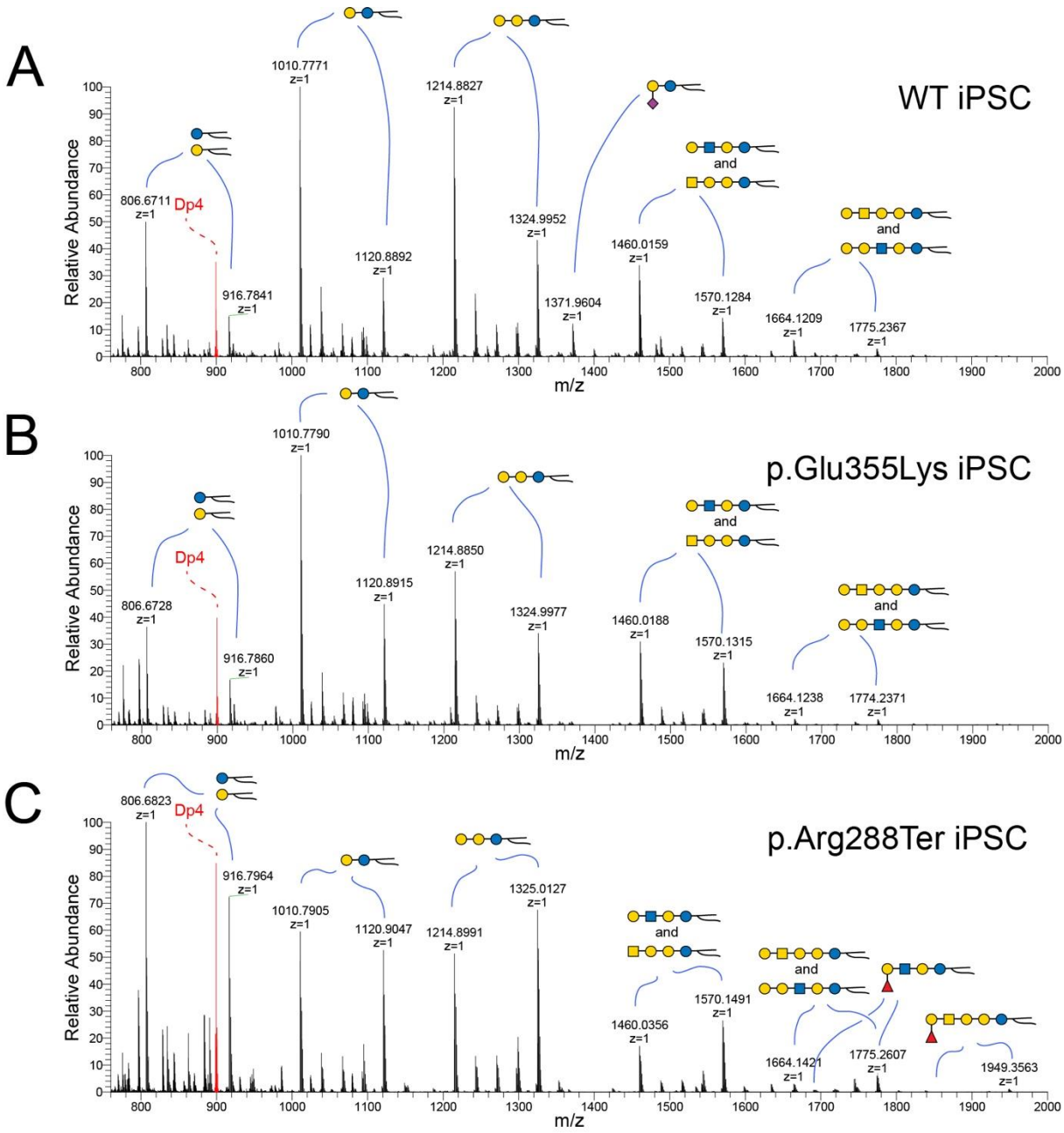

Figure 2.3. NSI-MS analysis of GSLs extracted from iPSCs detects minor differences in GSL biosynthesis and ceramide compositions. Mass spectra were obtained for permethylated intact GSLs extracted from WT (**A**), p.Glu355Lys (**B**), and p.Arg288Ter (**C**) iPSCs. GSLs with the same glycan headgroup are detected as families of related structures with differing ceramides (***highlighted by blue lines***). GM3 is a minor component of the GSL profile of WT iPSCs (***m/z 1372 in A***) but is not detected in either of the GM3SD iPSCs. Both of the GM3SD iPSCs produce a higher relative abundance of longer ceramides; compare the ratio of the LacCer form at m/z 1011 to the form at m/z 1121 across all three iPSCs. The shift in ceramide to higher mass is more pronounced in p.Arg288Ter than in p.Glu355Lys. Internal standard of permethylated maltotetraose (***m/z 885***) is shown in red (***Dp4***).

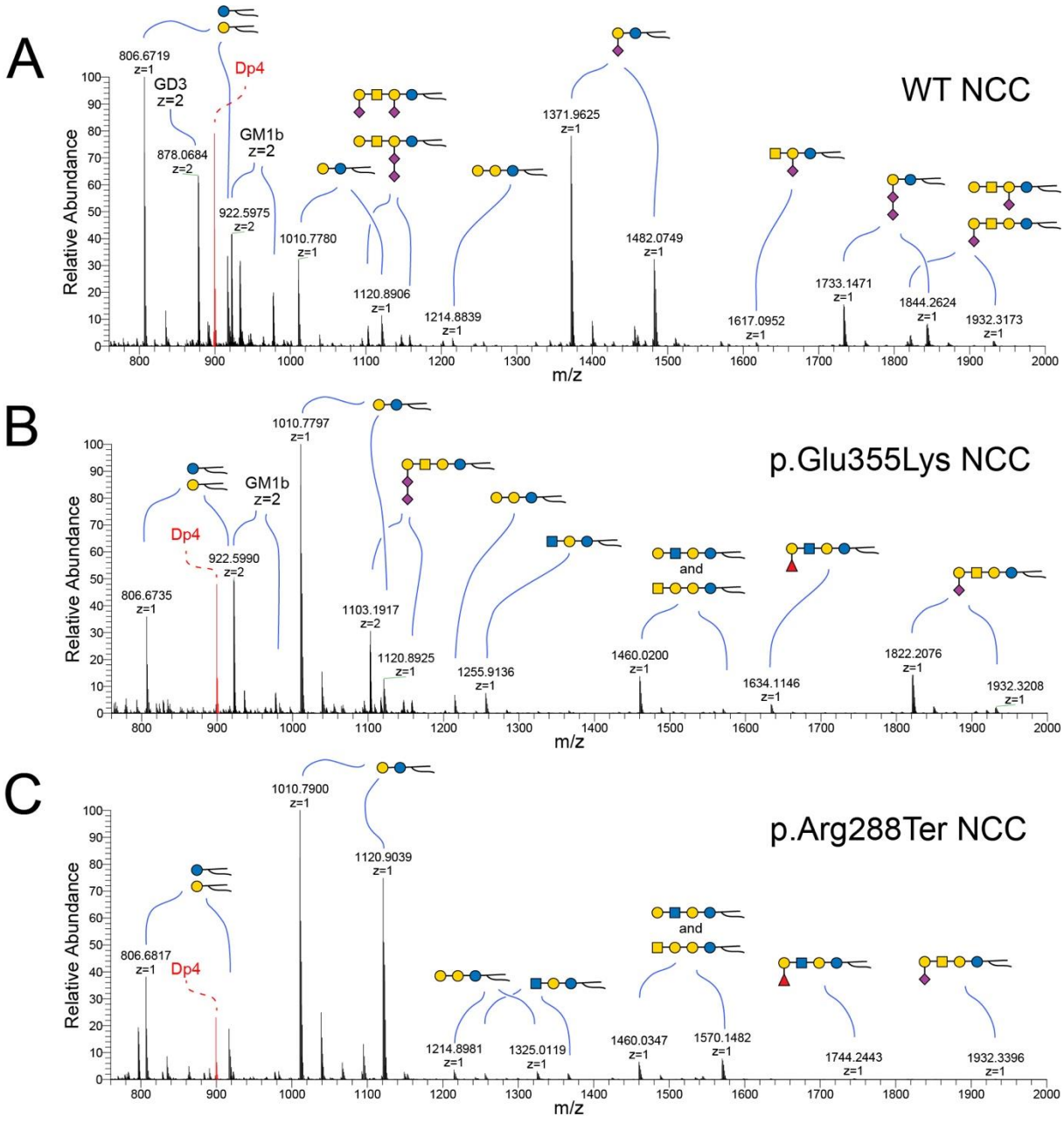

Figure 2.4. NSI-MS analysis of GSLs extracted from NCCs highlights neural cell-specific alterations in GSL biosynthesis and ceramide compositions. Mass spectra were obtained for permethylated intact GSLs extracted from WT (**A**), p.Glu355Lys (**B**), and p.Arg288Ter (**C**) NCCs. Upon differentiation of WT iPSCs to NCCs, GM3 becomes the most abundant GSL, but is not detectable in GM3SD NCCs. Both populations of GM3SD NCCs retain elevated LacCer (***m/z 1011-1103***). p.Glu355Lys NCCs synthesize alternatively sialylated GSLs, such as GM1b (***m/z 1822-1932***) and GD1c (***m/z 1103-1159, z=2***), at higher levels than p.Arg288Ter while p.Arg288Ter retains greater abundance of high mass ceramides and p.Glu355Lys exhibits reduced abundance of high mass ceramide compared to WT**.**

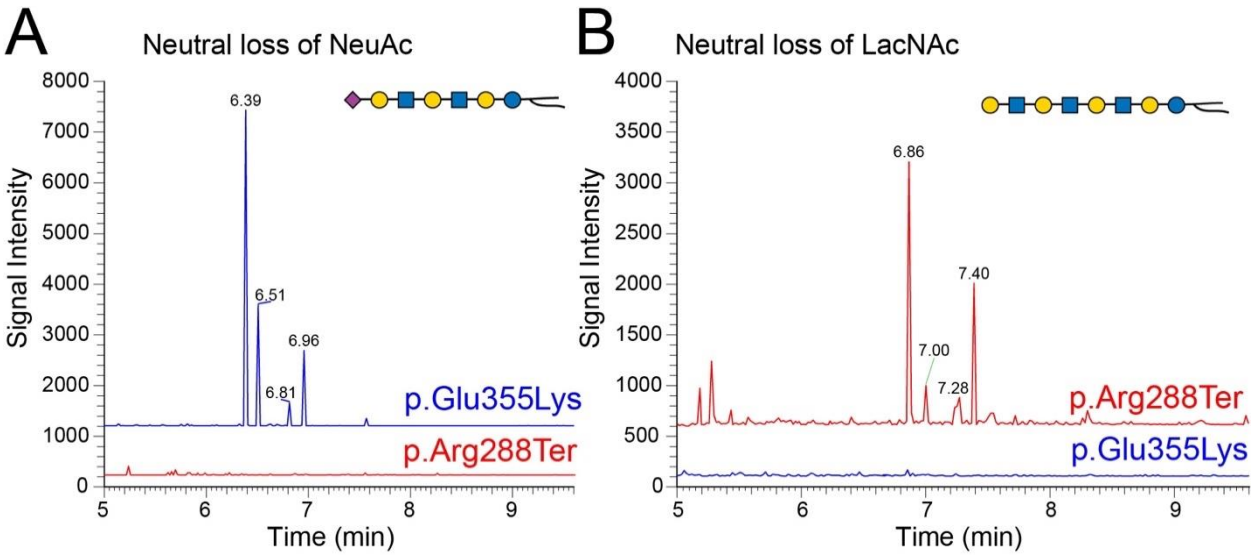

Figure 2.5. Unique GSL changes in GM3SD Variants. The results of Total Ion Monitoring workflows (TIM-chromatograms) were filtered for neutral loss of NeuAc or LacNAc. (**A**) Filtering for loss of NeuAc demonstrates that GSLs with extended LacNAc repeats capped with sialic acid are detected at higher abundance in p.Glu355Lys NCCs than in p.Arg288Ter NCCs. (**B**) Filtering for loss of LacNAc disaccharide demonstrates that non-sialylated forms of GSLs with LacNAc repeats are more abundant in p.Arg288Ter than in p.Glu355Lys NCCs. MS2 fragmentation profiles support the structural assignments at the inidicated TIM detection times (**Supplement Figure 2.1**). These less abundant unique GSLs, like the more abundant GSLs in NCCs, also show greater enrichment of higher mass ceramides in p.Arg288Ter than in p.Glu355Lys (e.g., compare the ratio of peaks at 6.96/6.39 in **A** to 7.40/6.86 in **B**).

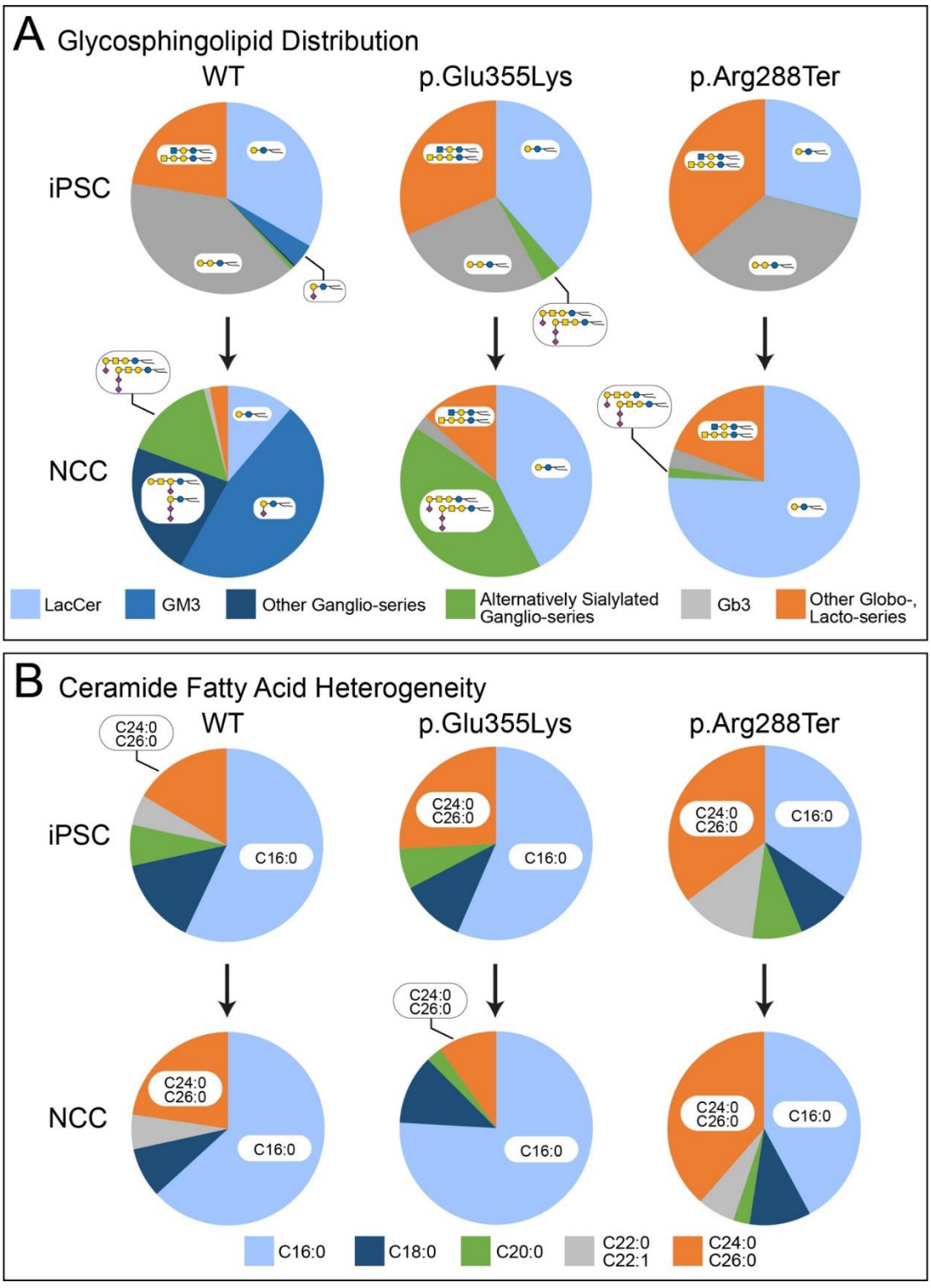

Figure 2.6. Summary of GSL and ceramide fatty acid abundance changes in iPSCs and NCCs of wildtype and GM3SD variants. The relative abundance of the major GSL types detected in iPSCs and NCCs demonstrate relatively minor differences in iPSCs but more significant changes upon differentiation to NCCs. (**A**) As WT iPSCs differentiate to NCCs, decreases in the relative abundance of LacCer, Gb3, and other Globo-, and Lacto-

series GSLs are mirrored by increases in GM3 and other Ganglio-series GSLs. Differentiation of GM3SD variant iPSCs to NCCs is accompanied by maintenance of LacCer as a major GSL and by complete lack of Ganglio-series GSLs that depend on ST3GAL5 activity. (**B**) The relative abundance of the ceramide fatty acids of LacCer were quantified. Although their iPSC fatty acid profiles are quite different, as WT and p.Arg288Ter cells differentiate to NCCs, relatively minor changes are observed, especially comparing the shortest (C16:0) to the longest (C24:0, C26:0) fatty acids. The fatty acid profile of p.Glu355Lys iPSCs is similar to WT iPSCs but as the p.Glu355Lys cells differentiate to NCCs, the relative abundance of the shortest chains (C16:0) expands at the expense of the longest chain fatty acids (C24:0, C26:0).

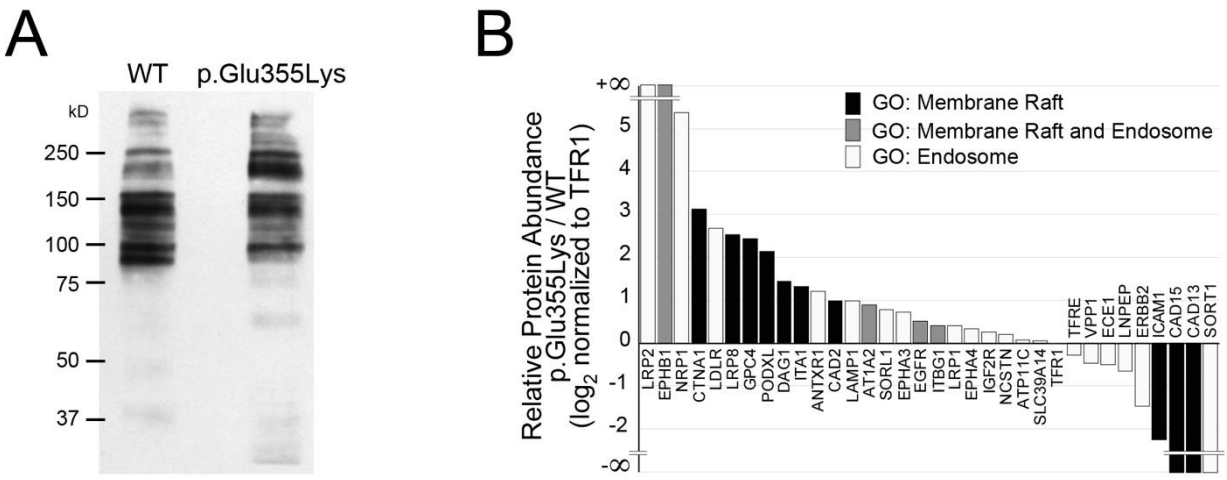

Figure 2.7. Cell surface protein abundance is altered in GM3SD cells. NCCs differentiated from WT or p.Glu355Lys iPSCs were subjected to selective-exoenzymatic labeling (SEEL) to install a biotin moiety specifically on cell surface glycoproteins. (**A**) Labeled proteins were resolved by SDS-PAGE and probed by western blot with anti-biotin antibody, revealing the presence of changes in the abundance of membrane proteins. (**B**) Gel-resolved proteins were harvested by in-gel digestion with trypsin and identified by LC-MS/MS. Identified proteins assigned to the indicated Gene Ontology (GO) categories were compared to assess the integrity of lipid rafts and the endosomal pathway. (**Supplement Table 1**).

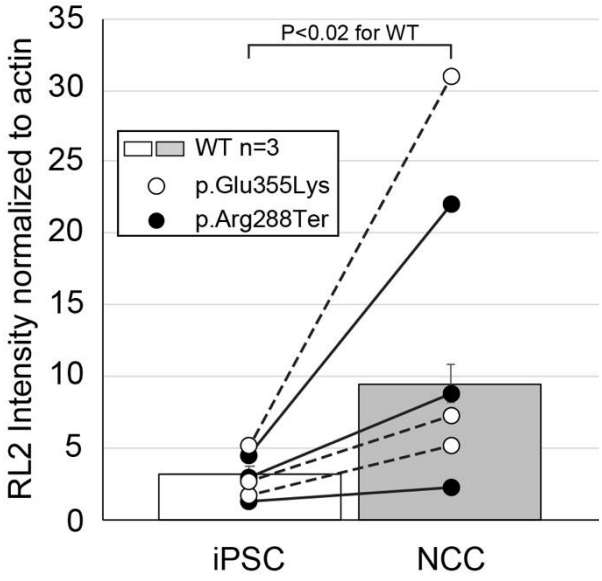

Figure 2.8. Protein O-GlcNAcylation increases upon differentiation of iPSCs to NCCs. Whole cell lysates from WT and GM3SD cells were resolved by SDS-PAGE, blotted, and probed with RL2, a monoclonal antibody that recognizes proteins modified by O-GlcNAc, and quantified by densitometry. Individual differentiation experiments for GM3SD cells are shown connected by a dashed or solid line (n=3 independent differentiations). GM3SD cell values are plotted on top of bars that represent the mean ± SEM for WT cells (n=3 independent differentiations). The statistical significance of the difference (P-value from pairwise T-test) are presented above the bars for comparison of WT iPSCs and WT NCCs O-GlcNAcylation.

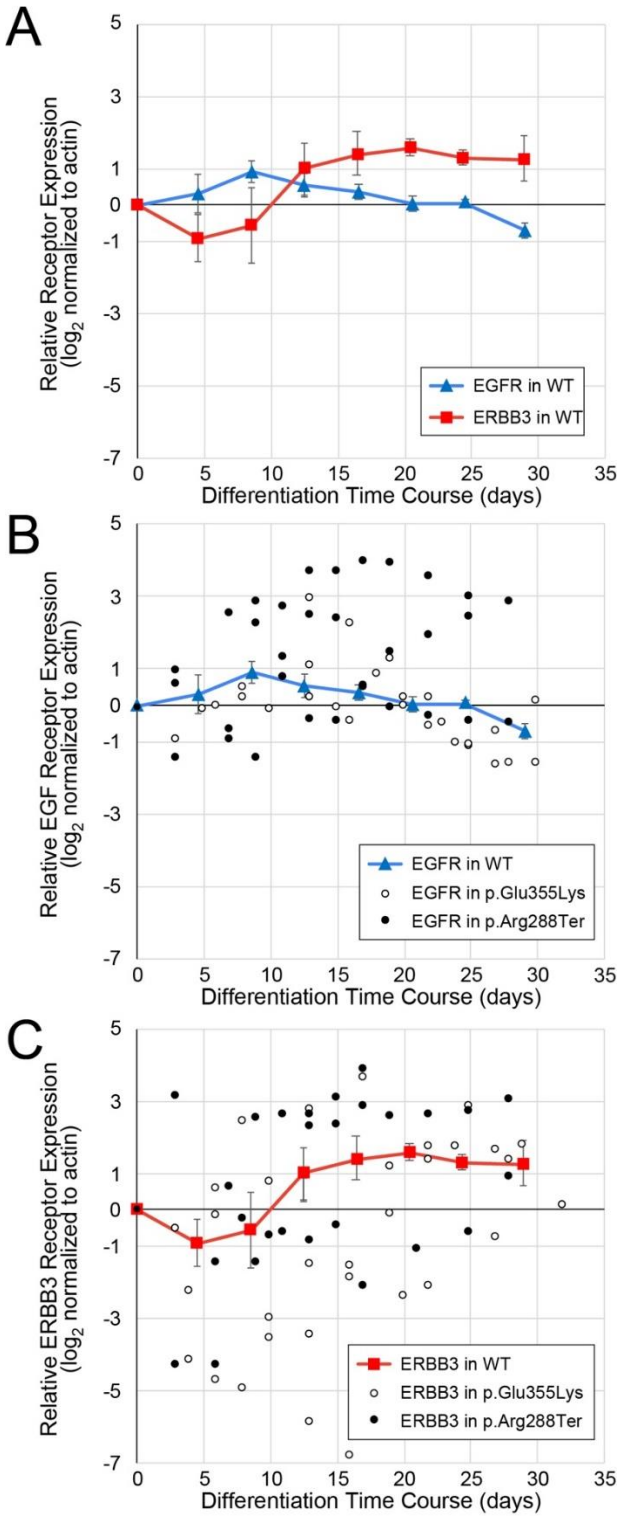

Figure 2.9. Dynamics of EGFR and ERBB3 expression during neural crest differentiation. Protein-specific, not phospho-specific, antibodies against EGFR and ERBB3 were used to quantify receptor expression in WT and GM3SD cells across full time courses of differentiation from iPSCs to NCCs (n=3 independent differentiations for

each cell type). (**A**) EGFR and ERBB3 expression mirror each other as WT iPSCs differentiate to NCCs. For simplicity of presentation and to provide a baseline reference for comparison with GM3SD cells, WT values were combined into bins that span 4 days of differentiation (mean ± SEM, n=4-6 determinations for each bin, total of 30 data points for each receptor). (**B**) Individual time points for EGFR abundance are plotted for three independent differentiations of GM3SD cells (n=27 data points for p.Glu355Lys, n=32 data points for p.Arg288Ter); WT EGFR profile is reproduced from panel A for reference. (**C**) Individual time points for ERBB3 abundance are plotted for three independent differentiations of GM3SD cells (n=37 data points for p.Glu355Lys, n=32 data points for p.Arg228Ter); WT ERBB3 profile is reproduced from panel A for reference. ***Table 2*** presents P-values for ANOVA and pairwise T-tests of ERBB3 and EGFR expression differences between WT and GM3SD cells during differentiation.

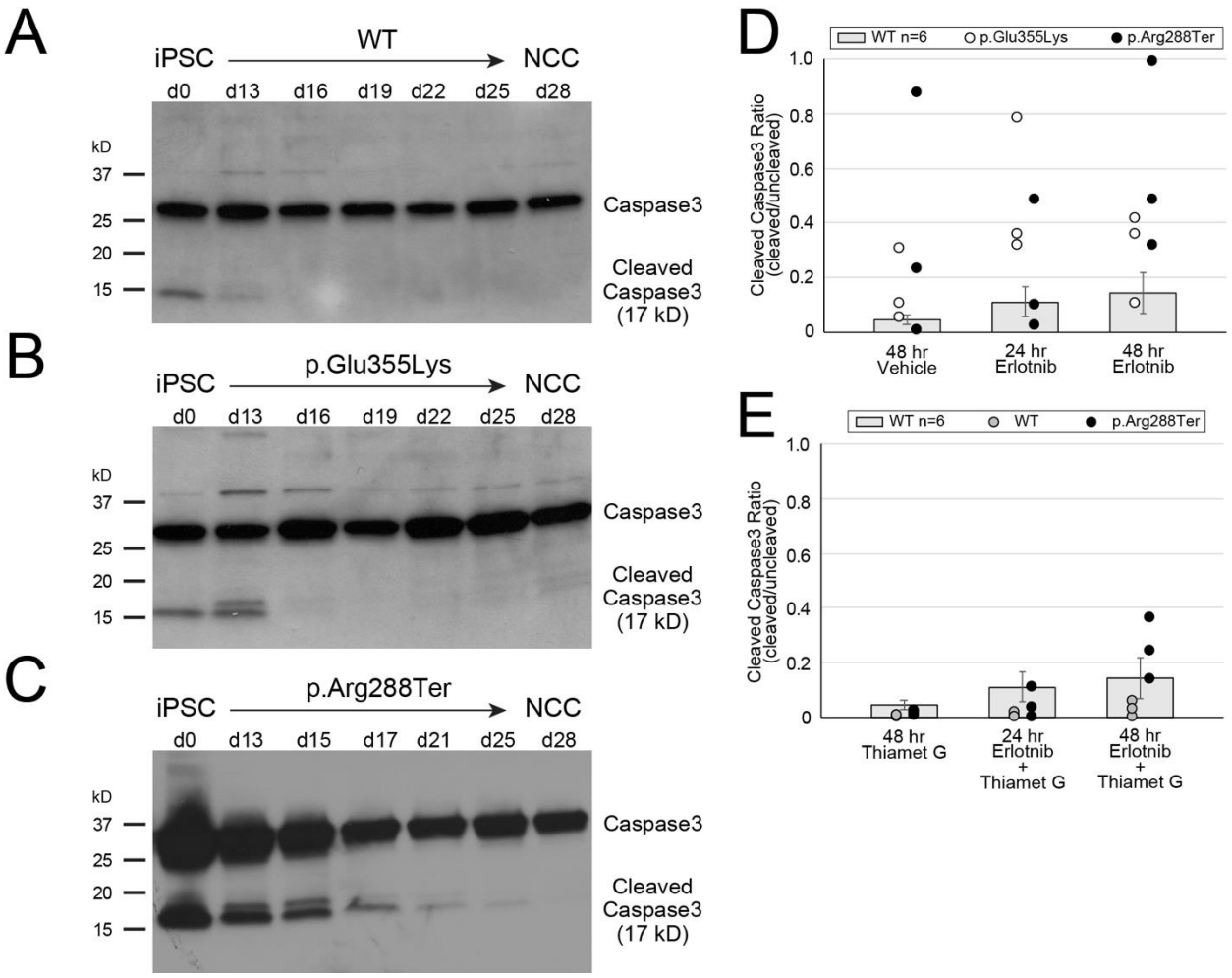

Figure 2.10. GM3SD apoptosis during differentiation is enhanced by altered EGFR signaling and rescued by increased protein O-GlcNAcylation. Apoptosis, reported by the abundance of cleaved Caspase3, is detectable in WT and GM3SD iPSC cultures (**A,B,C**) at day 0 (***d0***). As WT cells differentiate to NCCs (**A**), cleaved Caspase3 is barely detectable at the midpoint of the differentiation course (***d13***), whereas it remains at or above iPSC levels in p.Glu355Lys (**B**) and p.Arg288Ter (**C**) cells at the same time point and beyond. (**D**) GM3SD cells are more sensitive to erlotnib treatment than WT cells (GM3SD data points present 3 independent differentiations and are plotted on top of bars that present mean ± SEM for n=6 independent differentiations of WT cells treated similarly). ***Table 3*** presents P-values for ANOVA and pairwise T-tests of differences in cleaved Caspase3 between WT and GM3SD cells treated with erlotnib. (**E**) Thiamet G treatment, which enhances protein O-GlcNAcylation by inhibition of O-GlcNAcase, decreases Caspase3 cleavage in WT and p.Arg288Ter GM3SD cells. ***Table 4*** presents P-values for pairwise T-tests of differences in cleaved Caspase3 between WT and GM3SD cells treated with erlotnib and Thiamet G.

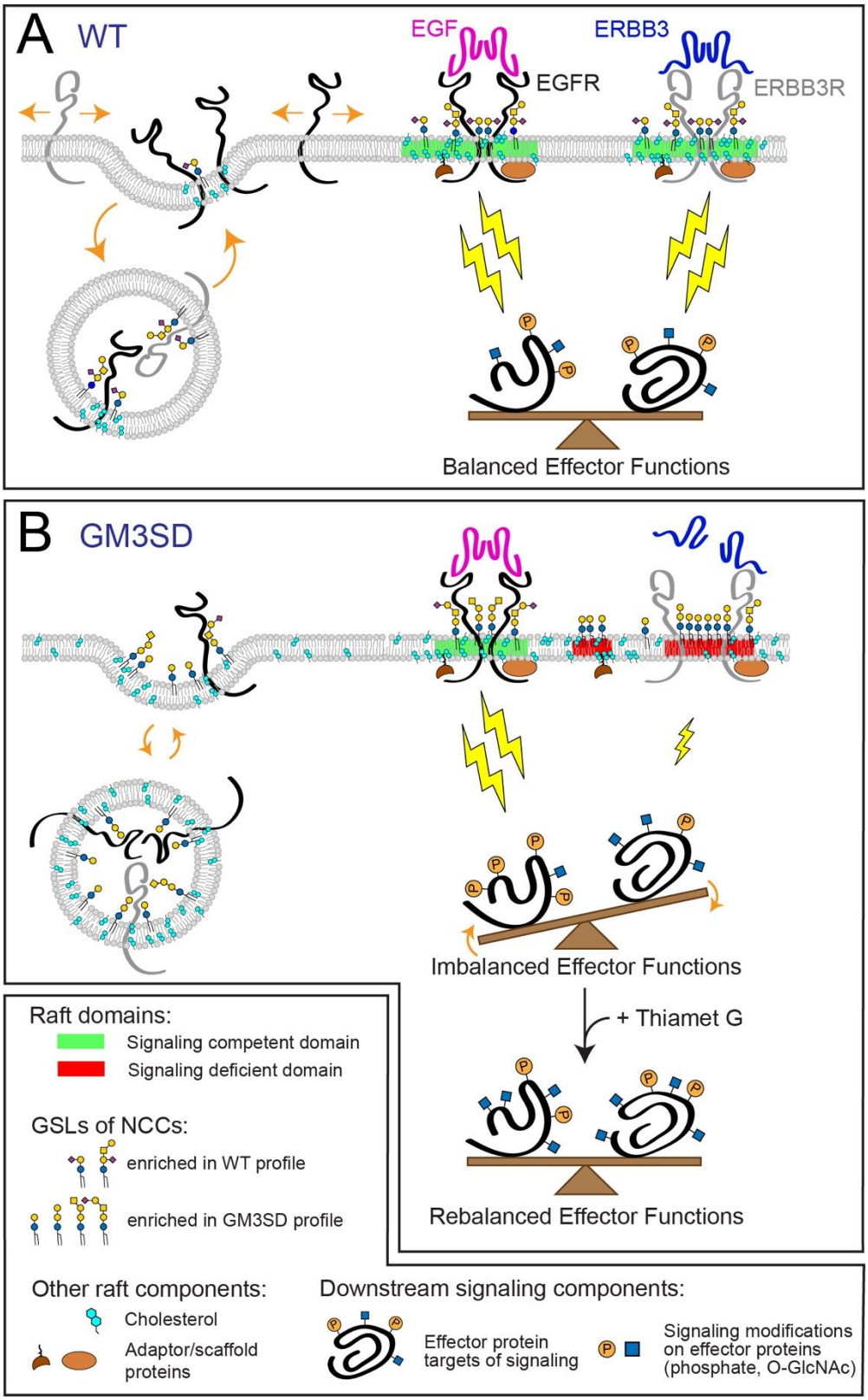

Figure 2.11. GSL composition impacts lipid rafts and cell signaling in GM3SD. Cell membrane lipid composition influences many cellular functions. Therefore, altered GSL

biosynthesis might be expected to have pleiotropic consequences, some of which are illustrated here in relation to their possible contribution to the cellular pathology associated with GM3SD. Cell surface signaling receptors are regulated by their migration in-and-out of membrane signaling domains and by the balance of their internalization/reinsertion kinetics. In WT and GM3SD cells, lipid raft characteristics reflect the physicochemical properties of the GSLs, phospholipids, and sterols that constitute the plasma membrane. (**A**) When cells are able to synthesize GM3 and its subsequent end-products, functional lipid rafts (***shaded green***) facilitate the association of signaling receptors and adaptor/scaffold proteins to appropriately stimulate downstream effectors (***lightning bolts***). Membrane recycling also buffers signaling responses by internalizing surface receptors and shuttling additional signaling capacity from intracellular storage. Effector functions are balanced by appropriate receptor activation, membrane insertion, and physical interactions within signaling domains. (**B**) In the absence of GM3, GSL compositions are shifted toward greater abundance of neutral lipids and toward the appearance of alternatively sialylated species. The characteristics of the resulting dysfunctional lipid rafts (***shaded red***) reflect deficiencies in the ability of these GSLs to interact with receptors and with other raft components. Consequently, increased or decreased signaling through modified rafts may generate imbalanced effector functions that impact cellular responses. Pharmacologic interventions, such as increasing protein O-GlcNAcylation (thiamet G), may establish an alternative balance in effector functions that counters otherwise deleterious downstream processes.

SUPPLEMENTAL FIGURES

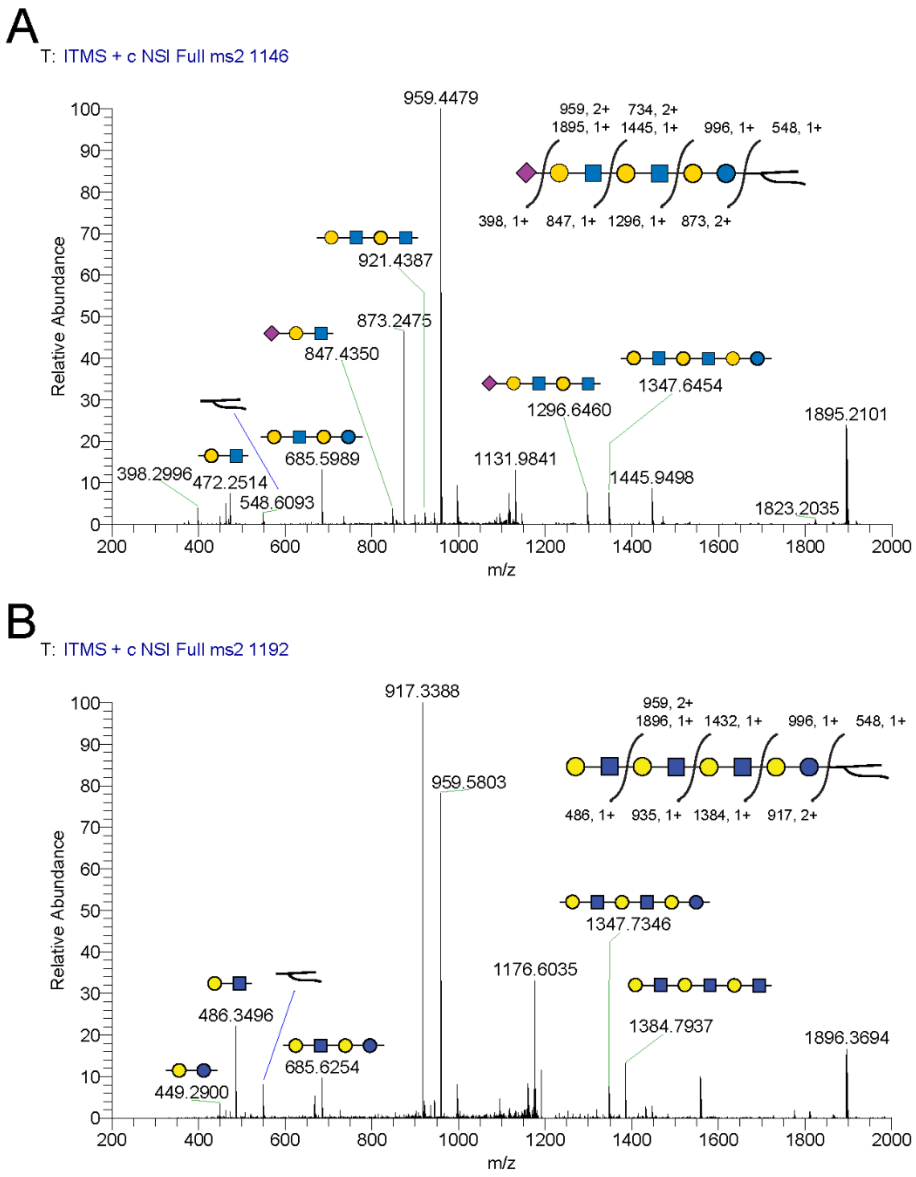

Supplement Figure 2.1. MS2 fragmentation supporting structural assignment of unique glycosphingolipids. NSI-MS/MS analysis of LacNAc-extended GSLs expressed by GM3SD NCCs. Top panel shows fragmentation of sialylated GSL detected at greater abundance in p.Glu355Lys NCCS than in p.Arg288Ter NCCs. Bottom panel shows fragmentation of non-sialylated GSL detected at greater abundance in p.Arg288Ter NCCs than in p.Arg288TerNCCs.

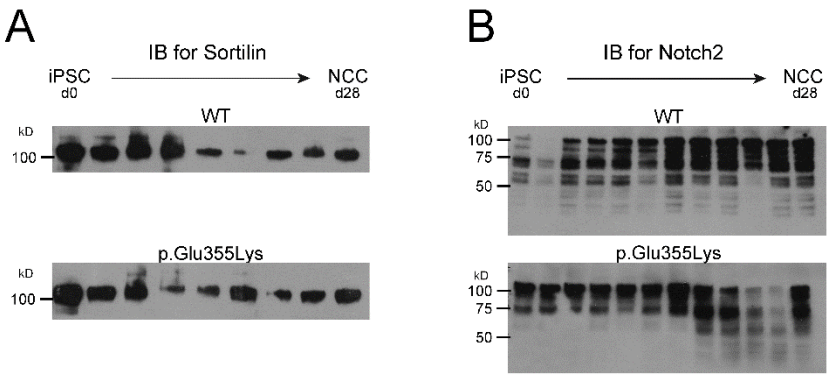

Supplement Figure 2.2. Altered abundances of SORT1 and NOTCH2 at the cell surface of GM3SD cells. (A) One of the proteins that was not detected by cell surface labelling of p.Glu355Lys cells, SORT1, was detectable in whole cell lysates. (B) NOTCH2, a cell surface receptor important for NC cell differentiation, was also undetectable by surface labeling of p.Glu355Lys cells but found in whole cell lysates (Supplement Table 1).

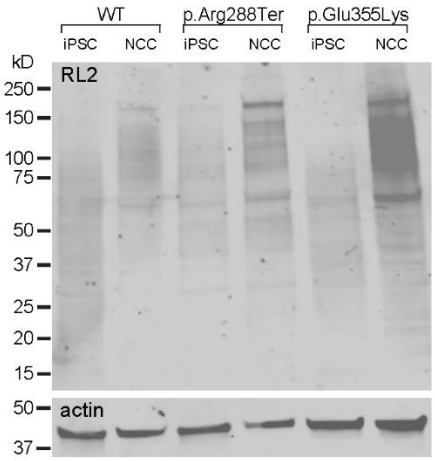

Supplement Figure 2.3. Protein O-GlcNAcylation increases upon differentiation of iPSCs to NCCs. Whole cell lysates from WT and GM3SD cells were resolved by SDS-PAGE, blotted, and probed with RL2, a monoclonal antibody that recognizes proteins modified by O-GlcNAc. As iPSCs differentiate to NCCs, the abundance of O-GlcNAcylated proteins increases and the profile of modified proteins also shifts to higher molecular weight.

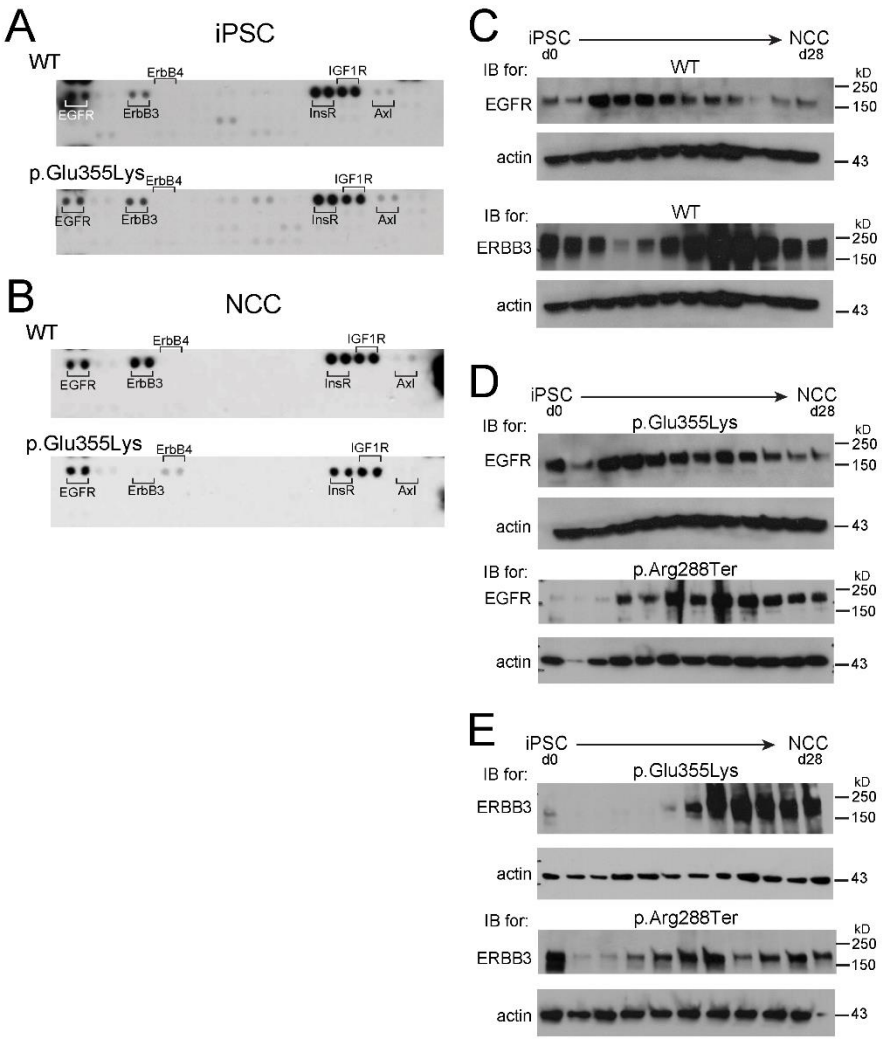

Supplement Figure 2.4. Expression/phosphorylation of receptor tyrosine kinases in WT and GM3SD cells. Blots bearing immobilized anti-RTK antibodies were overlayed with whole cell lysates from (A) iPSCs or (B) NCCs harvested at d19 of differentiation. Bound RTKs were then detected by sandwich with anti-phosphotyrosine antibody. Signal associated with ERBB3 increases in WT cells upon differentiation to NCCs, but ERBB3 is reduced in p.Glu355Lys NCCs. Other more subtle changes in RTK detection were also evident in p.Glu355Lys NCCs compared to WT. (C) Representative EGFR and ERBB3 western blots from one differentiation course of WT cells. (D) Representative EGFR western blots from one differentiation course of p.Glu355Lys and p.Arg288Ter cells. (E) Representative ERBB3 western blots from one differentiation course of p.Glu355Lys and p.Arg288Ter cells.

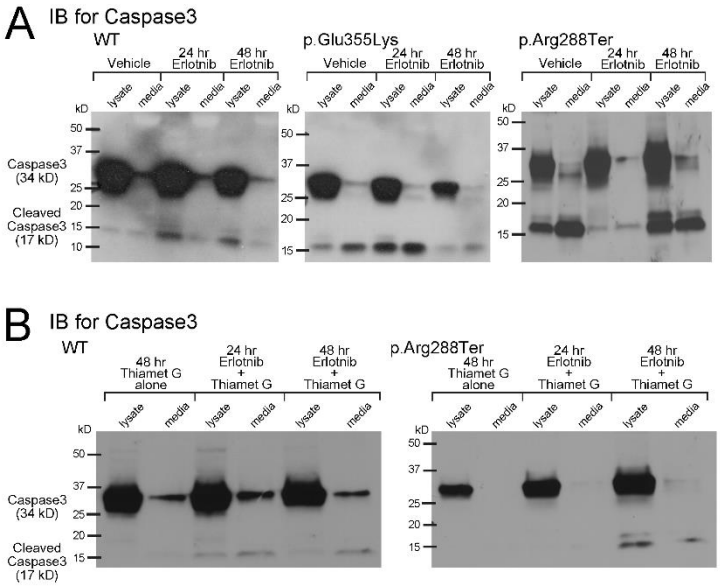

Supplement Figure 2.5. Representative cleaved caspase blots following pharmacologic perturbation. (A) Treatment of WT or GM3SD cells with erlotnib, an EGFR antagonist, during mid-differentiation to NCC (d11-14) induces increased Caspase3 cleavage. Caspase3 is detected in the cell lysate (*lysate*) of plated cells and in the cells recovered from the media (*media*) by centrifugation (quantified in Figure 2.10D). (D) Representative Caspase3 western blots demonstrate reduction in Caspase3 cleavage in presence of thiamet G (quantified in Figure 2.10E).

A

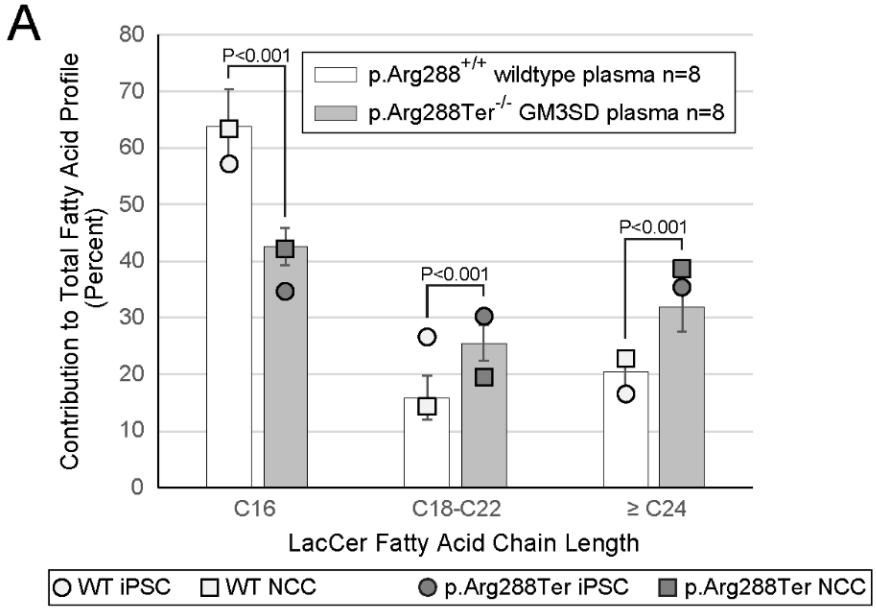

B

Fatty Acid Chain Lengths Associated with LacCer[a]	Contribution to Total Ceramide Fatty Acid Distribution (%)		
	Plasma[b] mean ± STD (n)	iPSC	NCC
Wildtype plasma (p.Arg288$^{+/+}$) and cells			
C16[c]	63.8 ± 6.6 (8)	57.0	63.2
C18-C22[d]	15.8 ± 3.9 (8)	26.5	14.2
≥C24[e]	20.4 ± 3.3 (8)	16.5	22.6
GM3SD plasma (p.Arg288Ter$^{-/-}$) and cells			
C16	42.5 ± 3.3 (8)	34.6	42.1
C18-C22	25.6 ± 3.3 (8)	30.1	19.3
≥C24	31.9 ± 4.4 (8)	35.3	38.6

[a]Chain length refers to the number of carbons detected for the indicated ceramide-associated fatty acids

[b]Fatty acid values for all plasma samples are taken from authors' previously published work: Aoki, K., et al. (2019) ***Clinical Mass Spectrometry 14***, 106-114

[c]C16 refers to C16:0 fatty acid

[d]C18-C22 refers to the sum of C18:0, C20:0, C22:0, and C22:1 fatty acids

[e]≥C24 refers to the sum of C24:0 and C26:0 fatty acids

Supplement Figure 2.6. Comparison of ceramide fatty acid distributions in plasma, iPSCs, and NCCs. The fatty acid distribution associated with the ceramide moiety of LacCer were quantified by mass spectrometry. (A) Bars in bar graph present the mean ± standard deviation (STD) for determinations of the relative abundance of the indicated LacCer fatty acids in normal patient plasma (p.Arg288$^{+/+}$ wildtype control, n=8 individuals,

white bar) or in GM3SD patient plasma (p.Arg288$^{-/-}$ GM3SD, n=8 individuals, light gray bar). These values are taken from authors' previous publication: Aoki, K., et al (2019) *Clinical Mass Spectrometry 14*, 106-114 and are presented here for comparison to the relative abundance of fatty acids detected in iPSCs and NCCs of WT and GM3SD. Fatty acid chain length denoted "C16" refers to C16:0. "C18-C22" refers to the summed abundances of C18, C20:0, C22:0, and C22:1. "≥C24" refers to the summed abundances of C24:0 and C26:0. Individual datapoints reporting the relative abundance of the same LacCer fatty acids in WT and p.Arg288Ter iPSCs and NCCs are plotted on top of the patient plasma bars for comparison. Statistical significance of differences (P-value from pairwise T-test) are presented above the bars for comparison of wildtype and p.Arg288Ter variant plasma samples. (B) Table presents the data plotted in panel A. The values in the "Plasma" column are plotted as bars in panel A and the values in the iPSC and NCC columns are plotted as individual data points in panel A. Panels A and B indicate that, despite reprogramming and differentiation, the iPSC and NCC cells derived from patient fibroblasts retain ceramide fatty acid chain length distributions that are remarkably similar to ceramide fatty acid distributions of plasma harvested from 8 unrelated individuals, whether the plasma sources were wildtype control or GM3SD patients.

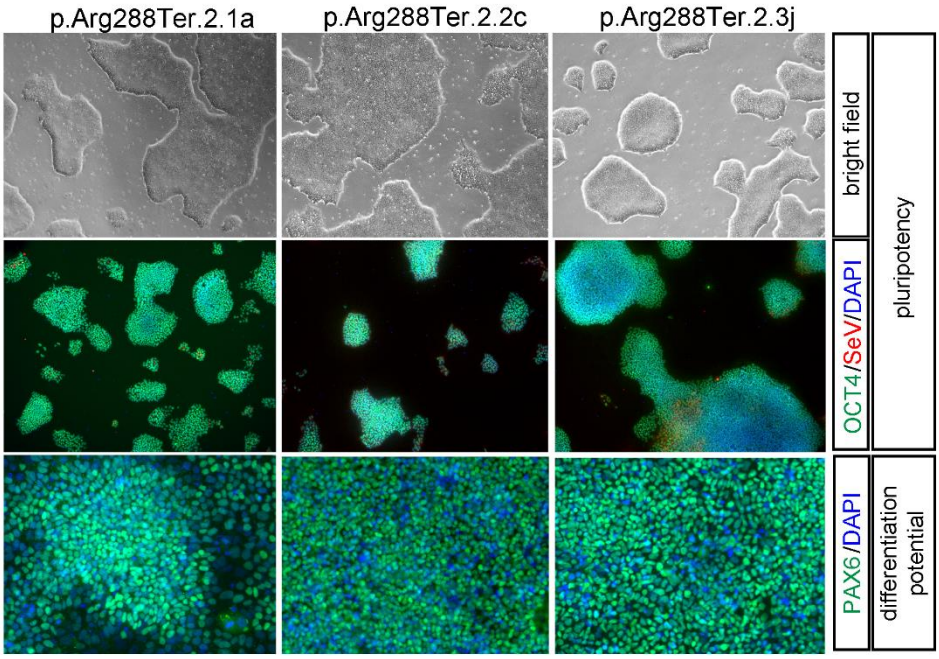

Supplement Figure 2.7. Generation and initial characterization of p.Arg288Ter iPS Cells. Fibroblasts harvested from a p.Arg288Ter patient were reprogrammed to iPS cells as described in Methods. The morphology and expression of pluripotency markers in three independent reprogrammed clones (2.1a, 2.2c, and 2.3j) are shown. All three clones possess the potential to differentiate to neuroectoderm as detected by PAX6 expression.

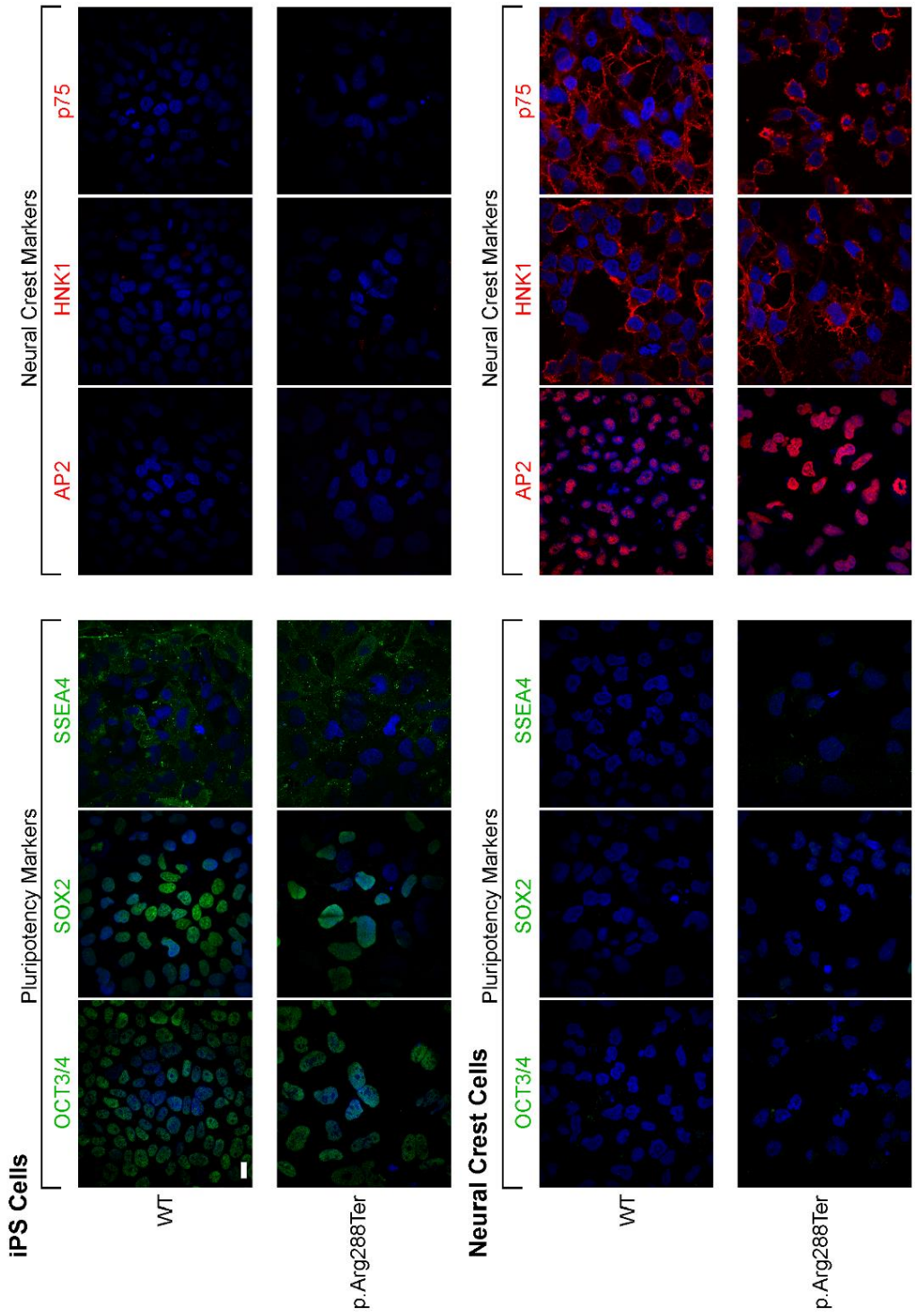

Supplement Figure 2.8. Immunofluorescence staining for pluripotency and neural crest markers in WT and p.Arg288Ter cells. iPSCs derived from p.Arg288Ter patient fibroblasts express appropriate pluripotency markers (Oct3/4, SOX2, SSEA4). Upon

differentiation to neural crest cells, expression of pluripotency markers is lost as expression of neural crest markers (AP2, HNK1, p75) is acquired.

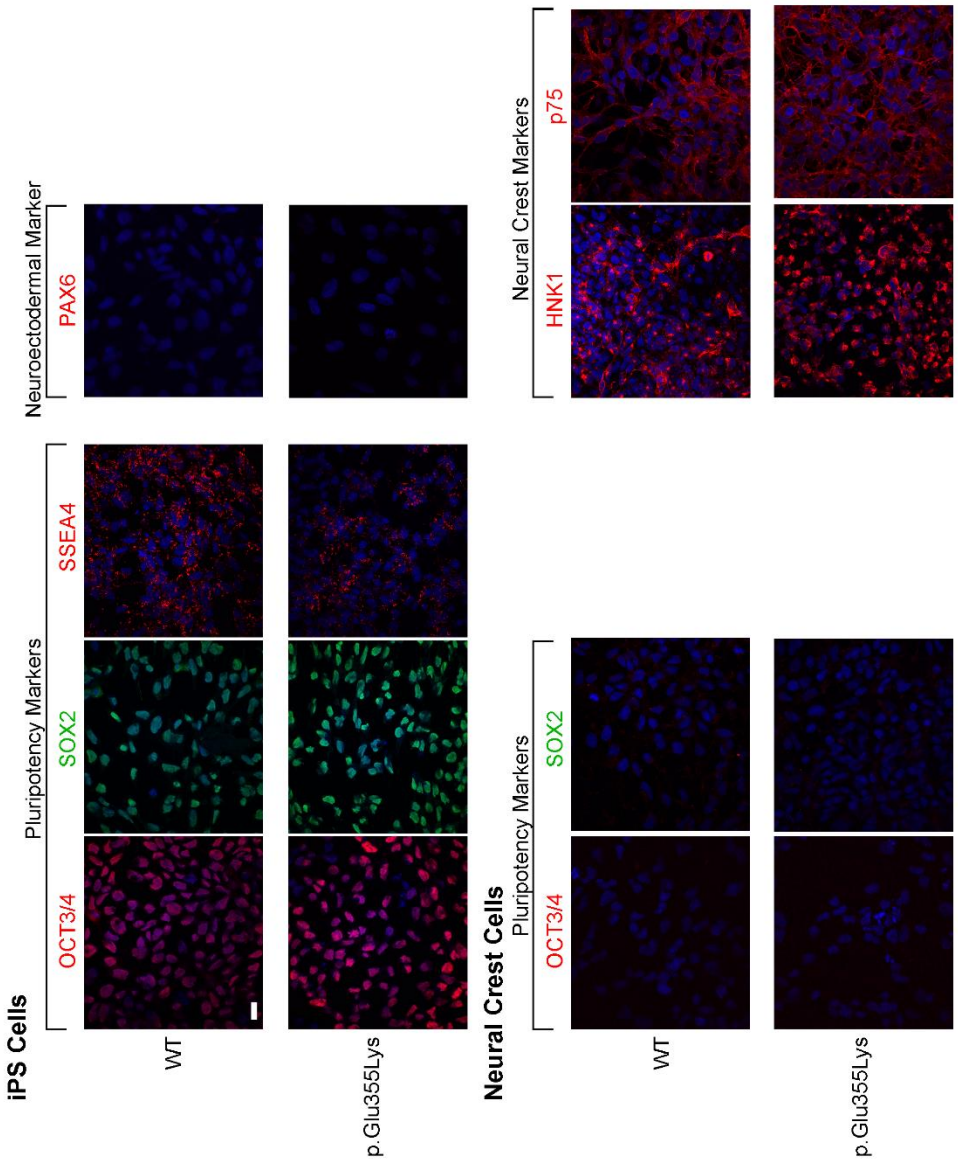

Supplement Figure 2.9. Immunofluorescence staining for pluripotency and neural crest markers in WT and p.Glu355Lys cells. iPSCs derived from p.Glu355Lys patient fibroblasts express appropriate pluripotency markers (Oct3/4, SOX2, SSEA4). Like the p.Arg288Ter iPSCs (Supplement Figure 2.1), p.Glu355Lys iPSCs are capable of differentiation to neuroectoderm (PAX6 positive) and can also acquire neural crest markers (HNK1, p75) concurrent with loss of pluripotency markers.

REFERENCES

Anumula, K. R., & Taylor, P. B. (1992). A comprehensive procedure for preparation of partially methylated alditol acetates from glycoprotein carbohydrates. *Anal Biochem, 203*(1), 101-108. doi:10.1016/0003-2697(92)90048-c

Aoki, K., Heaps, A. D., Strauss, K. A., & Tiemeyer, M. (2019). Mass spectrometric quantification of plasma glycosphingolipids in human GM3 ganglioside deficiency. *Clinical Mass Spectrometry, 14*, 106-114. doi:https://doi.org/10.1016/j.clinms.2019.03.001

Aoki, K., Perlman, M., Lim, J. M., Cantu, R., Wells, L., & Tiemeyer, M. (2007). Dynamic developmental elaboration of N-linked glycan complexity in the Drosophila melanogaster embryo. *J Biol Chem, 282*(12), 9127-9142. doi:10.1074/jbc.M606711200

Black, L. E., Longo, J. F., & Carroll, S. L. (2019). Mechanisms of Receptor Tyrosine-Protein Kinase ErbB-3 (ERBB3) Action in Human Neoplasia. *Am J Pathol, 189*(10), 1898-1912. doi:10.1016/j.ajpath.2019.06.008

Boccuto, L., Aoki, K., Flanagan-Steet, H., Chen, C. F., Fan, X., Bartel, F., . . . Schwartz, C. E. (2014). A mutation in a ganglioside biosynthetic enzyme, ST3GAL5, results in salt & pepper syndrome, a neurocutaneous disorder with altered glycolipid and glycoprotein glycosylation. *Hum Mol Genet, 23*(2), 418-433. doi:10.1093/hmg/ddt434

Bouchon, B., & Portoukalian, J. (1985). Purification of the peracetylated glycosphingolipids of the gala series (galactosyl- and galabiosylceramides). *J Chromatogr, 342*(2), 385-392. doi:10.1016/s0378-4347(00)84532-6

Bouchon, B., Portoukalian, J., & Bornet, H. (1985). Sex-specific difference of the galabiosylceramide level in the glycosphingolipids of human thyroid. *Biochim Biophys Acta, 836*(1), 143-152. doi:10.1016/0005-2760(85)90230-9

Bowser, L. E., Young, M., Wenger, O. K., Ammous, Z., Brigatti, K. W., Carson, V. J., . . . Strauss, K. A. (2019). Recessive GM3 synthase deficiency: Natural history, biochemistry, and therapeutic frontier. *Mol Genet Metab, 126*(4), 475-488. doi:10.1016/j.ymgme.2019.01.013

Bremer, E. G., Hakomori, S., Bowen-Pope, D. F., Raines, E., & Ross, R. (1984). Ganglioside-mediated modulation of cell growth, growth factor binding, and receptor phosphorylation. *J Biol Chem, 259*(11), 6818-6825.

Bremer, E. G., Schlessinger, J., & Hakomori, S. (1986). Ganglioside-mediated modulation of cell growth. Specific effects of GM3 on tyrosine phosphorylation of the epidermal growth factor receptor. *J Biol Chem, 261*(5), 2434-2440.

Brown, D. A., & London, E. (1997). Structure of Detergent-Resistant Membrane Domains: Does Phase Separation Occur in Biological Membranes? *Biochemical and Biophysical Research Communications, 240*(1), 1-7. doi:https://doi.org/10.1006/bbrc.1997.7575

Brown, D. A., & Rose, J. K. (1992). Sorting of GPI-anchored proteins to glycolipid-enriched membrane subdomains during transport to the apical cell surface. *Cell, 68*(3), 533-544. doi:10.1016/0092-8674(92)90189-j

Cederquist, G. Y., Tchieu, J., Callahan, S. J., Ramnarine, K., Ryan, S., Zhang, C., . . . Studer, L. (2020). A Multiplex Human Pluripotent Stem Cell Platform Defines Molecular and Functional Subclasses of Autism-Related Genes. *Cell Stem Cell, 27*(1), 35-49.e36. doi:10.1016/j.stem.2020.06.004

Chatterjee, S., Khullar, M., & Shi, W. Y. (1995). Digalactosylceramide is the receptor for staphylococcal enterotoxin-B in human kidney proximal tubular cells. *Glycobiology, 5*(3), 327-333. doi:10.1093/glycob/5.3.327

Collins, B. E., Ito, H., Sawada, N., Ishida, H., Kiso, M., & Schnaar, R. L. (1999). Enhanced Binding of the Neural Siglecs, Myelin-associated Glycoprotein and Schwann Cell Myelin Protein, to Chol-1 (α-Series) Gangliosides and Novel Sulfated Chol-1 Analogs *. *Journal of Biological Chemistry, 274*(53), 37637-37643. doi:10.1074/jbc.274.53.37637

Fragaki, K., Ait-El-Mkadem, S., Chaussenot, A., Gire, C., Mengual, R., Bonesso, L., . . . Paquis-Flucklinger, V. (2013). Refractory epilepsy and mitochondrial dysfunction due to GM3 synthase deficiency. *Eur J Hum Genet, 21*(5), 528-534. doi:10.1038/ejhg.2012.202

Gordon-Lipkin, E., Cohen, J. S., Srivastava, S., Soares, B. P., Levey, E., & Fatemi, A. (2018). ST3GAL5-Related Disorders: A Deficiency in Ganglioside Metabolism and a Genetic Cause of Intellectual Disability and Choreoathetosis. *J Child Neurol, 33*(13), 825-831. doi:10.1177/0883073818791099

Hart, G. W. (2019). Nutrient regulation of signaling and transcription. *J Biol Chem, 294*(7), 2211-2231. doi:10.1074/jbc.AW119.003226

Holbro, T., Beerli, R. R., Maurer, F., Koziczak, M., Barbas, C. F., 3rd, & Hynes, N. E. (2003). The ErbB2/ErbB3 heterodimer functions as an oncogenic unit: ErbB2 requires ErbB3 to drive breast tumor cell proliferation. *Proc Natl Acad Sci U S A, 100*(15), 8933-8938. doi:10.1073/pnas.1537685100

Huang, Y. F., Aoki, K., Akase, S., Ishihara, M., Liu, Y. S., Yang, G., . . . Fujita, M. (2021). Global mapping of glycosylation pathways in human-derived cells. *Dev Cell, 56*(8), 1195-1209.e1197. doi:10.1016/j.devcel.2021.02.023

Indellicato, R., Parini, R., Domenighini, R., Malagolini, N., Iascone, M., Gasperini, S., . . . Trinchera, M. (2019). Total loss of GM3 synthase activity by a normally

processed enzyme in a novel variant and in all ST3GAL5 variants reported to cause a distinct congenital disorder of glycosylation. *Glycobiology, 29*(3), 229-241. doi:10.1093/glycob/cwy112

Jennemann, R., Felding-Habermann, B., Geyer, R., Stirm, S., & Wiegandt, H. (1987). Carbohydrate analysis of chicken heart glycolipids. *Arch Biochem Biophys, 258*(1), 240-247. doi:10.1016/0003-9861(87)90341-9

Jiang, M., Yu, S., Yu, Z., Sheng, H., Li, Y., Liu, S., . . . Yang, W. (2017). XBP1 (X-Box–Binding Protein-1)–Dependent O-GlcNAcylation Is Neuroprotective in Ischemic Stroke in Young Mice and Its Impairment in Aged Mice Is Rescued by Thiamet-G. *Stroke, 48*(6), 1646-1654. doi:doi:10.1161/STROKEAHA.117.016579

Karlsson, K. A., & Larson, G. (1981). Molecular characterization of cell surface antigens of fetal tissue. Detailed analysis of glycosphingolipids of meconium of a human O Le(a--b+) secretor. *J Biol Chem, 256*(7), 3512-3524.

Klock, J. C., D'Angona, J. L., & Macher, B. A. (1981). Chemical characterization of neutral glycolipids in the human myeloid leukemias. *J Lipid Res, 22*(7), 1079-1083.

Laine, R. A., & Hakomori, S.-i. (1973). Incorporation of exogenous glycosphingolipids in plasma membranes of cultured hamster cells and concurrent change of growth behavior. *Biochemical and Biophysical Research Communications, 54*(3), 1039-1045. doi:https://doi.org/10.1016/0006-291X(73)90798-5

Lee, J. S., Yoo, Y., Lim, B. C., Kim, K. J., Song, J., Choi, M., & Chae, J.-H. (2016). GM3 synthase deficiency due to ST3GAL5 variants in two Korean female siblings: Masquerading as Rett syndrome-like phenotype. *American Journal of Medical Genetics Part A, 170*(8), 2200-2205. doi:https://doi.org/10.1002/ajmg.a.37773

Li, T. A., & Schnaar, R. L. (2018). Chapter Two - Congenital Disorders of Ganglioside Biosynthesis. In R. L. Schnaar & P. H. H. Lopez (Eds.), *Progress in Molecular Biology and Translational Science* (Vol. 156, pp. 63-82): Academic Press.

Lloyd, K. O., & Furukawa, K. (1998). Biosynthesis and functions of gangliosides: recent advances. *Glycoconjugate Journal, 15*(7), 627-636. doi:10.1023/A:1006924128550

Maccioni, H. J., Quiroga, R., & Ferrari, M. L. (2011). Cellular and molecular biology of glycosphingolipid glycosylation. *J Neurochem, 117*(4), 589-602. doi:10.1111/j.1471-4159.2011.07232.x

Maccioni, H. J. F., Quiroga, R., & Spessott, W. (2011). Organization of the synthesis of glycolipid oligosaccharides in the Golgi complex. *FEBS Letters, 585*(11), 1691-1698. doi:https://doi.org/10.1016/j.febslet.2011.03.030

Macher, B. A., Klock, J. C., Fukuda, M. N., & Fukuda, M. (1981). Isolation and structural characterization of human lymphocyte and neutrophil gangliosides. *J Biol Chem, 256*(4), 1968-1974.

Mbua, N. E., Li, X., Flanagan-Steet, H. R., Meng, L., Aoki, K., Moremen, K. W., . . . Boons, G. J. (2013). Selective exo-enzymatic labeling of N-glycans on the surface of living cells by recombinant ST6Gal I. *Angew Chem Int Ed Engl, 52*(49), 13012-13015. doi:10.1002/anie.201307095

Mehta, N., Porterfield, M., Struwe, W. B., Heiss, C., Azadi, P., Rudd, P. M., . . . Aoki, K. (2016). Mass Spectrometric Quantification of N-Linked Glycans by Reference to Exogenous Standards. *Journal of proteome research, 15*(9), 2969-2980. doi:10.1021/acs.jproteome.6b00132

Menendez, L., Kulik, M. J., Page, A. T., Park, S. S., Lauderdale, J. D., Cunningham, M. L., & Dalton, S. (2013). Directed differentiation of human pluripotent cells to neural crest stem cells. *Nat Protoc, 8*(1), 203-212. doi:10.1038/nprot.2012.156

Meng, L., Forouhar, F., Thieker, D., Gao, Z., Ramiah, A., Moniz, H., . . . Moremen, K. W. (2013). Enzymatic basis for N-glycan sialylation: structure of rat α2,6-sialyltransferase (ST6GAL1) reveals conserved and unique features for glycan sialylation. *J Biol Chem, 288*(48), 34680-34698. doi:10.1074/jbc.M113.519041

Miljan, E. A., Meuillet, E. J., Mania-Farnell, B., George, D., Yamamoto, H., Simon, H.-G., & Bremer, E. G. (2002). Interaction of the Extracellular Domain of the Epidermal Growth Factor Receptor with Gangliosides *. *Journal of Biological Chemistry, 277*(12), 10108-10113. doi:10.1074/jbc.M111669200

Rojas-Macias, M. A., Mariethoz, J., Andersson, P., Jin, C., Venkatakrishnan, V., Aoki, N. P., . . . Karlsson, N. G. (2019). Towards a standardized bioinformatics infrastructure for N- and O-glycomics. *Nature Communications, 10*(1), 3275. doi:10.1038/s41467-019-11131-x

Rukazenkov, Y., Speake, G., Marshall, G., Anderton, J., Davies, B. R., Wilkinson, R. W., . . . Swaisland, A. (2009). Epidermal growth factor receptor tyrosine kinase inhibitors: similar but different? *Anticancer Drugs, 20*(10), 856-866. doi:10.1097/CAD.0b013e32833034e1

Sandhoff, K., & Kolter, T. (2003). Biosynthesis and degradation of mammalian glycosphingolipids. *Philosophical transactions of the Royal Society of London. Series B, Biological sciences, 358*(1433), 847-861. doi:10.1098/rstb.2003.1265

Sandhoff, R., Geyer, R., Jennemann, R., Paret, C., Kiss, E., Yamashita, T., . . . Gröne, H.-J. (2005). Novel Class of Glycosphingolipids Involved in Male Fertility *. *Journal of Biological Chemistry, 280*(29), 27310-27318. doi:10.1074/jbc.M502775200

Saul, R., Wilkes, G., & Stevenson, R. (1983). Salt-And-Peper' pigmentary changes with severe mental retardation: a new neurocutaneous syndrome. .

Schnaar, R. L. (2016). Gangliosides of the Vertebrate Nervous System. *J Mol Biol, 428*(16), 3325-3336. doi:10.1016/j.jmb.2016.05.020

Schnaar, R. L., Gerardy-Schahn, R., & Hildebrandt, H. (2014). Sialic acids in the brain: gangliosides and polysialic acid in nervous system development, stability, disease, and regeneration. *Physiol Rev, 94*(2), 461-518. doi:10.1152/physrev.00033.2013

Shih, A. J., Telesco, S. E., & Radhakrishnan, R. (2011). Analysis of Somatic Mutations in Cancer: Molecular Mechanisms of Activation in the ErbB Family of Receptor Tyrosine Kinases. *Cancers, 3*(1), 1195-1231. Retrieved from https://www.mdpi.com/2072-6694/3/1/1195

Si-Tayeb, K., Noto, F. K., Sepac, A., Sedlic, F., Bosnjak, Z. J., Lough, J. W., & Duncan, S. A. (2010). Generation of human induced pluripotent stem cells by simple transient transfection of plasmid DNA encoding reprogramming factors. *BMC Dev Biol, 10*, 81. doi:10.1186/1471-213x-10-81

Silva, M., Videira, P. A., & Sackstein, R. (2017). E-Selectin Ligands in the Human Mononuclear Phagocyte System: Implications for Infection, Inflammation, and Immunotherapy. *Front Immunol, 8*, 1878. doi:10.3389/fimmu.2017.01878

Simons, K., & Ikonen, E. (1997). Functional rafts in cell membranes. *Nature, 387*(6633), 569-572. doi:10.1038/42408

Simpson, M. A., Cross, H., Proukakis, C., Priestman, D. A., Neville, D. C. A., Reinkensmeier, G., . . . Crosby, A. H. (2004). Infantile-onset symptomatic epilepsy syndrome caused by a homozygous loss-of-function mutation of GM3 synthase. *Nature Genetics, 36*(11), 1225-1229. doi:10.1038/ng1460

Sipione, S., Monyror, J., Galleguillos, D., Steinberg, N., & Kadam, V. (2020). Gangliosides in the Brain: Physiology, Pathophysiology and Therapeutic Applications. *Frontiers in neuroscience, 14*, 572965-572965. doi:10.3389/fnins.2020.572965

Steinkamp, M. P., Low-Nam, S. T., Yang, S., Lidke, K. A., Lidke, D. S., & Wilson, B. S. (2014). erbB3 is an active tyrosine kinase capable of homo- and heterointeractions. *Mol Cell Biol, 34*(6), 965-977. doi:10.1128/mcb.01605-13

Varki, A., Cummings, R. D., Aebi, M., Packer, N. H., Seeberger, P. H., Esko, J. D., . . . Kornfeld, S. (2015). Symbol Nomenclature for Graphical Representations of Glycans. *Glycobiology, 25*(12), 1323-1324. doi:10.1093/glycob/cwv091

Vukelić, Z., Zamfir, A. D., Bindila, L., Froesch, M., Peter-Katalinić, J., Usuki, S., & Yu, R. K. (2005). Screening and sequencing of complex sialylated and sulfated glycosphingolipid mixtures by negative ion electrospray Fourier transform ion

cyclotron resonance mass spectrometry. *J Am Soc Mass Spectrom, 16*(4), 571-580. doi:10.1016/j.jasms.2005.01.013

Wang, X. Q., Sun, P., & Paller, A. S. (2003). Ganglioside GM3 blocks the activation of epidermal growth factor receptor induced by integrin at specific tyrosine sites. *J Biol Chem, 278*(49), 48770-48778. doi:10.1074/jbc.M308818200

Wee, P., & Wang, Z. (2017). Epidermal Growth Factor Receptor Cell Proliferation Signaling Pathways. *Cancers (Basel), 9*(5). doi:10.3390/cancers9050052

Wells, L., Hart, G. W., & Athens Guidelines for the Publication of Glycomics, D. (2013). Glycomics: building upon proteomics to advance glycosciences. *Molecular & cellular proteomics : MCP, 12*(4), 833-835. doi:10.1074/mcp.e113.027904

Yamashita, T., Hashiramoto, A., Haluzik, M., Mizukami, H., Beck, S., Norton, A., . . . Proia, R. L. (2003). Enhanced insulin sensitivity in mice lacking ganglioside GM3. *Proceedings of the National Academy of Sciences of the United States of America, 100*(6), 3445-3449. doi:10.1073/pnas.0635898100

Yamashita, T., Wu, Y.-P., Sandhoff, R., Werth, N., Mizukami, H., Ellis, J. M., . . . Proia, R. L. (2005). Interruption of ganglioside synthesis produces central nervous system degeneration and altered axon–glial interactions. *Proceedings of the National Academy of Sciences, 102*(8), 2725-2730. doi:doi:10.1073/pnas.0407785102

York, W. S., Agravat, S., Aoki-Kinoshita, K. F., McBride, R., Campbell, M. P., Costello, C. E., . . . Kettner, C. (2014). MIRAGE: the minimum information required for a glycomics experiment. *Glycobiology, 24*(5), 402-406. doi:10.1093/glycob/cwu018

Yoshikawa, M., Go, S., Suzuki, S., Suzuki, A., Katori, Y., Morlet, T., . . . Inokuchi, J. (2015). Ganglioside GM3 is essential for the structural integrity and function of cochlear hair cells. *Hum Mol Genet, 24*(10), 2796-2807. doi:10.1093/hmg/ddv041

Yoshikawa, M., Go, S., Takasaki, K., Kakazu, Y., Ohashi, M., Nagafuku, M., . . . Inokuchi, J. (2009). Mice lacking ganglioside GM3 synthase exhibit complete hearing loss due to selective degeneration of the organ of Corti. *Proc Natl Acad Sci U S A, 106*(23), 9483-9488. doi:10.1073/pnas.0903279106

Yuzwa, S. A., Macauley, M. S., Heinonen, J. E., Shan, X., Dennis, R. J., He, Y., . . . Vocadlo, D. J. (2008). A potent mechanism-inspired O-GlcNAcase inhibitor that blocks phosphorylation of tau in vivo. *Nature Chemical Biology, 4*(8), 483-490. doi:10.1038/nchembio.96

CHAPTER 3

IRE1α DISPLAYS A PROPOSED PRO-SURVIVAL ROLE IN RESPONSE TO DECREASED PROTEIN O-GLCNACYLATION IN ALZHEIMER DISEASE NEURAL PROGENITOR CELLS.

INTRODUCTION

Alzheimer Disease (AD) is a neurodegenerative disorder characterized by cognitive decline, memory impairment, difficulty understanding images and spatial relationships, as well as changes in mood. The Alzheimer's Disease Association reported that 6.2 million individuals 65 and older were living with AD in 2021 ("2021 Alzheimer's disease facts and figures," 2021). The true cause for AD has not been deciphered; however, certain genes have been shown to have a large impact. Especially for familial AD where individuals inherit the disease in an autosomal dominant manner (Chen et al., 2017). Familial AD can be screened for and diagnosed in individuals by looking at mutations in the deterministic genes amyloid precursor protein (APP), presenilin 1 (PSEN1), presenilin 2 (PSEN2), and APOE-e4 allele on chromosome 19 (Bird, 1993). Sporadic AD received its name due to the fact it is not reliant on being inherited. However, it has been shown to be influenced by the interactions between risk genes APOE-e4, TREM2 and environmental factors (Chartier-Harlin et al., 1994; Guerreiro, Brás, & Hardy, 2013; Liu, Kanekiyo, Xu, & Bu, 2013; Sherrington et al., 1995). The pathophysiological characteristics seen with AD are amyloid-β (Aβ) plaques,

neurofibrillary tangles (NFT), synaptic loss, and neural death in multiple regions of the brain (Chi, Chang, & Sang, 2018). Recently, soluble Aβ and hyper-phosphorylated tau (phospho-tau) have been shown to display a large neurotoxic stress signaling role in the cell prior to plaque and NFT formation (Li & Selkoe, 2020).

Even though the causes of AD are poorly understood, there are many reasons to speculate as to why neuron death increases in the diseased state. One possible explanation for the increased neural death seen could be from the high levels of cellular stress associated with AD. The endoplasmic reticulum (ER) has been shown to be stressed in AD neural cultures and post-mortem human brain (Hoozemans et al., 2009; J. H. Lin, Li, Zhang, Ron, & Walter, 2009). The ER is the initial compartment in the secretory pathway and is responsible for the proper folding of nascent polypeptides. It responds to changes in the environment and protein folding to alter overall protein folding load as well as transcription or translation of certain genes. Since AD is associated with the aggregation of misfolded proteins such as hyperphosphorylated tau, amyloid precursor protein, and Aβ, it makes sense as to why we see this elevation of ER stress (Uddin et al., 2020). When the ER becomes stressed glucose-regulatory protein 78 (also known as BIP) releases from the membrane proteins that make up the unfolded protein response (UPR). When it releases from these proteins, it causes them to activate. The UPR consist of three different membrane proteins: inositol-requiring enzyme (IRE1α), protein kinase RNA-like endoplasmic reticulum kinase (PERK) and activating transcription factor 6 (ATF6) (Uddin et al., 2020; Wodrich, Scott, Shukla, Harris, & Giniger, 2022). To attempt to bring the ER back to homeostasis, IRE1α and ATF6 signals to increase transcription and reduce protein-folding burden by initiating the splicing of X-box binding protein (XBP1).

Once spliced XBP1 is in its activated form and can translocate to the nucleus to increase transcription of a wide variety of genes involved in protein trafficking, folding, and degradation (Lee, Iwakoshi, & Glimcher, 2003; Yoshida, Matsui, Yamamoto, Okada, & Mori, 2001). Ultimately, XBP1 has a very large impact on cell fate and recovery (Acosta-Alvear et al., 2007). The other branch of the UPR is controlled by PERK, which once activated stops the influx of newly synthesized proteins into the ER by inhibiting translation. PERK does this by phosphorylating eukaryotic initiation factor 2α (eIF2α) (Harding, Zhang, & Ron, 1999). However, a few proteins can still be translated such as activating transcription 4 (ATF4) which will promote cell death when the ER has been stressed for a prolonged amount of time (Lu, Harding, & Ron, 2004).

O-linked-β-N-acetylglucosamine (O-GlcNAc) has been defined as a signal integrator and relay system affecting upstream and downstream target proteins and mechanisms. It acts by modifying serine or threonine residues on nucleocytoplasmic proteins. Many of these proteins that could be modified with O-GlcNAc could also be modified via phosphorylation at the same sites (Hart & Akimoto, 2009; Kamemura & Hart, 2003). With the known information on how phosphorylation can affect signaling it is not surprising that dynamic changes in phosphorylation and O-GlcNAcylation would cause drastic effects. Protein O-GlcNAcylation has been shown to have a pro-survival affect in many stressed environments (Zachara et al., 2004). This is especially the case for AD where decreased protein O-GlcNAcylation leads to increased production of Aβ and NFTs (Park, Lai, Arumugam, & Jo, 2020; Yuzwa et al., 2008). O-GlcNAc levels and specific O-GlcNAcylation of proteins has been shown to affect the ER (Ngoh, Hamid, Prabhu, & Jones, 2009). As stated previously, IRE1α's role in the UPR is to increase the

transcription of chaperones. However, it has also been shown to effect different components of AD pathogenesis such as the amount of Aβ oligomers, astrocyte activation (Duran-Aniotz et al., 2017), glucose metabolism and O-GlcNAcylation (van der Harg et al., 2017).

Using human induced pluripotent stem cells (iPSCs) and differentiated neural crest cells (NCC) we investigated protein O-GlcNAcylation and IRE1α to obtain preliminary data on the consequences of AD. We chose NCCs for our differentiations because they are neural progenitors of the peripheral nervous system (PNS). The PNS has not been extensively studied in AD leading to a large gap in knowledge. The PNS is crucial for relaying external signals and internal signals to the CNS. Additionally, it directly affects the release of glucose from peripheral metabolic tissues and cells (E. E. Lin, Scott-Solomon, & Kuruvilla, 2021). The amount of glucose available to be used by the hexosamine biosynthetic pathway (HBP) affects the amount of protein O-GlcNAcylation. This study found changes in protein O-GlcNAcylation in AD compared to the non-diseased state once the population became NCCs (post day 15). This result was accompanied by increased expression of IRE1α in AD signifying the possible cellular changes occurring in NCCs. These results can be further studied to define the mechanisms of how the PNS is affected in AD.

MATERIALS AND METHODS

Generation of induced pluripotent stem cells

Wild-type iPSC lines were acquired from Steve Duncan, University of Wisconsin (Si-Tayeb et al., 2010). AD iPSC lines were generated from fibroblasts sourced from a patient's skin sample (Israel et al., 2012). These–iPSC clones were initially tested for

pluripotency by assessing expression of pluripotency markers Oct4 (Cell Signaling, # C30A3), SSEA3/4 (Santa Cruz, # sc-21704), and Sox2 (R&D, # MAB2018).

Neural Crest differentiation of iPSCs

Patient and WT iPSCs were differentiated to NCCs according to (Menendez, Yatskievych, Antin, & Dalton, 2011). Briefly, a 60 mm dish of ~90% confluent iPSCs was dissociated with Accutase (Innovative Cell Technologies, # AT104) and resuspended to a density of ~$9.2x10^4$ cells per cm^2 on Geltrex-coated plates in neural crest media composed of DMEM/F12 without glutamine (Cellgro), 2% Probumin, Life Science Grade (Millipore), 1x Non-essential amino acids (Cellgro), 2 mM GlutaGro (Cellgro), 1x Antibiotic/Antimycotic (Cellgro), 10 µg/ml Human Transferrin, (Athens Research & Tech),1x Trace elements A, B, & C (Cellgro), 50 µg/ml L-Ascorbic acid 2-phosphate sesqimagnesium salt hydrate (Sigma), 10 ng/ml Heregulin β (Peprotech), 200 ng/ml Long R3-IGF1 (SAFC/Sigma), 8 ng/ml bFGF (RnD Systems), 2 µM GSK3 inhibitor IX (BIO) (Tocris), and 20 µM SB431542 (Tocris). Media was changed daily, and at confluence, cells were split 1:4-1:6 (vol/vol) onto Geltrex-coated plates. By Day 15, cells tested positive by immunohistochemistry for NC markers HNK1 (Sigma Aldrich, # C6680) and p75 (Advanced Targeting Systems, # AB-N07), and negative for iPSC markers Oct4, SSEA3/4, and Sox2. When assessing cell characteristics at specific time points of differentiation, cells were collected on specified days by scraping, spun down at 200 x g for 5 minutes, and frozen after aspiration of the supernatant. Successful differentiation of WT and AD iPSCs to NCCs was monitored by endpoint analysis for the acquisition of NCC markers and loss of pluripotency markers by immunofluorescence as described below. Marker assessment was performed over multiple independent differentiations and repeated upon thaw of each

new aliquot of an iPSC line. In all cases, the iPSCs acquired NCC and lost pluripotency markers as expected based on previous publications (Menendez et al., 2011).

Immunofluorescence staining

Antibodies and dilutions were as follows: Anti-HNK-1 antibody (Sigma Aldrich, Monoclonal Anti-HNK-1/N-CAM (CD57), # C6680), 1:200 dilution in 5% donkey serum prepared in 0.2% Triton X-100 in PBS (PBS-T); Anti-Sox2 antibody (R&D, # MAB2018), 1:200 dilution in 5% donkey serum in PBS-T; Anti-Oct4 antibody (Santa Cruz, # sc-8628), 1:200 dilution in 5% donkey serum in PBS-T; Anti-SSEA3/4 antibody (Santa Cruz, # sc-21704), 1:200 dilution in 5% donkey serum in PBS-T; Anti-p75 antibody (Advanced Targeting Systems, # AB-N07), 1:100 dilution in PBS-T; Anti-110.6 antibody (Hart Laboratory (Comer, Vosseller, Wells, Accavitti, & Hart, 2001)), 1:300 dilution in 5% goat serum in PBS-T. All antibodies were incubated overnight at 4ºC. Immunofluorescent images were captured using an Olympus Fluoview FV1000 laser confocal microscope or a LionheartFX (BioTek) fluorescence microscope.

Western blot analysis

Antibodies for detection of proteins by western blot of whole cell lysates were used as provided and were from the following sources: anti-caspase 3 (Santa Cruz, caspase-3 Antibody 31A1067, # sc-56053) at 1:1000 dilution with detection by goat anti-mouse secondary at 1:10,00 dilution; anti- IRE1α (Cell Signaling, IRE1α (14C10) Rabbit mAb #3294) at 1:1000 dilution with detected by goat anti-mouse secondary at 1:10,000 dilution; anti-β-actin (Cell Signaling, β-Actin Antibody 13E5, #4970) at 1:5000 dilution with detection by goat anti-rabbit secondary at 1:10,000 dilution. O-GlcNAcylation of proteins of nucleocytoplasmic extracts (NCEs) was detected by western blot with anti-O-GlcNAc

monoclonal antibody RL-2 (Enzo Life Sciences, ALX-804-11-R100) at 1:1000 dilution with detection by goat anti-mouse secondary at 1:10,000 and 110.6 (Hart Laboratory, (Comer et al., 2001)) at 1:500 dilution with detection by goat anti- mouse IgM 1:20,000. Actin was detected in parallel with O-GlcNAc by incubation with anti-β-actin (Cell Signaling Technology, Actin Antibody 13E5, #4790) at 1:5000 with detection by goat anti-rabbit secondary at 1:10,000. Protein concentrations were measured by BCA assay and aliquots were reduced, alkylated, resolved by SDS-PAGE, and transferred to PVDF membranes for probing with primary antibodies at 4°C overnight. All primary antibody binding was detected by Alexa Fluor IRDye secondary antibodies: IRDye®680RD goat anti-mouse (LI-COR, catalog number 926-68070) and IRDye®800CW goat anti-rabbit (LI-COR catalog number 926-32211). Densitometric quantification was performed with ImageJ Software. For developmental time courses that assessed the change in abundance of receptors across differentiation from iPSC to NCC, signal intensities for proteins were normalized to ß-actin (loading control) and then expressed relative to the normalized signal intensity detected in NC (d26-28 of differentiation).

Statistical analysis

Western blot analyses were performed on cells harvested at indicated time points between 3 independent differentiation courses. Multiple parametric tests were utilized to assess the statistical significance of the resulting data. Pairwise T-tests were used to assess the similarity of one population compared to another for specific features. For all three tests, a P-value less than or equal to 0.05 was considered indicative of a significant difference between the tested populations. The results of pairwise T-tests identified the same population differences as significant. In tables and graphs, population means are

reported ± standard error of the mean. For the analysis, immunoblot band intensities for each receptor were normalized to actin intensity to control for loading variability and then each time point was presented relative to terminal NCC of the differentiation course. For the analysis of cleaved Caspase3, the ratio of the immunoblot intensity associated with the cleavage product at 17kD was divided by the ratio of the intensity associated with the intact protein at 34kD detected in the same lane; normalization to actin was not performed since the ratios are independent of sample load.

RESULTS

Alzheimer Disease neural crest cells possess decreased O-GlcNAcylation of nuclear core proteins.

The addition and removal of O-GlcNAc can happen on nuclear and cytoplasmic proteins in response to different cellular signaling, but it can also act to affect cell signaling pathways (Hart & Akimoto, 2009). To decipher the role of O-GlcNAc in the PNS, neural crest cells (NCCs) were differentiated from human induced pluripotent stem cells (iPSC) (**Figure 3.1**). Using nucleocytoplasmic extracts (NCE) from WT and AD time points throughout the differentiation from iPSC to NCC we probed for protein O-GlcNAcylation with antibodies, RL2 and 110.6 (**Figure 3.2**). The expression of RL2 significantly decreased ($p<0.05$) in AD compared to WT starting at day 17 of the differentiation (**Figure 3.2A**). It continued to reach statistical significance till Day 23 prior to increasing at the last time point of the differentiation. Protein O-GlcNAcylation detected by 110.6 displayed no significant change between WT and AD throughout the differentiation (**Figure 3.2B**).

The localization of O-GlcNAcylated proteins is dynamic throughout the differentiation.

The localization of O-GlcNAcylated proteins in the cells greatly affects their function and activity. Previous research has shown that O-GlcNAcylation of certain proteins can affect their translocation and activity (Yang & Qian, 2017). To judge if there are possible changes in localization of O-GlcNAcylated proteins in a cell type specific manner we completed immunofluorescence probing for 110.6 throughout the WT differentiation from iPSC to NCC. Qualitative analysis shows that 110.6 expression was located predominantly outside of the nucleus prior to moving more nuclear around day 23 of the differentiation (**Figure 3.3**). This result provides initial feedback that the cellular localization of O-GlcNAcylated proteins could also be making a difference in function, not necessarily just the amount.

The Unfolded Protein Response is stimulated in Alzheimer's Disease and may help protect against Apoptotic signaling

Due to the known research displaying the impact of AD on cellular stress and cellular death we chose to assess the activity of the Unfolded Protein Response (UPR) and cleaved caspase3 levels in AD. Once activated the membrane receptor IRE1α, acts initially to promote cell survival and homeostasis (Lee et al., 2003; Yoshida et al., 2001). Thus, we probed for IRE1α using whole-cell lysates prepared from the different time points throughout the differentiation from IPSC to NCC in both WT and AD. The expression of IRE1α significantly increases in AD during the time frame day 17 - 21 of the differentiation ($p<0.05$) compared to WT (**Figure 3.4A**).

Increased expression of IRE1α could allow the ER to continue down two different pathways. Firstly, IRE1α can initiate pro-survival signaling to bring the cell back to homeostasis. But if the cell is not able to restore homeostasis and the UPR undergoes prolonged activation, PERK will be stimulated resulting in the activation of ATF4 and CHOP mediated cell death (Uddin et al., 2020). Thus, to gauge over all changes in the survival of differentiating cells we assessed the appearance of cleaved caspase3, an apoptotic effector, in the last three-time ranges of WT and AD cells (**Figure 3.4B**). Cleaved caspase3 was not detectable in WT and AD cells throughout these time points. This result suggests that AD cells despite possessing decreased protein O-GlcNAcylation and increased cellular stress starting around day 17 of the differentiation were not subject to increased cell death compared to WT.

DISCUSSION

O-GlcNAcylation is a complex PTM on Ser/ Thr residues that has been shown to be crucial in mediating cell signaling (Dias & Hart, 2007). The presence or absence of this modification is driven by the environment, nutrient availability, cellular stress, growth factors, and other signaling events (Hart, 2019). Thus, changes in O-GlcNAcylation can act as a signal integrator with the ability to cause or resolve stresses (Zachara et al., 2004). For instance, increased protein O-GlcNAcylation has been shown to reduce inflammation and decrease mitochondrial stress (Huang & Hart, 2021; Mannino & Hart, 2022). However, in the CNS of individuals with AD O-GlcNAc levels are reduced. This reduction and lack of modification present causes alterations in a variety of different proteins activity (Dias & Hart, 2007; Hart, 2019). Specifically, this decrease in protein O-GlcNAcylation has been shown to drastically affect the production of Aβ plaques, NFTs, and cell survival (Park et

al., 2020). It has been shown that a healthy cell could function to increase glucose uptake in response to stress and other environmental factors (Zachara et al., 2004). Increasing the uptake of glucose provides additional starting material for the Hexosamine Biosynthetic Pathway thus promoting increased protein O-GlcNAcylation of certain proteins. Increased protein O-GlcNAcylation then can act to protect against cellular damage and promote cell survival unlike what is seen in AD (Zachara et al., 2004). This proposes a theory that AD neurons, which are prone to cell death, have a decreased capacity to respond to cellular stress from disease pathology.

To judge if AD neural progenitors of the PNS showed similar characteristics to AD neurons of the CNS, we analyzed the amount of protein O-GlcNAcylation in WT and AD. Using biological replicates from these two populations we showed that RL2 expression, a monoclonal antibody against protein O-GlcNAcylation, was decreased at day 17 in AD NCC compared to the non-diseased state. This decreased expression continued till day 23 prior to increasing to WT levels. Expression of 110.6 which is an antibody used for detecting broader changes in protein O-GlcNAcylation did not show any significant changes in expression between WT and AD throughout the differentiation. With this result in mind, we aimed to question why RL2 expression would change between the diseased and non-diseased state and not 110.6. These antibodies do detect different subsets of proteins (Comer et al., 2001; Holt et al., 1987) allowing us to see that the O-GlcNAcylation of more transcription factors and nuclear proteins, detected by RL2, decreases in AD. However, there is also a possibility the localization of proteins modified with O-GlcNAc is changing and not necessarily the amount (Yang & Qian, 2017). Preliminary results showed that the localization of proteins modified with O-GlcNAc detected by 110.6 did

change throughout a WT differentiation. This result proposes the question the O-GlcNAcylation of different proteins in different compartments could have different effects on cell signaling, transcription, etc. and it is not necessarily the amount of O-GlcNAcylation that could be causing changes in cell signaling.

Research has highlighted that significantly increased (hyperglycemic environment) or significantly decreased (hypoglycemic environment) O-GlcNAcylation can cause cellular stress (Hart, 2019). Thus, to judge ER stress and the activation of the UPR, we demonstrated that IRE1α expression is significantly elevated in AD between day 17 and 21 ($p<0.5$). This time frame is the same time frame associated with decreased protein O-GlcNAcylation revealing a possible correlation between protein O-GlcNAcylation and activation of the UPR. Knowing the downstream consequences of decreased O-GlcNAc and cellular stress, we explored how apoptosis was affected in the last three-time frames of the differentiation. Cleaved caspase3 levels, an indicator of apoptosis, were undetectable in both WT and AD. These findings suggest that AD neural progenitors of the PNS do experience changes in protein O-GlcNAcylation that would be suspected to affect cellular stress and downstream signaling pathways; however, due to the lack of cell death we believe there are compensatory mechanisms occurring that may be initiating pro-survival signaling in the PNS (**Figure 3.5**).

These studies provide preliminary data that can stimulate further work studying AD in the PNS to possibly find a pro-survival mechanism that is contrary to the CNS. However, it is important to note that these results are based on multiple differentiations from a single WT and 2x APP familial AD representative (Israel et al., 2012). It would be crucial for researchers to further study these items in additional patient-derived cell types to judge if

there are individual to individual variation. Using iPSC provide a very novel opportunity to judge changes in cell signaling and mechanisms.

FIGURES AND TABLES

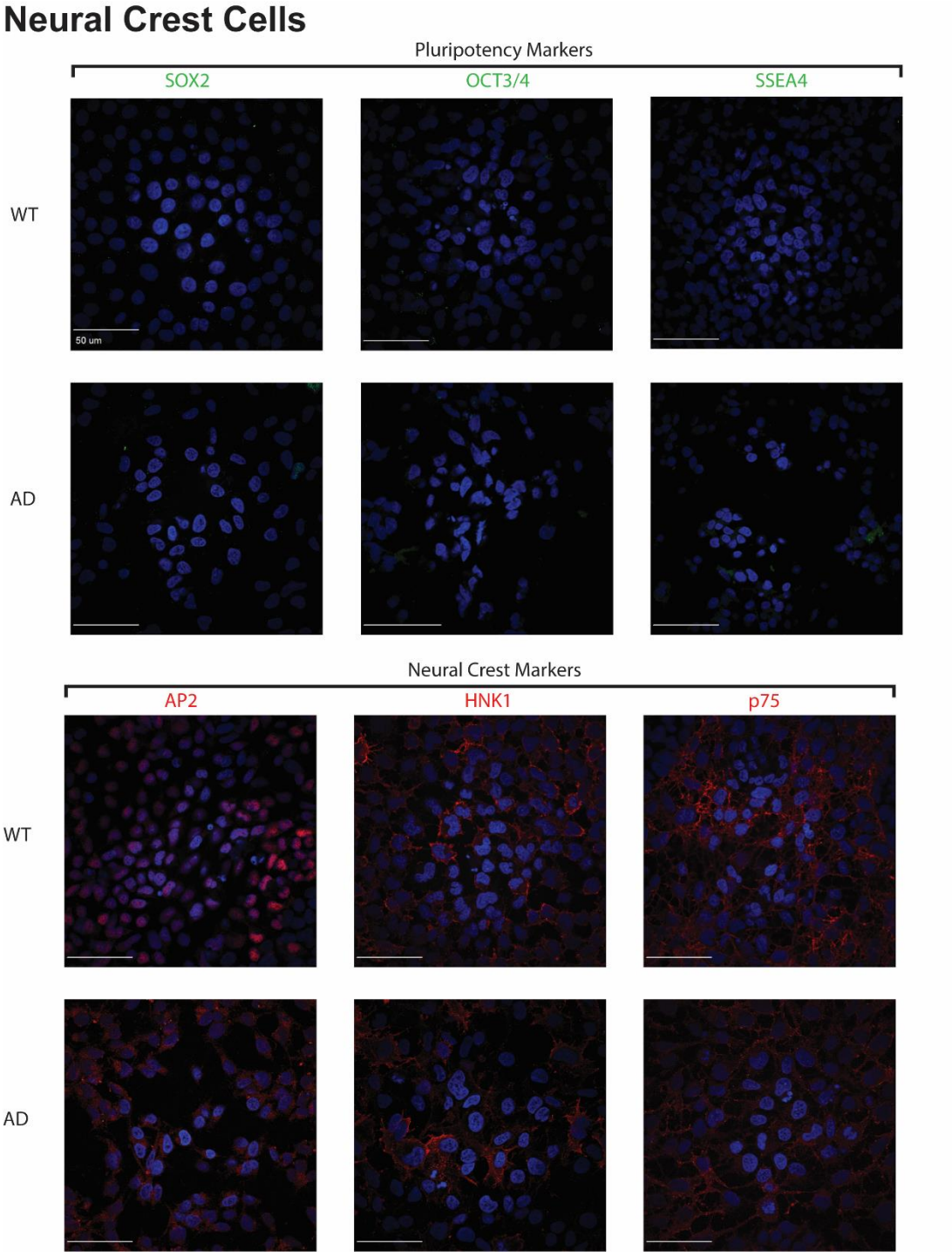

Figure 3.1. Immunofluorescence staining for pluripotency and neural crest markers in WT and AD cells. Upon differentiation to neural crest cells, expression of pluripotency markers (Oct3/4, SOX2, SSEA4) is lost as expression of neural crest markers (AP2, HNK1, p75) is acquired.

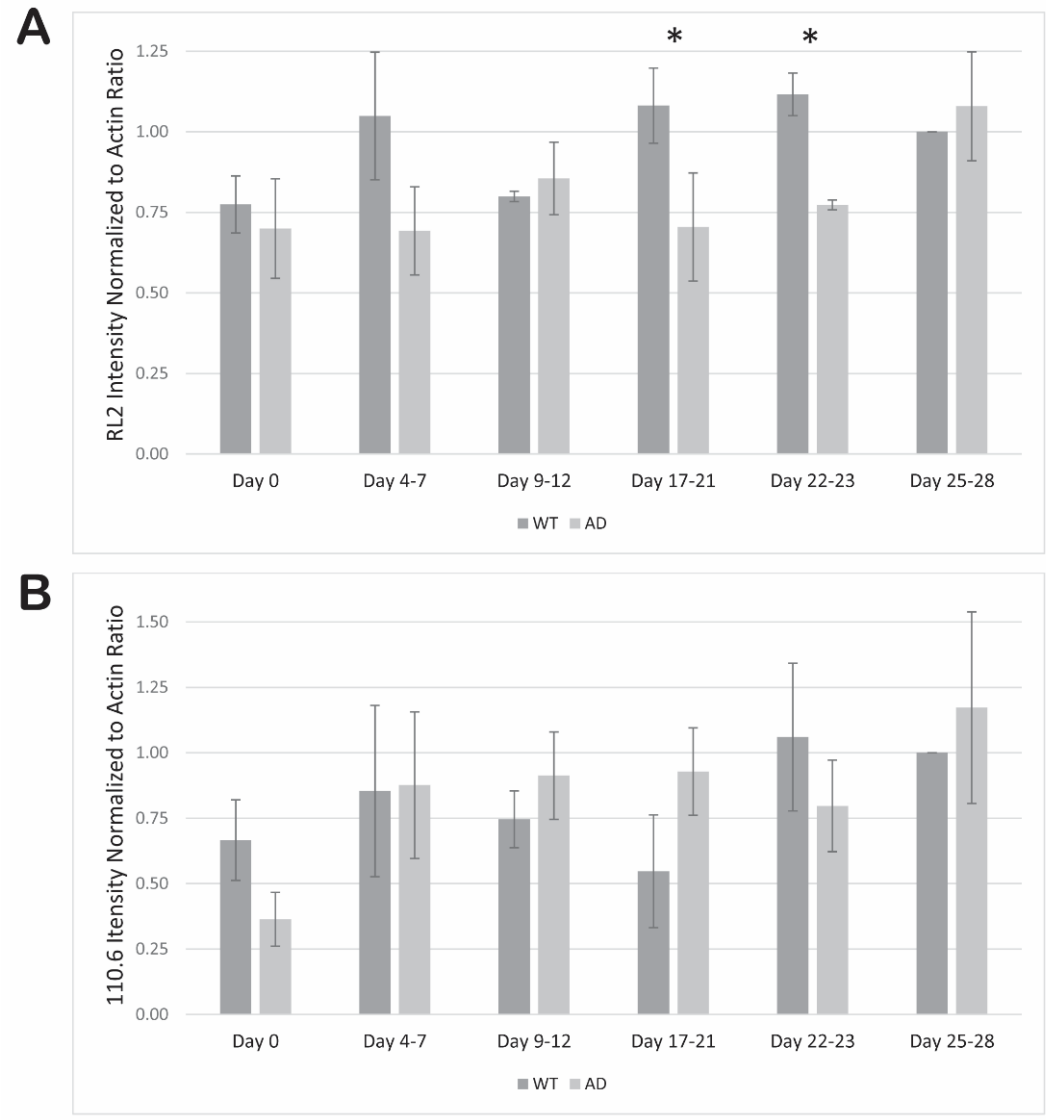

Figure 3.2. Protein O-GlcNAcylation detected by RL2 decreases upon differentiation of iPSCs to NCCs in Alzheimer Disease. Nucleocytoplasmic extracts from WT and AD cells were resolved by SDS-PAGE, blotted, and probed with **(A)** RL2 and **(B)** 110.6, monoclonal antibodies that recognize proteins modified by O-GlcNAc then quantified by densitometry. For developmental time courses that assessed the change in abundance across from iPSC to NCC (n=3 independent differentiations), signal intensities for receptor proteins were normalized to ß-actin (loading control) and then normalized to the signal intensity detected in K3 NCC. WT and AD values were combined into ranges that span 2-4 days of differentiation. The statistical significance of the difference (P-value from pairwise T-test) are presented above the bars for comparison of WT and AD cells O-GlcNAcylation.

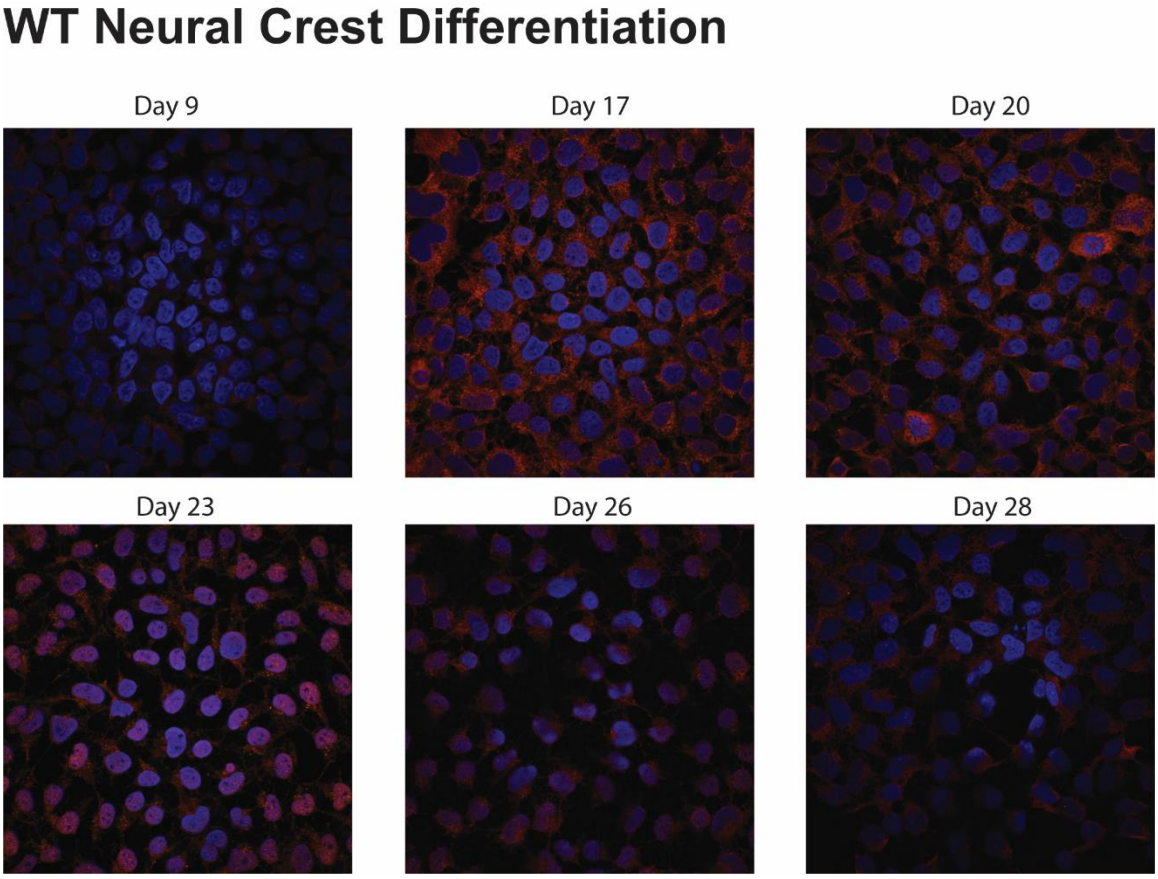

Figure 3.3. WT-derived human induced pluripotent stem cells differentiated to neural crest cells posses' changes in the localization of protein O-GlcNAcylation. WT iPSCs were differentiated to NCC via dual SMAD inhibition using small molecules. Expression and localization of protein O-GlcNAcylation was analyzed by staining with 110.6 and completing immunofluorescence at different time points throughout the differentiation.

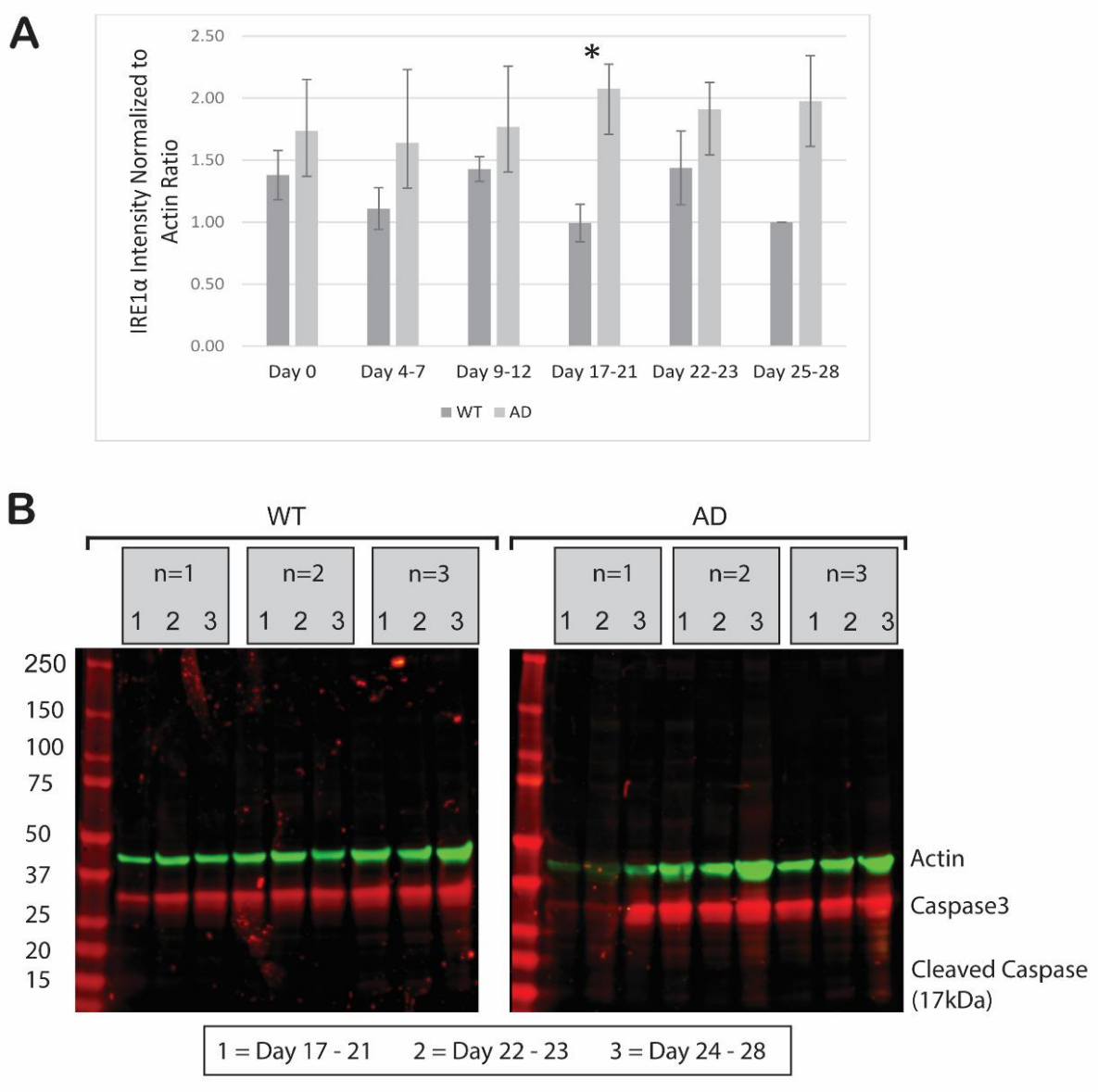

Figure 3.4. Dynamics of IRE1α and downstream signaling during neural crest differentiation. (A) Antibody against IRE1α and Actin was used to quantify receptor expression in WT and AD cells across full time courses of differentiation from iPSCs to NCCs (n=3 independent differentiations for each cell type). For simplicity of presentation and to provide a baseline reference for comparison, WT and AD values were combined into ranges that span 2-4 days of differentiation (mean ± SEM, n=3 determinations for each bin). (**B**) Apoptosis, reported by the abundance of cleaved Caspase3, is not detectable in WT and AD NCC cultures (Post Day 17). For simplicity of presentation, WT and AD samples were labeled by 1, 2, or 3 representation a span of 2-4 days of differentiation. As WT and AD cells differentiate to NCCs, cleaved Caspase3 is barely detectable.

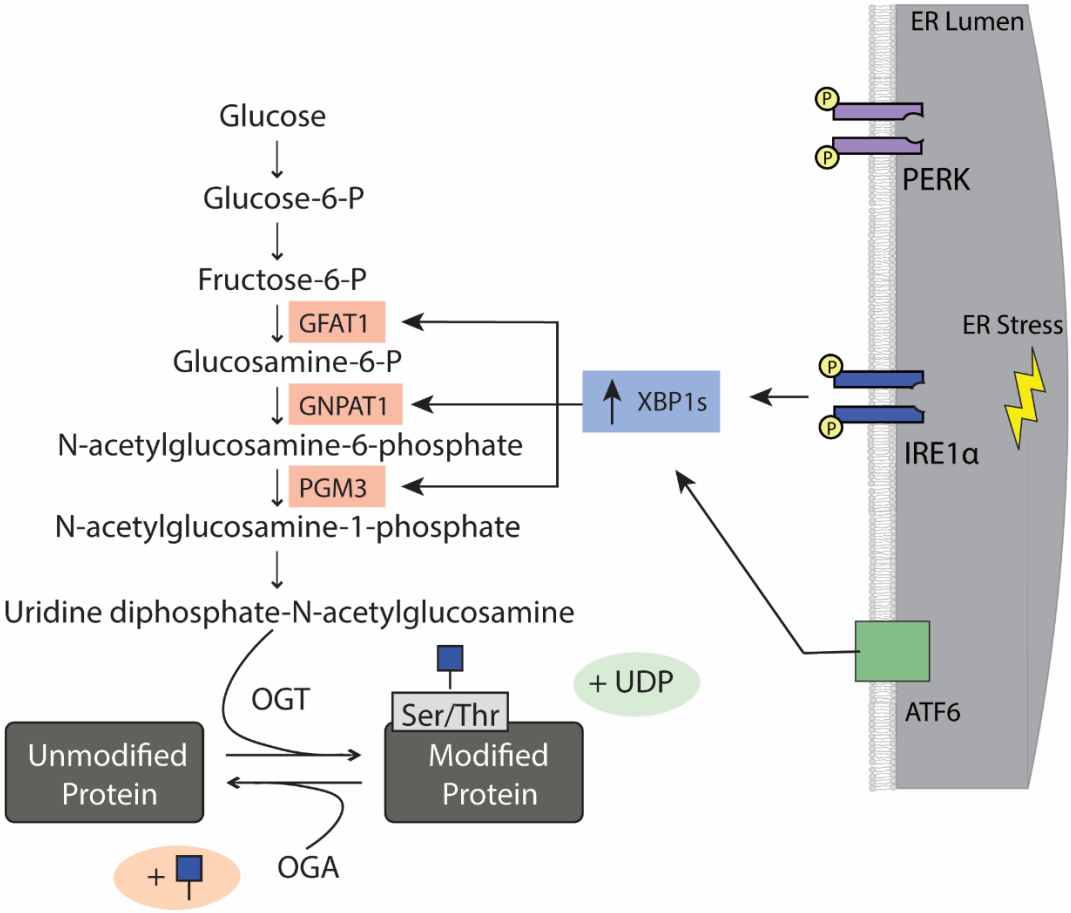

Figure 3.5. IRE1α signals for increased production of UDP-GlcNAc in response to reduced O-GlcNac levels. The unfolded protein response (UPR) signals for a variety of different pathways in response to ER stress. Therefore, the activation of UPR has many downstream consequences. When the ER becomes stressed IRE1α and ATF6 work to splice XBP1 (XBP1s). Increased expression of spliced XPB1 has been shown to directly increase the presence of the enzymes GFAT1, GNPAT1, and PGM3 which are involved in the Hexosamine Biosynthetic Pathway. The HBP produces uridine diphosphate – N -acetylglucosamine (UDP-GlcNAc) which then is used by O-GlcNAc transferase (OGT) as a donor substrate. The resulting protein is modified with a GlcNAc moiety changing the possible activity and localization of the protein.

REFERENCES

2021 Alzheimer's disease facts and figures. (2021). *Alzheimers Dement, 17*(3), 327-406. doi:10.1002/alz.12328

Acosta-Alvear, D., Zhou, Y., Blais, A., Tsikitis, M., Lents, N. H., Arias, C., . . . Dynlacht, B. D. (2007). XBP1 controls diverse cell type- and condition-specific transcriptional regulatory networks. *Mol Cell, 27*(1), 53-66. doi:10.1016/j.molcel.2007.06.011

Bird, T. D. (1993). Alzheimer Disease Overview. In M. P. Adam, H. H. Ardinger, R. A. Pagon, S. E. Wallace, L. J. H. Bean, K. W. Gripp, G. M. Mirzaa, & A. Amemiya (Eds.), *GeneReviews((R))*. Seattle (WA).

Chartier-Harlin, M. C., Parfitt, M., Legrain, S., Pérez-Tur, J., Brousseau, T., Evans, A., . . . et al. (1994). Apolipoprotein E, epsilon 4 allele as a major risk factor for sporadic early and late-onset forms of Alzheimer's disease: analysis of the 19q13.2 chromosomal region. *Hum Mol Genet, 3*(4), 569-574. doi:10.1093/hmg/3.4.569

Chen, X., Bisschops, M. M. M., Agarwal, N. R., Ji, B., Shanmugavel, K. P., & Petranovic, D. (2017). Interplay of Energetics and ER Stress Exacerbates Alzheimer's Amyloid-β (Aβ) Toxicity in Yeast. *Front Mol Neurosci, 10*, 232. doi:10.3389/fnmol.2017.00232

Chi, H., Chang, H. Y., & Sang, T. K. (2018). Neuronal Cell Death Mechanisms in Major Neurodegenerative Diseases. *Int J Mol Sci, 19*(10). doi:10.3390/ijms19103082

Comer, F. I., Vosseller, K., Wells, L., Accavitti, M. A., & Hart, G. W. (2001). Characterization of a mouse monoclonal antibody specific for O-linked N-acetylglucosamine. *Anal Biochem, 293*(2), 169-177. doi:10.1006/abio.2001.5132

Dias, W. B., & Hart, G. W. (2007). O-GlcNAc modification in diabetes and Alzheimer's disease. *Mol Biosyst, 3*(11), 766-772. doi:10.1039/b704905f

Duran-Aniotz, C., Cornejo, V. H., Espinoza, S., Ardiles Á, O., Medinas, D. B., Salazar, C., . . . Hetz, C. (2017). IRE1 signaling exacerbates Alzheimer's disease pathogenesis. *Acta Neuropathol, 134*(3), 489-506. doi:10.1007/s00401-017-1694-x

Guerreiro, R., Brás, J., & Hardy, J. (2013). SnapShot: genetics of Alzheimer's disease. *Cell, 155*(4), 968-968.e961. doi:10.1016/j.cell.2013.10.037

Harding, H. P., Zhang, Y., & Ron, D. (1999). Protein translation and folding are coupled by an endoplasmic-reticulum-resident kinase. *Nature, 397*(6716), 271-274. doi:10.1038/16729

Hart, G. W. (2019). Nutrient regulation of signaling and transcription. *J Biol Chem, 294*(7), 2211-2231. doi:10.1074/jbc.AW119.003226

Hart, G. W., & Akimoto, Y. (2009). The O-GlcNAc Modification. In nd, A. Varki, R. D. Cummings, J. D. Esko, H. H. Freeze, P. Stanley, C. R. Bertozzi, G. W. Hart, & M. E. Etzler (Eds.), *Essentials of Glycobiology*. Cold Spring Harbor (NY).

Holt, G. D., Snow, C. M., Senior, A., Haltiwanger, R. S., Gerace, L., & Hart, G. W. (1987). Nuclear pore complex glycoproteins contain cytoplasmically disposed O-linked N-acetylglucosamine. *J Cell Biol, 104*(5), 1157-1164. doi:10.1083/jcb.104.5.1157

Hoozemans, J. J., van Haastert, E. S., Nijholt, D. A., Rozemuller, A. J., Eikelenboom, P., & Scheper, W. (2009). The unfolded protein response is activated in pretangle neurons in Alzheimer's disease hippocampus. *Am J Pathol, 174*(4), 1241-1251. doi:10.2353/ajpath.2009.080814

Huang, C.-W., & Hart, G. W. (2021). Decreased O-GlcNAcylation and mitochondrial dysfunction are involving in low glucose induced Alzheimer's disease-like phenotype in induced pluripotent stem cell-derived neurons. *Alzheimer's & Dementia, 17*(S2), e058620. doi:https://doi.org/10.1002/alz.058620

Israel, M. A., Yuan, S. H., Bardy, C., Reyna, S. M., Mu, Y., Herrera, C., . . . Goldstein, L. S. (2012). Probing sporadic and familial Alzheimer's disease using induced pluripotent stem cells. *Nature, 482*(7384), 216-220. doi:10.1038/nature10821

Kamemura, K., & Hart, G. W. (2003). Dynamic interplay between O-glycosylation and O-phosphorylation of nucleocytoplasmic proteins: a new paradigm for metabolic control of signal transduction and transcription. *Prog Nucleic Acid Res Mol Biol, 73*, 107-136. doi:10.1016/s0079-6603(03)01004-3

Lee, A. H., Iwakoshi, N. N., & Glimcher, L. H. (2003). XBP-1 regulates a subset of endoplasmic reticulum resident chaperone genes in the unfolded protein response. *Mol Cell Biol, 23*(21), 7448-7459. doi:10.1128/mcb.23.21.7448-7459.2003

Li, S., & Selkoe, D. J. (2020). A mechanistic hypothesis for the impairment of synaptic plasticity by soluble Aβ oligomers from Alzheimer's brain. *J Neurochem, 154*(6), 583-597. doi:10.1111/jnc.15007

Lin, E. E., Scott-Solomon, E., & Kuruvilla, R. (2021). Peripheral Innervation in the Regulation of Glucose Homeostasis. *Trends in Neurosciences, 44*(3), 189-202. doi:https://doi.org/10.1016/j.tins.2020.10.015

Lin, J. H., Li, H., Zhang, Y., Ron, D., & Walter, P. (2009). Divergent effects of PERK and IRE1 signaling on cell viability. *PLoS One, 4*(1), e4170. doi:10.1371/journal.pone.0004170

Liu, C.-C., Kanekiyo, T., Xu, H., & Bu, G. (2013). Apolipoprotein E and Alzheimer disease: risk, mechanisms and therapy. *Nature Reviews Neurology, 9*(2), 106-118. doi:10.1038/nrneurol.2012.263

Lu, P. D., Harding, H. P., & Ron, D. (2004). Translation reinitiation at alternative open reading frames regulates gene expression in an integrated stress response. *J Cell Biol, 167*(1), 27-33. doi:10.1083/jcb.200408003

Mannino, M. P., & Hart, G. W. (2022). The Beginner's Guide to O-GlcNAc: From Nutrient Sensitive Pathway Regulation to Its Impact on the Immune System. *Front Immunol, 13*, 828648. doi:10.3389/fimmu.2022.828648

Menendez, L., Yatskievych, T. A., Antin, P. B., & Dalton, S. (2011). Wnt signaling and a Smad pathway blockade direct the differentiation of human pluripotent stem cells to multipotent neural crest cells. *Proceedings of the National Academy of Sciences, 108*(48), 19240-19245. doi:10.1073/pnas.1113746108

Ngoh, G. A., Hamid, T., Prabhu, S. D., & Jones, S. P. (2009). O-GlcNAc signaling attenuates ER stress-induced cardiomyocyte death. *Am J Physiol Heart Circ Physiol, 297*(5), H1711-1719. doi:10.1152/ajpheart.00553.2009

Park, J., Lai, M. K. P., Arumugam, T. V., & Jo, D.-G. (2020). O-GlcNAcylation as a Therapeutic Target for Alzheimer's Disease. *NeuroMolecular Medicine, 22*(2), 171-193. doi:10.1007/s12017-019-08584-0

Sherrington, R., Rogaev, E. I., Liang, Y., Rogaeva, E. A., Levesque, G., Ikeda, M., . . . St George-Hyslop, P. H. (1995). Cloning of a gene bearing missense mutations in early-onset familial Alzheimer's disease. *Nature, 375*(6534), 754-760. doi:10.1038/375754a0

Si-Tayeb, K., Noto, F. K., Sepac, A., Sedlic, F., Bosnjak, Z. J., Lough, J. W., & Duncan, S. A. (2010). Generation of human induced pluripotent stem cells by simple transient transfection of plasmid DNA encoding reprogramming factors. *BMC Dev Biol, 10*, 81. doi:10.1186/1471-213x-10-81

Uddin, M. S., Tewari, D., Sharma, G., Kabir, M. T., Barreto, G. E., Bin-Jumah, M. N., . . . Ashraf, G. M. (2020). Molecular Mechanisms of ER Stress and UPR in the Pathogenesis of Alzheimer's Disease. *Molecular Neurobiology, 57*(7), 2902-2919. doi:10.1007/s12035-020-01929-y

van der Harg, J. M., van Heest, J. C., Bangel, F. N., Patiwael, S., van Weering, J. R., & Scheper, W. (2017). The UPR reduces glucose metabolism via IRE1 signaling. *Biochim Biophys Acta Mol Cell Res, 1864*(4), 655-665. doi:10.1016/j.bbamcr.2017.01.009

Wodrich, A. P. K., Scott, A. W., Shukla, A. K., Harris, B. T., & Giniger, E. (2022). The Unfolded Protein Responses in Health, Aging, and Neurodegeneration: Recent

Advances and Future Considerations. *Front Mol Neurosci, 15*, 831116. doi:10.3389/fnmol.2022.831116

Yang, X., & Qian, K. (2017). Protein O-GlcNAcylation: emerging mechanisms and functions. *Nat Rev Mol Cell Biol, 18*(7), 452-465. doi:10.1038/nrm.2017.22

Yoshida, H., Matsui, T., Yamamoto, A., Okada, T., & Mori, K. (2001). XBP1 mRNA is induced by ATF6 and spliced by IRE1 in response to ER stress to produce a highly active transcription factor. *Cell, 107*(7), 881-891. doi:10.1016/s0092-8674(01)00611-0

Yuzwa, S. A., Macauley, M. S., Heinonen, J. E., Shan, X., Dennis, R. J., He, Y., . . . Vocadlo, D. J. (2008). A potent mechanism-inspired O-GlcNAcase inhibitor that blocks phosphorylation of tau in vivo. *Nature Chemical Biology, 4*(8), 483-490. doi:10.1038/nchembio.96

Zachara, N. E., O'Donnell, N., Cheung, W. D., Mercer, J. J., Marth, J. D., & Hart, G. W. (2004). Dynamic O-GlcNAc modification of nucleocytoplasmic proteins in response to stress. A survival response of mammalian cells. *J Biol Chem, 279*(29), 30133-30142. doi:10.1074/jbc.M403773200

CHAPTER 4

DISCUSSION

Based on our initial work on GM3 Synthase Deficiency (GM3SD) and Alzheimer's Disease (AD) this chapter will highlight our findings as well as future directions to further understand neurological diseases and the consequences of altered glycosylation.

CONCLUSIONS FROM OUR RESEARCH AND FUTURE DIRECTIONS

Both diseases discussed in this thesis are devastating diseases that disrupt normal cognitive functioning and standard of living. In addition to causing cognitive changes GM3SD affects the peripheral nervous system greatly. It is a rare disease, so up until recently not much was known about it. In past years it was found to be caused by mutations in the *ST3GAL5* gene, which is responsible for the production of GM3 and all GM3-derived gangliosides. Since the original work other variants have been found, but despite changes in the mutation they all show loss of ST3Gal5s' activity (Boccuto et al., 2014; Gordon-Lipkin et al., 2018; Indellicato et al., 2019; J. S. Lee et al., 2016; Simpson et al., 2004). Focusing on two patients in Chapter 2 of this thesis, we see that there are molecular similarities even though their mutations causing GM3SD are different. We show that both the Salt and Pepper population (p.Glu355Lys) and Amish Population (p.Arg288Ter) do not possess any GM3 or GM3-derived gangliosides as iPSC or NCC. This result is consistent with previous work done (Boccuto et al., 2014; Bowser et al., 2019; Simpson et al., 2004); however, our mass spectrometry did show an increase

accumulation of LacCer in the variants compared to wildtype. This result contrasts with the work completed by Boccuto et al. which showed an increase in globo-series GSLs that are also not reliant on GM3 synthase. Our result showing increased accumulation of LacCer has been reported in a paper previously published by our lab. Specifically, the plasma of Amish (p.Arg288Ter) GM3-deficient patients showed elevated levels of LacCer (Aoki, Heaps, Strauss, & Tiemeyer, 2019). Increased levels of LacCer have been shown to be correlated with increased levels of cell death (Bodas, Min, & Vij, 2015; Martin, Williams, & Chatterjee, 2006). Thus, to understand the downstream consequences of the loss of GM3 and GM3-derived gangliosides we analyzed different receptors, modifications, and cleaved caspase3 levels to see if these cells are more prone to cell death. Inhibiting EGFR in the GM3SD variants and WT showed that the variants are more susceptible to cell death indicated by increased levels of cleaved caspase3. Protein O-GlcNAcylation has been shown to have a pro-survival role affecting many different aspects of cell fate (Hart, 2019). The amount of protein O-GlcNAcylation can be increased by pharmacologically inhibiting O-GlcNAcase (OGA) with Thiamet- G (Jiang et al., 2017; Yuzwa et al., 2008). When we inhibited OGA in the presence or absence of erlotinib, we saw reduced levels of cleaved caspase3.

Due to the difficulty isolating lipid rafts there is a lack of information on what effector proteins influence the overall signaling (Pike, 2009). In our SEEL studies we identified different proteins associated with the membrane and endosomes. Many of these proteins were either upregulated or downregulated in comparison to wildtype. It is speculated that the changes in these effector proteins could affect the lipid raft domains and the decreased sialylation of GSLs. If the domains are affected it could be assumed that

overall signaling activity, localization at the cell surface, and the receptors position in the domain could be altered (Pike, 2009). Despite the lack of research studying these domains, it has been expressed how crucial lipid rafts are for proper signaling and development. Thus, as we study these aspects in our iPSC and differentiated NCCs it makes sense why we see changes in receptor signaling and responses. A key signaling aspect that we analyzed was O-GlcNAcylation. As the WT and GM3SD cells differentiated to NCCs the overall amount of protein O-GlcNAcylation increased, but the overall level varied much more in the different replicates of GM3SD cells. Additionally, the ability to reduce cleaved caspase3 levels by pharmacologically enhancing O-GlcNAcylation with thiamet G in the presence or absence of erlotnib (Jiang et al., 2017; Yuzwa et al., 2008) shows that it affects cell signaling in some form. To fully understand the magnitude of this result, it would be beneficial to further look at what effector proteins are becoming O-GlcNAcylated and how this could be directly affecting lipid rafts.

In contract to GM3SD, Alzheimer's disease has become very common and has been studied extensively regarding the central nervous system, amyloid β and phospho-tau pathology (Bird, 1993; Hardy & Higgins, 1992). The previous work done makes sense due to the main consequences of AD, Aβ plaques, neurofibrillary tangles, and neuron death, are primarily found in the central nervous system and brain. However, the work illustrated in chapter 3 of this thesis attempts to study AD in a different light then previously done. It focuses on neural crest cells which are progenitors to the PNS (Gilbert, 2000; Yntema & Hammond, 1954). The PNS has not been extensively studied in AD. However, because the PNS directly supplies the CNS with information from the internal and external

environment it makes it very interesting to see if it possesses any upstream signaling events that could have a cascade of responses (Goldstein, 2001).

Our preliminary data showcases O-GlcNAcylation on nuclear core proteins and transcription factors detected by RL2 expression is significantly decreased compared to WT. O-GlcNAcylation has been previously described to be a crucial signal integrator responsible for decreasing stress in many different aspects of the cell (Mannino & Hart, 2022; Yang & Suh, 2014; Zachara et al., 2004). However, in diseases like AD it has also been shown to be a cause of stress. This decrease in protein O-GlcNAcylation has been shown to drastically affect protein activity and translation as well as the aggregation of Aβ and hyperphosphorylated tau (Dias & Hart, 2007; Hart, 2019; Park, Lai, Arumugam, & Jo, 2020).

The endoplasmic reticulum (ER) is necessary for the proper production and folding of nascent polypeptides (Helenius & Aebi, 2004; Sun & Brodsky, 2019). The ER has a quality control system called the Unfolded Protein Response (UPR) which acts to bring the ER back to homeostasis if the ER becomes stressed. The ER can become stressed in response to accumulation of misfolded proteins, like hyperphosphorylated tau or amyloid precursor protein, environmental factors, and signaling events (Ron & Walter, 2007; Schröder & Kaufman, 2005). The UPR consists of three membrane receptors: inositol-requiring enzyme (IRE1α), protein kinase RNA-like endoplasmic reticulum kinase (PERK) and activating transcription factor 6 (ATF6) (Uddin et al., 2020; Wodrich, Scott, Shukla, Harris, & Giniger, 2022). One of the main receptors of the UPR is IRE1α and its role is to increase transcription of chaperones and promote cell survival by initiating the splicing of X-box binding protein (XBP1). (Adams, Kopp, Larburu, Nowak, & Ali, 2019;

Lin, Li, Zhang, Ron, & Walter, 2009; McCarthy et al., 2020). Once spliced XBP1 is in its activated form and can translocate to the nucleus to increase transcription of a wide variety of genes involved in protein trafficking, folding, degradation, and metabolism (A. H. Lee, Iwakoshi, & Glimcher, 2003; Yoshida, Matsui, Yamamoto, Okada, & Mori, 2001). Thus, the IRE1α and XBP1 pathway has a very large impact on cell fate and recovery (Acosta-Alvear et al., 2007). Blots probing for IRE1α showed that the receptor expression increased during the same time frame that O-GlcNAcylation decreased in AD, highlighting a possible correlation between the decreased protein O-GlcNAcylation and increased ER stress. If the ER stays stressed for a prolonged period of time, then PERK will become activated signaling for CHOP mediated cell death (Lin et al., 2009). Thus, to judge the consequences of changes in cell signaling we analyzed cleaved caspase3 levels for the last three-time frames of the differentiation. We showed that there were undetectable levels of cleaved caspase3 in both WT and AD. This result suggests that AD NCCs mechanisms to promote pro-survival are effective at restoring homeostasis and preventing cell death. This would contrast with cells from the central nervous system such as cortical neurons that have been shown to be prone to extensive cell stress and death (Morrison & Hof, 2007).

These preliminary results are found in NCCs. NCCs formed at the dorsal most portion of the neural tube are only progenitors of the PNS. There are three main pathways that NCC can migrate through which produces a broad span of different cell types. If the NCC migrate ventrally they will form dorsal root ganglia (sensory division) and sympathetic and enteric neurons (autonomic division). Pigment cells are produced from NCC migrating dorsolaterally. Following these migratory pathways the NCC commit to a neuronal fate (Marmigère & Ernfors, 2007). Peripheral sensory neurons integrate signals

from the peripheral organs, tissues, and limbs. These neurons can be divided into three different groups: nociceptors, mechanoreceptors, and proprioceptors (Saito-Diaz, Street, Ulrichs, & Zeltner, 2021) The different types of neurons have different roles and chemical properties meaning that certain changes may affect one cell type differently than another (Marmigère & Ernfors, 2007). Thus, it would be advantageous to judge if these neurons also exhibit similar changes seen in our NCCs.

To further define this possible mechanism, it would be crucial to study other components of cellular stress in NCCs to judge if more components are involved in this response and recovery. For instance, individuals with AD have been shown to have oxidative stress and mitochondrial disfunction (Huang & Hart, 2021; Perez Ortiz & Swerdlow, 2019; Weidling & Swerdlow, 2020). Many speculate that mitochondria dysfunction could be a cause or response of AD pathology. Like the ER the mitochondria can become stressed in response to changes in glucose metabolism and O-GlcNAcylation. This relationship has been extensively studied in terms of cancer and diabetes which are two diseases that rely heavily on glucose metabolism (Haythorne et al., 2019; Raut, Chakrabarti, Pamarthy, & Bhadra, 2019; Sutherland, Bomhof, Capozzi, Basaraba, & Wright, 2009). The mitochondria also possess an unfolded protein response (UPR^{mt}) which is not as understood as the ERs. In addition to the mitochondria becoming stressed from glucose metabolism, it has been shown that ER stress affects the transcription of genes encoding mitochondrial proteins. The expression of certain proteins such as mitochondrial ATP-dependent proteases will cause stress in the mitochondria (Hori et al., 2002). To understand more of the cellular mechanisms occurring in AD NCC it would be beneficial to detect what other compartments could be under stress from AD pathology as well as if

there is a certain sequence of events leading to the different compartments becoming stressed.

As seen many aspects of glucose metabolism and protein O-GlcNAcylation have been correlated with stress. Firstly, overall increased transport of glucose has been associated with pro-survival mechanisms allowing the cell to survive difficult environmental conditions (Zachara et al., 2004). Adding in inhibitors of glycolysis and the hexosamine biosynthetic pathway (HBP) overall stopping the production of UDP-GlcNAc, results in increased cell death (Kan, Baldwin, & Whetton, 1994; Liu, Schoenkerman, & Lowe, 2000; Malhotra & Brosius, 1999). This supports the notion that decreased O-GlcNAcylation causes the cells to be more prone to cell death. If the decreased protein O-GlcNAcylation seen in our AD NCC is the cause of stress it would be ideal to see what proteins are experiencing a change in O-GlcNAcylation in AD NCC compared to WT. Since O-GlcNAcylation is a transient PTM it is difficult to analyze site specific modification. However, to gauge overall changes in O-GlcNAcylation on individual proteins immunoprecipitation and mass spectrometry analysis can be completed. Completing this analysis would give insight to see what proteins are not being modified with a O-GlcNAc moiety in AD and what functions of those proteins could be altered as a response.

Despite these neurological diseases being drastically different we sought to further study as well as compare the mechanistic changes occurring in both diseases. My individual work on both projects revolved around protein O-GlcNAcylation as a center link. Based on our work on GM3SD variants and preliminary data on AD, O-

GlcNAcylation could serve as a potential target and/or treatment for therapeutics in many types of neurological diseases.

REFERENCES

Acosta-Alvear, D., Zhou, Y., Blais, A., Tsikitis, M., Lents, N. H., Arias, C., . . . Dynlacht, B. D. (2007). XBP1 controls diverse cell type- and condition-specific transcriptional regulatory networks. *Mol Cell, 27*(1), 53-66. doi:10.1016/j.molcel.2007.06.011

Adams, C. J., Kopp, M. C., Larburu, N., Nowak, P. R., & Ali, M. M. U. (2019). Structure and Molecular Mechanism of ER Stress Signaling by the Unfolded Protein Response Signal Activator IRE1. *Front Mol Biosci, 6*, 11. doi:10.3389/fmolb.2019.00011

Aoki, K., Heaps, A. D., Strauss, K. A., & Tiemeyer, M. (2019). Mass spectrometric quantification of plasma glycosphingolipids in human GM3 ganglioside deficiency. *Clinical Mass Spectrometry, 14*, 106-114. doi:https://doi.org/10.1016/j.clinms.2019.03.001

Bird, T. D. (1993). Alzheimer Disease Overview. In M. P. Adam, H. H. Ardinger, R. A. Pagon, S. E. Wallace, L. J. H. Bean, K. W. Gripp, G. M. Mirzaa, & A. Amemiya (Eds.), *GeneReviews((R))*. Seattle (WA).

Boccuto, L., Aoki, K., Flanagan-Steet, H., Chen, C. F., Fan, X., Bartel, F., . . . Schwartz, C. E. (2014). A mutation in a ganglioside biosynthetic enzyme, ST3GAL5, results in salt & pepper syndrome, a neurocutaneous disorder with altered glycolipid and glycoprotein glycosylation. *Hum Mol Genet, 23*(2), 418-433. doi:10.1093/hmg/ddt434

Bodas, M., Min, T., & Vij, N. (2015). Lactosylceramide-accumulation in lipid-rafts mediate aberrant-autophagy, inflammation and apoptosis in cigarette smoke induced emphysema. *Apoptosis, 20*(5), 725-739. doi:10.1007/s10495-015-1098-0

Bowser, L. E., Young, M., Wenger, O. K., Ammous, Z., Brigatti, K. W., Carson, V. J., . . . Strauss, K. A. (2019). Recessive GM3 synthase deficiency: Natural history, biochemistry, and therapeutic frontier. *Mol Genet Metab, 126*(4), 475-488. doi:10.1016/j.ymgme.2019.01.013

Dias, W. B., & Hart, G. W. (2007). O-GlcNAc modification in diabetes and Alzheimer's disease. *Mol Biosyst, 3*(11), 766-772. doi:10.1039/b704905f

Gilbert, S. (2000). *The Neural Crest* [6th edition]*Developmental Biology*.

Goldstein, B. (2001). Anatomy of the peripheral nervous system. *Phys Med Rehabil Clin N Am, 12*(2), 207-236.

Gordon-Lipkin, E., Cohen, J. S., Srivastava, S., Soares, B. P., Levey, E., & Fatemi, A. (2018). ST3GAL5-Related Disorders: A Deficiency in Ganglioside Metabolism

and a Genetic Cause of Intellectual Disability and Choreoathetosis. *J Child Neurol, 33*(13), 825-831. doi:10.1177/0883073818791099

Hardy, J. A., & Higgins, G. A. (1992). Alzheimer's disease: the amyloid cascade hypothesis. *Science, 256*(5054), 184-185. doi:10.1126/science.1566067

Hart, G. W. (2019). Nutrient regulation of signaling and transcription. *J Biol Chem, 294*(7), 2211-2231. doi:10.1074/jbc.AW119.003226

Haythorne, E., Rohm, M., van de Bunt, M., Brereton, M. F., Tarasov, A. I., Blacker, T. S., . . . Ashcroft, F. M. (2019). Diabetes causes marked inhibition of mitochondrial metabolism in pancreatic β-cells. *Nature Communications, 10*(1), 2474. doi:10.1038/s41467-019-10189-x

Helenius, A., & Aebi, M. (2004). Roles of N-linked glycans in the endoplasmic reticulum. *Annu Rev Biochem, 73*, 1019-1049. doi:10.1146/annurev.biochem.73.011303.073752

Hori, O., Ichinoda, F., Tamatani, T., Yamaguchi, A., Sato, N., Ozawa, K., . . . Ogawa, S. (2002). Transmission of cell stress from endoplasmic reticulum to mitochondria: enhanced expression of Lon protease. *J Cell Biol, 157*(7), 1151-1160. doi:10.1083/jcb.200108103

Huang, C.-W., & Hart, G. W. (2021). Decreased O-GlcNAcylation and mitochondrial dysfunction are involving in low glucose induced Alzheimer's disease-like phenotype in induced pluripotent stem cell-derived neurons. *Alzheimer's & Dementia, 17*(S2), e058620. doi:https://doi.org/10.1002/alz.058620

Indellicato, R., Parini, R., Domenighini, R., Malagolini, N., Iascone, M., Gasperini, S., . . . Trinchera, M. (2019). Total loss of GM3 synthase activity by a normally processed enzyme in a novel variant and in all ST3GAL5 variants reported to cause a distinct congenital disorder of glycosylation. *Glycobiology, 29*(3), 229-241. doi:10.1093/glycob/cwy112

Jiang, M., Yu, S., Yu, Z., Sheng, H., Li, Y., Liu, S., . . . Yang, W. (2017). XBP1 (X-Box–Binding Protein-1)–Dependent O-GlcNAcylation Is Neuroprotective in Ischemic Stroke in Young Mice and Its Impairment in Aged Mice Is Rescued by Thiamet-G. *Stroke, 48*(6), 1646-1654. doi:doi:10.1161/STROKEAHA.117.016579

Kan, O., Baldwin, S. A., & Whetton, A. D. (1994). Apoptosis is regulated by the rate of glucose transport in an interleukin 3 dependent cell line. *J Exp Med, 180*(3), 917-923. doi:10.1084/jem.180.3.917

Lee, A. H., Iwakoshi, N. N., & Glimcher, L. H. (2003). XBP-1 regulates a subset of endoplasmic reticulum resident chaperone genes in the unfolded protein response. *Mol Cell Biol, 23*(21), 7448-7459. doi:10.1128/mcb.23.21.7448-7459.2003

Lee, J. S., Yoo, Y., Lim, B. C., Kim, K. J., Song, J., Choi, M., & Chae, J.-H. (2016). GM3 synthase deficiency due to ST3GAL5 variants in two Korean female siblings: Masquerading as Rett syndrome-like phenotype. *American Journal of Medical Genetics Part A, 170*(8), 2200-2205. doi:https://doi.org/10.1002/ajmg.a.37773

Lin, J. H., Li, H., Zhang, Y., Ron, D., & Walter, P. (2009). Divergent effects of PERK and IRE1 signaling on cell viability. *PLoS One, 4*(1), e4170. doi:10.1371/journal.pone.0004170

Liu, W., Schoenkerman, A., & Lowe, W. L., Jr. (2000). Activation of members of the mitogen-activated protein kinase family by glucose in endothelial cells. *Am J Physiol Endocrinol Metab, 279*(4), E782-790. doi:10.1152/ajpendo.2000.279.4.E782

Malhotra, R., & Brosius, F. C., III. (1999). Glucose Uptake and Glycolysis Reduce Hypoxia-induced Apoptosis in Cultured Neonatal Rat Cardiac Myocytes *. *Journal of Biological Chemistry, 274*(18), 12567-12575. doi:10.1074/jbc.274.18.12567

Mannino, M. P., & Hart, G. W. (2022). The Beginner's Guide to O-GlcNAc: From Nutrient Sensitive Pathway Regulation to Its Impact on the Immune System. *Front Immunol, 13*, 828648. doi:10.3389/fimmu.2022.828648

Marmigère, F., & Ernfors, P. (2007). Specification and connectivity of neuronal subtypes in the sensory lineage. *Nature Reviews Neuroscience, 8*(2), 114-127. doi:10.1038/nrn2057

Martin, S. F., Williams, N., & Chatterjee, S. (2006). Lactosylceramide is required in apoptosis induced by N-Smase. *Glycoconj J, 23*(3-4), 147-157. doi:10.1007/s10719-006-7920-8

McCarthy, N., Dolgikh, N., Logue, S., Patterson, J. B., Zeng, Q., Gorman, A. M., . . . Fulda, S. (2020). The IRE1 and PERK arms of the unfolded protein response promote survival of rhabdomyosarcoma cells. *Cancer Letters, 490*, 76-88. doi:https://doi.org/10.1016/j.canlet.2020.07.009

Morrison, J. H., & Hof, P. R. (2007). Life and Death of Neurons in The Aging Cerebral Cortex. In *International Review of Neurobiology* (Vol. 81, pp. 41-57): Academic Press.

Park, J., Lai, M. K. P., Arumugam, T. V., & Jo, D.-G. (2020). O-GlcNAcylation as a Therapeutic Target for Alzheimer's Disease. *NeuroMolecular Medicine, 22*(2), 171-193. doi:10.1007/s12017-019-08584-0

Perez Ortiz, J. M., & Swerdlow, R. H. (2019). Mitochondrial dysfunction in Alzheimer's disease: Role in pathogenesis and novel therapeutic opportunities. *Br J Pharmacol, 176*(18), 3489-3507. doi:10.1111/bph.14585

Pike, L. J. (2009). The challenge of lipid rafts. *J Lipid Res, 50 Suppl*(Suppl), S323-328. doi:10.1194/jlr.R800040-JLR200

Raut, G. K., Chakrabarti, M., Pamarthy, D., & Bhadra, M. P. (2019). Glucose starvation-induced oxidative stress causes mitochondrial dysfunction and apoptosis via Prohibitin 1 upregulation in human breast cancer cells. *Free Radical Biology and Medicine, 145*, 428-441. doi:https://doi.org/10.1016/j.freeradbiomed.2019.09.020

Ron, D., & Walter, P. (2007). Signal integration in the endoplasmic reticulum unfolded protein response. *Nat Rev Mol Cell Biol, 8*(7), 519-529. doi:10.1038/nrm2199

Saito-Diaz, K., Street, J. R., Ulrichs, H., & Zeltner, N. (2021). Derivation of Peripheral Nociceptive, Mechanoreceptive, and Proprioceptive Sensory Neurons from the same Culture of Human Pluripotent Stem Cells. *Stem Cell Reports, 16*(3), 446-457. doi:10.1016/j.stemcr.2021.01.001

Schröder, M., & Kaufman, R. J. (2005). ER stress and the unfolded protein response. *Mutat Res, 569*(1-2), 29-63. doi:10.1016/j.mrfmmm.2004.06.056

Simpson, M. A., Cross, H., Proukakis, C., Priestman, D. A., Neville, D. C. A., Reinkensmeier, G., . . . Crosby, A. H. (2004). Infantile-onset symptomatic epilepsy syndrome caused by a homozygous loss-of-function mutation of GM3 synthase. *Nature Genetics, 36*(11), 1225-1229. doi:10.1038/ng1460

Sun, Z., & Brodsky, J. L. (2019). Protein quality control in the secretory pathway. *J Cell Biol, 218*(10), 3171-3187. doi:10.1083/jcb.201906047

Sutherland, L. N., Bomhof, M. R., Capozzi, L. C., Basaraba, S. A., & Wright, D. C. (2009). Exercise and adrenaline increase PGC-1{alpha} mRNA expression in rat adipose tissue. *J Physiol, 587*(Pt 7), 1607-1617. doi:10.1113/jphysiol.2008.165464

Uddin, M. S., Tewari, D., Sharma, G., Kabir, M. T., Barreto, G. E., Bin-Jumah, M. N., . . . Ashraf, G. M. (2020). Molecular Mechanisms of ER Stress and UPR in the Pathogenesis of Alzheimer's Disease. *Molecular Neurobiology, 57*(7), 2902-2919. doi:10.1007/s12035-020-01929-y

Weidling, I. W., & Swerdlow, R. H. (2020). Mitochondria in Alzheimer's disease and their potential role in Alzheimer's proteostasis. *Exp Neurol, 330*, 113321. doi:10.1016/j.expneurol.2020.113321

Wodrich, A. P. K., Scott, A. W., Shukla, A. K., Harris, B. T., & Giniger, E. (2022). The Unfolded Protein Responses in Health, Aging, and Neurodegeneration: Recent Advances and Future Considerations. *Front Mol Neurosci, 15*, 831116. doi:10.3389/fnmol.2022.831116

Yang, Y. R., & Suh, P.-G. (2014). O-GlcNAcylation in cellular functions and human diseases. *Advances in Biological Regulation, 54*, 68-73. doi:https://doi.org/10.1016/j.jbior.2013.09.007

Yntema, C. L., & Hammond, W. S. (1954). The origin of intrinsic ganglia of trunk viscera from vagal neural crest in the chick embryo. *J Comp Neurol, 101*(2), 515-541. doi:10.1002/cne.901010212

Yoshida, H., Matsui, T., Yamamoto, A., Okada, T., & Mori, K. (2001). XBP1 mRNA is induced by ATF6 and spliced by IRE1 in response to ER stress to produce a highly active transcription factor. *Cell, 107*(7), 881-891. doi:10.1016/s0092-8674(01)00611-0

Yuzwa, S. A., Macauley, M. S., Heinonen, J. E., Shan, X., Dennis, R. J., He, Y., . . . Vocadlo, D. J. (2008). A potent mechanism-inspired O-GlcNAcase inhibitor that blocks phosphorylation of tau in vivo. *Nature Chemical Biology, 4*(8), 483-490. doi:10.1038/nchembio.96

Zachara, N. E., O'Donnell, N., Cheung, W. D., Mercer, J. J., Marth, J. D., & Hart, G. W. (2004). Dynamic O-GlcNAc modification of nucleocytoplasmic proteins in response to stress. A survival response of mammalian cells. *J Biol Chem, 279*(29), 30133-30142. doi:10.1074/jbc.M403773200